

RS-8232-2/67832

NUREG/CR-4993
SAND87-1858

ay1

J. A. Wackerly, 85243



8232-2/067832



00000001 -

A Standard Problem for HECTR-MAAP Comparison: Incomplete Burning

Prepared by C. C. Wong

Sandia National Laboratories

Prepared for
U.S. Nuclear Regulatory
Commission

NOTICE

This report was prepared as an account of work sponsored by an agency of the United States Government. Neither the United States Government nor any agency thereof, or any of their employees, makes any warranty, expressed or implied, or assumes any legal liability of responsibility for any third party's use, or the results of such use, of any information, apparatus, product or process disclosed in this report, or represents that its use by such third party would not infringe privately owned rights.

NOTICE

Availability of Reference Materials Cited in NRC Publications

Most documents cited in NRC publications will be available from one of the following sources:

1. The NRC Public Document Room, 1717 H Street, N.W.
Washington, DC 20555
2. The Superintendent of Documents, U.S. Government Printing Office, Post Office Box 37082,
Washington, DC 20013-7082
3. The National Technical Information Service, Springfield, VA 22161

Although the listing that follows represents the majority of documents cited in NRC publications, it is not intended to be exhaustive.

Referenced documents available for inspection and copying for a fee from the NRC Public Document Room include NRC correspondence and internal NRC memoranda; NRC Office of Inspection and Enforcement bulletins, circulars, information notices, inspection and investigation notices; Licensee Event Reports; vendor reports and correspondence; Commission papers; and applicant and licensee documents and correspondence.

The following documents in the NUREG series are available for purchase from the GPO Sales Program: formal NRC staff and contractor reports, NRC-sponsored conference proceedings, and NRC booklets and brochures. Also available are Regulatory Guides, NRC regulations in the *Code of Federal Regulations*, and *Nuclear Regulatory Commission Issuances*.

Documents available from the National Technical Information Service include NUREG series reports and technical reports prepared by other federal agencies and reports prepared by the Atomic Energy Commission, forerunner agency to the Nuclear Regulatory Commission.

Documents available from public and special technical libraries include all open literature items, such as books, journal and periodical articles, and transactions. *Federal Register* notices, federal and state legislation, and congressional reports can usually be obtained from these libraries.

Documents such as theses, dissertations, foreign reports and translations, and non-NRC conference proceedings are available for purchase from the organization sponsoring the publication cited.

Single copies of NRC draft reports are available free, to the extent of supply, upon written request to the Division of Information Support Services, Distribution Section, U.S. Nuclear Regulatory Commission, Washington, DC 20555.

Copies of industry codes and standards used in a substantive manner in the NRC regulatory process are maintained at the NRC Library, 7920 Norfolk Avenue, Bethesda, Maryland, and are available there for reference use by the public. Codes and standards are usually copyrighted and may be purchased from the originating organization or, if they are American National Standards, from the American National Standards Institute, 1430 Broadway, New York, NY 10018.

A Standard Problem for HECTR-MAAP Comparison: Incomplete Burning

Manuscript Completed: July 1988
Date Published: August 1988

Prepared by
C. C. Wong

Sandia National Laboratories
Albuquerque, NM 87185

Prepared for
Division of Systems Research
Office of Nuclear Regulatory Research
U.S. Nuclear Regulatory Commission
Washington, DC 20555
NRC FIN A1246

ABSTRACT

To assist in the resolution of differences between the NRC and IDCOR on the hydrogen combustion issue, a standard problem has been defined to compare the results of HECTR and MAAP analyses of hydrogen transport and combustion in a nuclear reactor containment. The first part of this standard problem, which addresses incomplete burning of hydrogen in the lower and upper compartments, has been completed. In this report, a critical review and comparison of the combustion models in HECTR and in MAAP will be presented, and HECTR analyses of this standard problem and its comparison with MAAP predictions will be discussed. Review of these two combustion models shows that HECTR and MAAP yield very different pictures of the burning process. MAAP calculations, which implicitly employ a 5% hydrogen ignition criterion, yield a burn time on the order of two hours, i.e., the burning process resembles a standing diffusion flame, rather than a flame propagating through a homogeneous mixture. Such predictions are not unreasonable for some accidents in ice-condenser plants. However, there are accident scenarios in which high concentrations of steam exist in the lower compartment (e.g., about 27% as in this standard problem). Ignition occurs at a higher concentration of hydrogen (about 7%). This will produce a propagating flame rather than a diffusion flame. Hence MAAP-calculated combustion pressures and temperatures appear to be much lower than one would expect. HECTR, on the other hand, predicts that ignition occurs at hydrogen concentration of 7% and the burning takes only a few seconds. This leads to a sharp, short but higher pressure increase.

CONTENTS

	<u>Page</u>
1. Introduction	1
2. Description of the HECTR-MAAP Standard Problem	4
3. Modeling Differences Between HECTR and MAAP	8
3.1 Description of the Combustion Model in HECTR	8
3.2 Description of the Combustion Model in MAAP	10
3.3 Case Study Comparing HECTR and MAAP Combustion Models	12
3.4 Summary of Modeling Differences	33
4. HECTR Results of the Standard Problem	35
4.1 Modeling of the Reactor Containment	35
4.2 HECTR Default Calculations	38
4.3 Modified HECTR Calculations to Match MAAP Results	43
4.4 Sensitivity Studies	46
4.5 Summary of Findings	52
5. Conclusion	54
6. References	55
Appendix A Computer Program TFLAME	A.1
Appendix B HECTR Input for the Standard Problem	B.1

LIST OF FIGURES

<u>Figure</u>	<u>Page</u>
1. Simplified Diagram of Ice-Condenser Containment	2
2. Hydrogen Release Rate from the Primary Reactor System into Containment Predicted by the MAAP Code	5
3. Steam Release Rate from the Primary Reactor System into Containment Predicted by the MAAP Code	6
4. Adiabatic Flame Temperature as a Function of Hydrogen Concentration	14
5. Burning Velocity as a Function of Hydrogen and Steam Concentrations	16
6. Flammability of Hydrogen:Air:Steam Mixture in a Quiescent Environment	17
7. Comparison of Combustion Completeness Between Measured Data and Predictions by the HECTR and MAAP Models for VGES Fans-off Experiments	19
8. Comparison of Combustion Completeness Between Measured Data and Predictions by the HECTR and MAAP Models for VGES Fans-on Experiments	20
9. Comparison of Combustion Completeness Between Measured Data and Predictions by the HECTR and MAAP Models for NTS Low-Steam Experiments	21
10. Comparison of Combustion Completeness Between Measured Data and Predictions by the HECTR and MAAP Models for NTS High-Steam Experiments	22
11. Comparison of Upward Flame Speed Between Measured Data and Predictions by the HECTR and MAAP Models for VGES Fans-off Experiments	24
12. Comparison of Upward Flame Speed Between Measured Data and Predictions by the HECTR and MAAP Models for VGES Fans-on Experiments	25
13. Comparison of Upward Flame Speed Between Measured Data and Predictions by the HECTR and MAAP Models for NTS Low-Steam Experiments	26
14. Comparison of Upward Flame Speed Between Measured Data and Predictions by the HECTR and MAAP Models for NTS High-Steam Experiments	27
15. Comparison of Burn Time Between Measured Data and Predictions by the HECTR and MAAP Models for VGES Fans-off Experiments	28
16. Comparison of Burn Time Between Measured Data and Predictions by the HECTR and MAAP Models for VGES Fans-on Experiments	29
17. Comparison of Burn Time Between Measured Data and Predictions by the HECTR and MAAP Models for NTS Low-Steam Experiments	30

LIST OF FIGURES
(continued)

<u>Figure</u>	<u>Page</u>
18. Comparison of Burn Time Between Measured Data and Predictions by the HECTR and MAAP Models for NTS High-Steam Experiments	31
19. Pressure and Temperature Responses in the Lower Compartment Predicted by HECTR Using the HECTR/MAAP 6-Compartment Model (Default Calculation)	40
20. Pressure and Temperature Responses in the Lower Compartment Predicted by HECTR Using the HECTR 6-Compartment Model (Default Calculation)	41
21. Pressure and Temperature Responses in the Lower Compartment Predicted by HECTR Using the HECTR 15-Compartment Model (Default Calculation)	42
22. Pressure and Temperature Responses in the Lower Compartment Predicted by HECTR Using the HECTR/MAAP 6-Compartment Model (MAAP Ignition Time, Burn Time, and Combustion Completeness)	45
23. Surface Temperature Responses of Steel Equipment (Top) and Concrete (Bottom) in the Lower Compartment Predicted by HECTR Using the HECTR/MAAP 6-Compartment Model (MAAP Ignition Time, Burn Time, and Combustion Completeness)	47
24. Total Heat Flux to the Surface of Steel Equipment (Top) and Concrete (Bottom) in the Lower Compartment Predicted by HECTR Using the HECTR/MAAP 6-Compartment Model (MAAP Ignition Time, Burn Time, and Combustion Completeness)	48
25. Surface Temperature Responses of Steel Equipment (Top) and Concrete (Bottom) in the Lower Compartment Predicted by HECTR Using the HECTR 15-Compartment Model (Default Calculation)	49
26. Total Heat Flux to the Surface of Steel Equipment (Top) and Concrete (Bottom) in the Lower Compartment Predicted by HECTR Using the HECTR 15-Compartment Model (Default Calculation)	50
27. Pressure and Temperature Responses in the Lower Compartment Predicted by HECTR Using the HECTR 15-Compartment Model (Ignition Criterion: 6% of H ₂)	51
28. Pressure and Temperature Responses in the Upper Plenum Predicted by HECTR Using the HECTR 15-Compartment Model (Ignition Criterion: 8% of H ₂)	53
29. Pressure and Temperature Responses in the Dome Predicted by HECTR Using the HECTR 15-Compartment Model (Combustion Occurred at 8% H ₂ Concentration in the Dome)	54

LIST OF FIGURES
(continued)

<u>Figure</u>	<u>Page</u>
30. Pressure Comparison Between HECTR and MAAP Predictions	55
31. Temperature Comparison Between HECTR and MAAP Predictions	57
32. Calculated Stability Boundaries for a 5 cm. Diameter Jet as a Function of Hydrogen and Steam Flow Rates	58

LIST OF TABLES

<u>Table</u>	<u>Page</u>
1. Modeling Differences between HECTR and MAAP	9
2. Default Ignition and Propagation Limits in HECTR (F is a factor based on the LaChatelier formula to account for carbon monoxide)	11
3. Parameters Used for Case Study of the MAAP Combustion Model	13
4. Summary of HECTR Analyses of the Standard Problem	36
5. Major Differences between HECTR and MAAP Input Data	37
6. Combustion Parameters Used in the Modified HECTR Calculations	44

ACKNOWLEDGMENTS

This work was supported by the U. S. Nuclear Regulatory Commission under the direction of Dr. Patricia Worthington. Her interest and concern about the hydrogen combustion issue led to the development of this standard problem. Many thanks to Bob Palla of NRC for numerous discussions related to this subject, and also to Marty Plys of Fauske and Associates for providing information about the combustion model in MAAP. The author also acknowledges Marshall Berman, Susan Dingman, and Douglas Stamps of Sandia National Laboratories for their review of and comments on this report.

EXECUTIVE SUMMARY

Sandia National Laboratories, with the support of the U. S. Nuclear Regulatory Commission, developed the HECTR code to analyze the transport and combustion of hydrogen during reactor accidents. IDCOR developed the MAAP code to perform similar analyses. Both of these codes are lumped-parameter codes, but they differ in the way that various phenomena are modeled, especially in the areas of (1) ignition criteria, (2) flame propagation criteria, (3) burn time, (4) combustion completeness, (5) continuous in-cavity oxidation of combustible gases from core-concrete interactions, and (6) natural circulation. In order to assist in the resolution of differences between the NRC and IDCOR on the hydrogen combustion issue, a standard problem has been defined to compare the results of HECTR and MAAP analyses of hydrogen transport and combustion in a nuclear reactor containment. This standard problem is an S2HF accident sequence in a PWR ice-condenser containment. The objective of this comparison is to determine the impact of the modeling differences for risk assessment.

There are two parts to this standard problem. The first part, which addresses the question of deflagration in the upper and lower compartments, will be presented in this report. The second part, which concentrates on the questions of natural circulation between the reactor cavity and lower compartment and continuous oxidation of combustible gases in the reactor cavity, will appear in a separate report.

For the first part of the standard problem - incomplete burning in the lower and upper compartments - a comprehensive review of the two combustion models has been performed, and it shows that HECTR and MAAP yield very different pictures of the burning process. In HECTR, the reaction rate and combustion completeness of the incomplete burning process is determined by two empirical correlations generated from the VGES and FITS experiments. On the other hand, MAAP predictions of the combustion process rely heavily on the force balance between the buoyancy force of the burnt gases and the drag force against the upward motion. When these two models are used to analyze the VGES, FITS, and NTS premixed hydrogen combustion experiments, HECTR predictions are better and compare reasonably well against the test data, while the model used in MAAP has difficulty predicting the combustion process accurately. It predicts that ignition always occurs at a low hydrogen concentration (about 5%) even though steam inerting would require higher hydrogen concentration or prevent any burning. No matter at what hydrogen concentration ignition occurs, the model in MAAP substantially overpredicts the burn time, which leads to much slower pressure and temperature rises.

When comparing HECTR and MAAP analyses of the standard problem, HECTR predicts that if ignition occurs at 7% hydrogen concentration, there will be three global deflagrations. A very sharp, but brief pressure peak will be associated with each burn. However MAAP predicts that ignition occurs at a lower hydrogen concentration (about 4.6%); this leads to a much more gradual increase in pressure and long burn time, which has the characteristics of a standing diffusion flame, rather than a flame propagating through a homogeneous mixture. Obviously HECTR-calculated combustion pressures and temperatures are much higher than MAAP predictions. HECTR has the capability to model the standing flame. However in this S2HF drain-close accident, the combustion process is likely to be a propagating flame rather than a standing flame because of the high steam-to-hydrogen mixture ratio at the break. Such a high ratio will make the standing flame very unstable or even extinguished.

In conclusion, the most important differences between HECTR and MAAP calculations involve the assessment of the threat to containment integrity. MAAP does not distinguish between the clearly separate processes of flame ignition and flame propagation - ignition is defined to occur immediately upon the achievement of a particular hydrogen concentration. For incomplete burns, MAAP calculations, which implicitly employ a 5% hydrogen ignition criterion, yield a burn time on the order of two hours and relatively low pressure increase, i.e., the burning process resembles a standing diffusion flame, rather than a flame propagating through a homogeneous mixture. Such predictions are not unreasonable for some accidents in ice-condenser plants. However, there are accident scenarios in which high steam concentration exists in the lower compartment (e.g., about 27% as in this standard problem) and ignition occurs at a higher concentration of hydrogen (about 7%). This will produce a sharp, short but very high pressure increase.

For global burns, as in the case of loss of offsite power accident, MAAP can never yield pressures in excess of that corresponding to 7.3% hydrogen in dry air because a "flame temperature criterion" is used instead of experimentally determined flammability limits and ignition thresholds. Since essentially all containments can survive combustion under these conditions, MAAP never predicts any threat. However, since ignition can be random due to loss of power, burns at concentrations much higher than 7.3% are possible. Furthermore in some accident scenarios, a plant may be steam inerted, which would prevent combustion after high concentrations of hydrogen have developed. When the steam condensed (by natural condensation or by spray initiation), deflagrations could take place at high hydrogen concentrations. MAAP does not account for the possibility of steam inerting.

1. INTRODUCTION

Sandia National Laboratories developed the HECTR (Hydrogen Event: Containment Transient Responses) code primarily to analyze the transport and combustion of hydrogen during reactor accidents [1, 2]. IDCOR (Industry Degraded Core Rulemaking Program) uses the MAAP (Modular Accident Analysis Program) code [3] to perform similar analyses. Both of these codes are lumped-parameter codes, but they differ in the way that various phenomena are modeled, especially in the areas of (1) ignition criteria, (2) flame propagation criteria, (3) burn time, (4) combustion completeness, (5) continuous in-cavity oxidation of combustible gases from core-concrete interactions, and (6) natural circulation. These differences will give different predictions of pressure and temperature loadings imposed on the containment and equipment by the accumulation and combustion of hydrogen during a severe accident. We are trying to determine the impact of these differences and to assist the NRC in determining the acceptability of the models for performing risk assessments.

The listed modeling differences are particularly pronounced in multicompartment systems such as the Ice-Condenser (IC) and Mark III containments. HECTR calculations tend to allow higher concentrations of hydrogen to develop, which leads to the prediction of higher containment pressures and temperatures. HECTR also permits flames to propagate into the IC upper plenum region, where potentially detonable mixtures can develop for some accident scenarios (e.g., TMLB'). Flame propagation into the IC upper compartment is also possible in the HECTR model, and the global burns, which ensue, generate much higher pressures than burns restricted to the lower compartment. MAAP code calculations generally do not predict these effects [4].

In order to assist in resolution of differences between the NRC and IDCOR on the hydrogen combustion issue, a standard problem has been defined to compare HECTR and MAAP analyses of hydrogen transport and combustion in a nuclear reactor containment. The important phenomena to be addressed include: (1) incomplete burning in the lower and upper compartments, (2) continuous in-cavity oxidation of combustible gases from core-concrete interactions, and (3) natural circulation between the reactor cavity and lower compartment. The problem selected is an S2HF accident sequence in a PWR ice-condenser containment (Figure 1). The selection of the S2HF accident sequence is for code comparison only.

In this report, the first part of the standard problem that addresses the phenomenon of incomplete burning in the upper and lower compartments of hydrogen generated by in-vessel metal-water reaction will be discussed. The other two phenomena

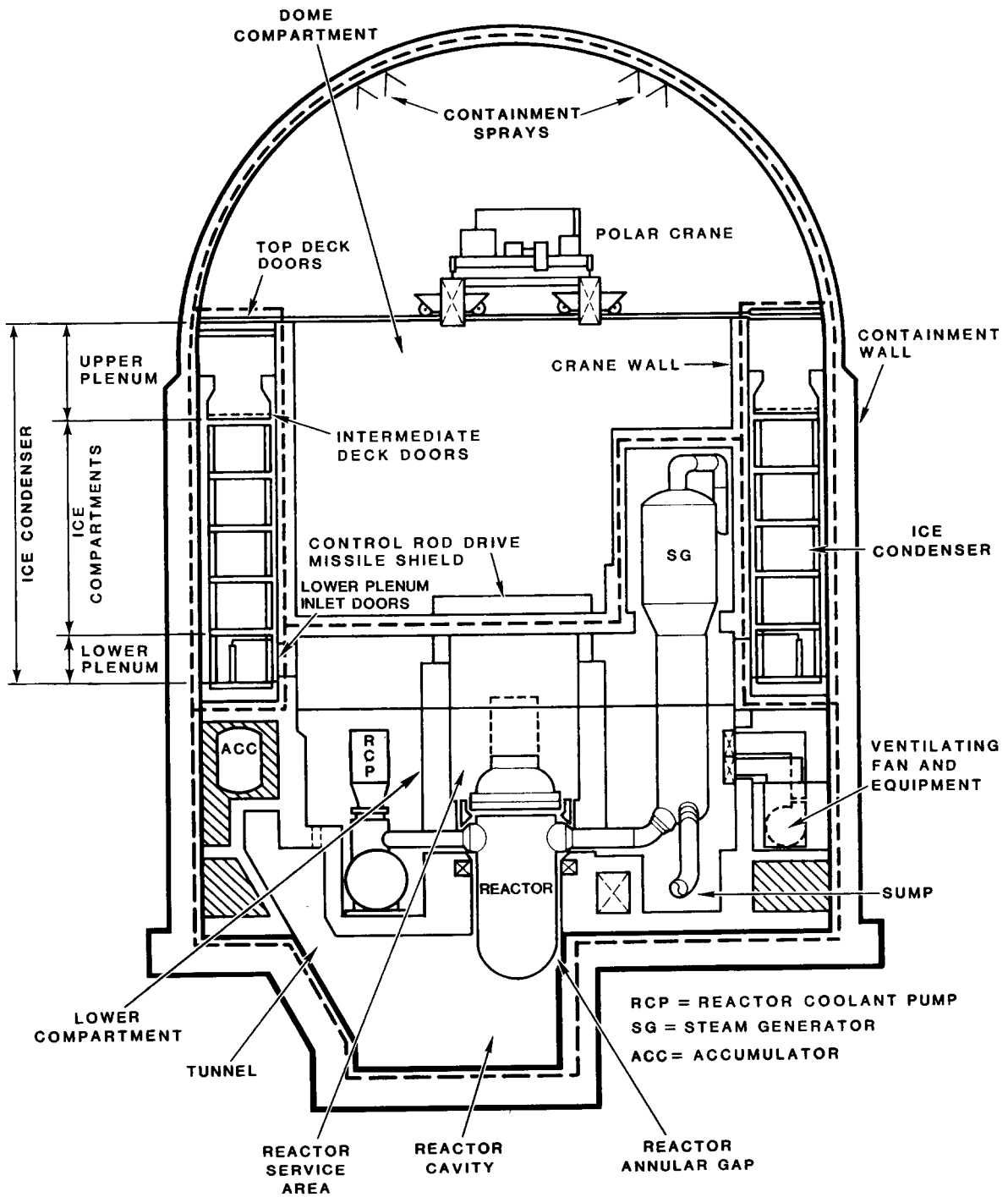


Figure 1. Simplified Diagram of Ice-Condenser Containment

(natural convection and continuous in-cavity oxidation), which are very important with respect to containment failure during a core-melt accident, will be addressed in a different report.

2. DESCRIPTION OF THE HECTR-MAAP STANDARD PROBLEM

The S2HF accident scenario involves a small break (0.5- to 2-inch in diameter) loss-of-coolant accident with failure of emergency coolant and containment-spray recirculation. All of the water inventory from the sprays, which are only operated in the injection mode, is trapped in the upper compartment due to the failure to remove upper-to-lower-compartment drain plugs. This failure causes the reactor cavity to remain dry throughout the transient. Incomplete hydrogen burns initiated by the deliberate ignition system are expected in the lower and upper compartments. When the reactor vessel fails, the molten fuel slumps onto the floor of the cavity and results in a core-concrete interaction. This interaction generates a substantial amount of combustible gases, which may oxidize continuously in the reactor cavity. The stability of this continuous in-cavity oxidation strongly depends on the amount of oxygen present in the reactor cavity and the concentrations of steam, CO₂, and other diluents. A complete in-cavity oxidation will prevent any accumulation of combustible gases in the lower and upper compartments and minimize the threat to containment integrity from combustion.

Because our main objective is to assess the importance of modeling differences of hydrogen transport and combustion in the HECTR and MAAP codes, the sources (either steam or any noncondensable gases) and initial conditions predicted by the MAAP code will be put into HECTR to study the containment response. Moreover, for better comparison of both computer codes, we redefined the standard problem into a two-part transient problem in October 1985 [5]. The first part of the transient problem will study hydrogen behavior during the period of in-vessel hydrogen production (from the metal-water reaction) and the second part will cover hydrogen behavior during the period of ex-vessel hydrogen production (from the core-concrete interaction). By setting up the standard problem this way, any discrepancies of the results between HECTR and MAAP in the first part of the problem will not affect the second part.

In the MAAP analysis of the S2HF accident in an ice-condenser containment [4], an average clad oxidation of 30% was calculated. This corresponds to 248 kg (547 lb) of hydrogen being generated. The hydrogen and steam release rates predicted by the MAAP code for the S2HF accident sequence are plotted in Figures 2 and 3. Comparing these sources to those given in the MARCH-HECTR analyses of an ice-condenser containment for the S2D, S1D, and S1HF accident scenarios [6] shows that MAAP predictions of the hydrogen and steam release rates are very different. MAAP predicts a lesser amount of steam being released and estimates a lower release rate of both sources into the reactor containment compared to MARCH. It is very important to accurately predict

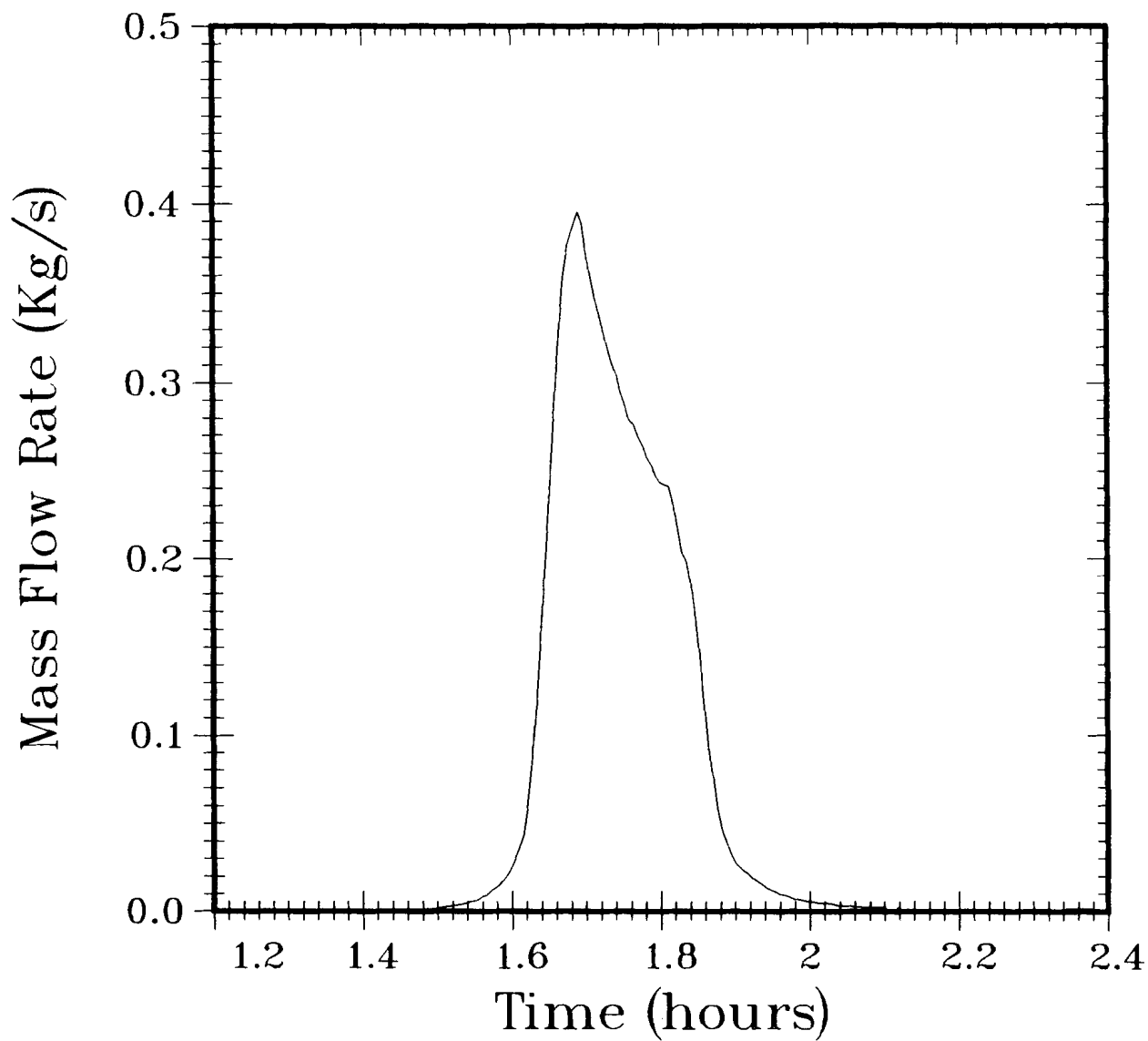


Figure 2. Hydrogen Release Rate from the Primary Reactor System into Containment Predicted by the MAAP Code

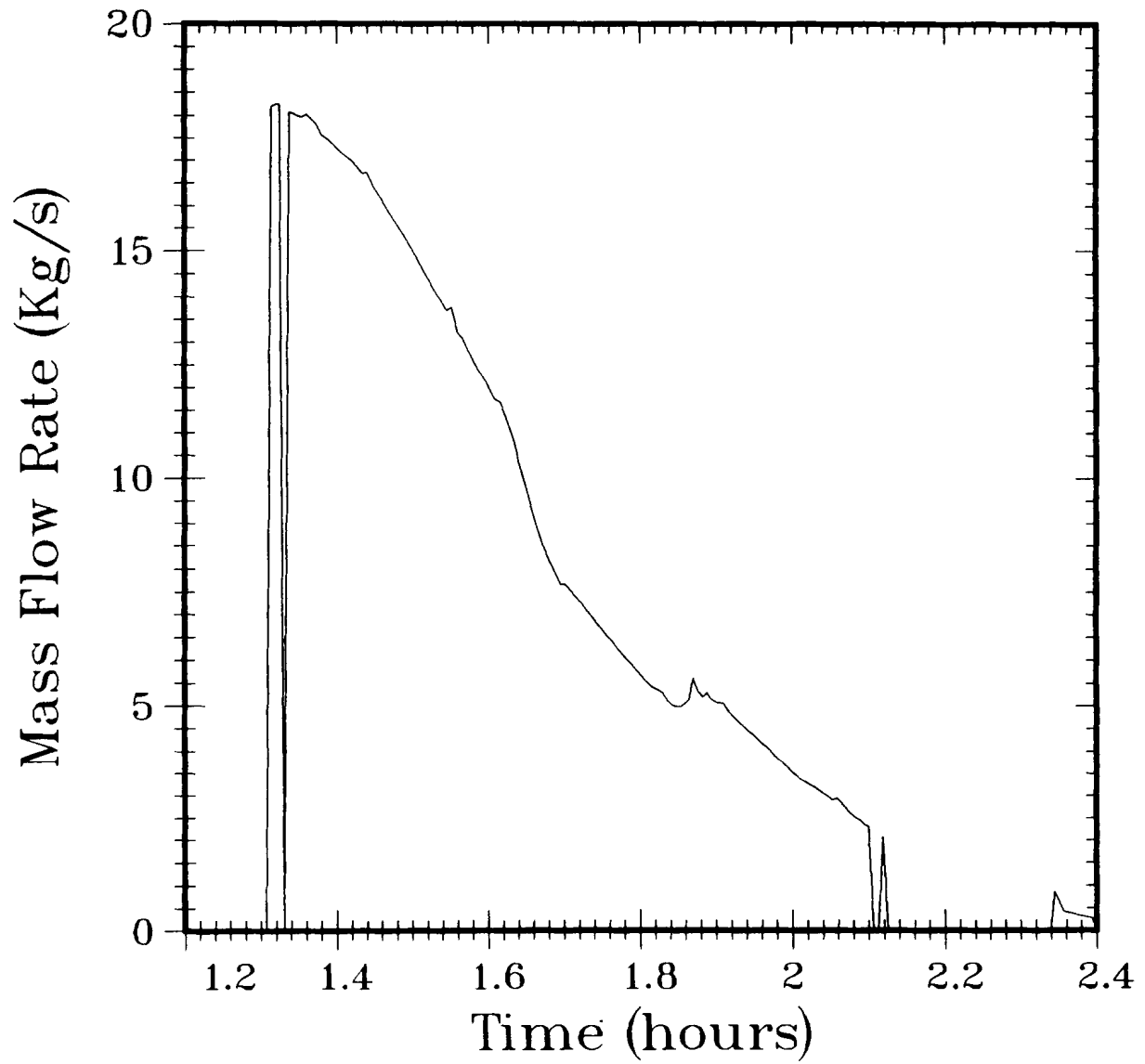


Figure 3. Steam Release Rate from the Primary Reactor System into Containment Predicted by the MAAP Code

the amount of gases generated and their release rate when performing an integrated containment analysis.

Since HECTR is using the sources and initial conditions generated by the MAAP code, the following HECTR results do not represent our best estimate of the pressure and temperature responses of an ice-condenser containment during an S2HF accident. These HECTR analyses are only designed to better understand differences in the combustion model between two computer codes.

3. MODELING DIFFERENCES BETWEEN HECTR AND MAAP

Before presenting HECTR analyses of the first part of the standard problem, a review of the combustion models in HECTR and in MAAP will be useful. Since most key parameters in combustion modeling, such as ignition criteria, combustion completeness, burn time, and propagation criteria, are expressed either as an algebraic formula (as in HECTR) or as an analytical expression (as in MAAP), it is not necessary to perform a large amount of HECTR or MAAP calculations in order to compare the combustion models in both codes. By comparing these key combustion parameters, based on the predictions made by both algebraic and analytical formulas, with the measured data obtained from experiments, a better understanding of differences between the combustion models in both codes can be achieved. This approach works well when addressing the modeling of incomplete burning in the lower and upper compartments.

Besides comparing these two models in term of those key combustion parameters listed above, it is still necessary to perform and compare HECTR and MAAP calculations to understand the impact of modeling differences on the containment responses (pressure and temperature rises) for a selected severe accident involving hydrogen combustion. Theoretically, both codes are not chartered to model the complex combustion phenomenon in detail such as multistep chemical kinetics or flame acceleration induced by turbulent effect, but rather to predict the global containment responses with respect to hydrogen combustion for a nuclear reactor safety study. Hence at least one HECTR and one MAAP calculation for the comparison of containment responses are needed.

In the following sections, the combustion models in both HECTR and MAAP are reviewed first. Next, predictions made by both models are compared with the experimental results in terms of the key parameters used in combustion modeling. Table 1 lists major differences of the combustion model between these two codes.

3.1 Description of the Combustion Model in HECTR

Most combustion parameters in HECTR are determined primarily by experimental correlations or are specified by the user. Such a procedure allows the accident analyst the option to perform parametric or conservative calculations, and to address phenomena which may be highly stochastic. For example, in the absence of deliberate ignition systems, the timing and location of ignition can be random. Concentrations of hydrogen in air ranging from 4% to 74% are flammable. Flammability limits for mixtures of hydrogen, oxygen, nitrogen, carbon monoxide and

Table 1. Modeling Differences between HECTR and MAAP.

	HECTR	MAAP
<u>Combustion Model</u>		
Ignition Criterion	Depends on mixture concentration (user input; can be varied parametrically).	For global burn, uses flame speed criterion. For incomplete burn, checks if calculated burning velocity is greater than 1 cm/s.
Combustion Completeness	Calculates based on an empirical formula (a function of H ₂ concentration).	Predicts a complete burn if flame temperature criterion is satisfied. For incomplete burn, uses an analytical formula (function of burning velocity, drag coeff., igniter location).
Burn Time	Characteristic length divided by flame speed.	Regional radius divided by burning velocity for global burn. For incomplete burn, uses an analytical formula (function of burning velocity, drag coef., and density)
Flame Propagation	Upward, downward, horizontal propagations depend on H ₂ concentration	Upward propagation

dioxide, and steam have been determined empirically and are employed in HECTR. However, any "flammable" concentration can exist stably without burning in a containment until an adequate ignition source is provided. In the TMI accident, ignition occurred accidentally when the concentration reached about 8% [7]. In a TMLB' accident, ignition may not occur until power is restored.

HECTR does not model the details of a propagating flame front moving through a compartment; rather, it calculates the rate at which the chemical reaction takes place. The duration of a burn and the final mole fractions of combustible gases and oxygen are calculated at the start of a burn. Burn time is calculated as the ratio of a user-specified characteristic length to an experimentally determined flame speed [8]. Final mole fractions depend on the combustion completeness correlation. Once a flame has been ignited and after a delay equal to a specified fraction of the burnout time, it will propagate upwards, sideways, or downwards if the concentrations in the neighboring compartments are greater than or equal to 4%, 6%, or 9% respectively (Table 2); these propagation concentrations have been determined experimentally [9].

3.2 Description of the Combustion Model in MAAP

MAAP distinguishes between two types of burns, "global" and "incomplete." The "global burn" is the analog of the HECTR deflagration model. A "flame temperature criterion" is used to control these burns. An adiabatic, isobaric flame temperature of 983 K is defined as a critical threshold for both ignition and propagation. This flame temperature corresponds to a burn involving a hydrogen concentration in dry air of about 7.3%. For global burns, combustion is always 100% complete. Burn time is determined by dividing a characteristic length by the flame speed. Flame speed is given by the density ratio of unburned to burned gases times the laminar burning velocity [10].

For plants equipped with deliberate ignition systems, the "incomplete burning" model is employed if the igniters are assumed to be operating. A characteristic volume is assigned to each igniter; ignition is assumed to take place at the bottom and propagate up. The duration of the burn, and the fraction of combustible gases burned are determined by analytical expressions. The flame will ignite and propagate upwards if the calculated flame speed exceeds 1 cm/s, corresponding to a hydrogen concentration in dry air of about 4.8%, or 5.5% for a mixture containing about 55% steam. Propagation in directions other than upwards is not allowed.

Table 2. Default Ignition and Propagation Limits in HECTR (F is a factor based on the LaChatelier formula to account for carbon monoxide)

Parameter	Mole Fraction			
	Combustible Gas F	($H_2 + F \cdot CO$)	O_2	Diluents ($H_2O + CO_2$)
Ignition Limits	0.541	≥ 0.07	≥ 0.05	≤ 0.55
Upward Propagation	0.328	≥ 0.041	≥ 0.05	≤ 0.55
Horizontal Propagation	0.435	≥ 0.06	≥ 0.05	≤ 0.55
Downward Propagation	0.600	≥ 0.09	≥ 0.05	≤ 0.55

Neither the "global" nor the "incomplete" burning models in MAAP recognize the well-known phenomenon of steam inerting. Burning is calculated to occur regardless of steam concentration.

3.3 Case Study Comparing HECTR and MAAP Combustion Models

Important combustion parameters, such as ignition criteria, combustion completeness, burn time, and propagation criteria predicted by algebraic formulas as in HECTR and by analytical expression as in MAAP, are compared with existing experimental data. The calculated results that are presented in this section are not generated from HECTR and MAAP. They are the results of simple calculations based upon the combustion models in HECTR and MAAP (Appendix A). This is the best approach to compare both combustion models without performing a substantial number of HECTR and MAAP calculations.

The experiments that are used in this comparison are the VGES [11] and NTS [12] experiments. The required input data for both models are listed in Table 3. A burning velocity multiplier of 1.0 and drag coefficient of 100.0 are used in this comparison because these are the values used in containment analyses in Reference 4.

3.3.1 Ignition Criteria

The ignition criteria in both HECTR and MAAP codes depend heavily on the mixture chemistry. Neither combustion model considers the availability of ignition sources or activation energy required to initiate combustion. For example, air motion driven by sprays may substantially cool the igniters, degrade their performance, and prevent any ignition; neither model accounts for this effect. In HECTR and in MAAP, as long as the built-in ignition criteria are satisfied, combustion will occur. The default ignition criteria in HECTR are: $H_2 \geq 7\%$, $O_2 \geq 5\%$, and steam $\leq 55\%$. The user can vary the criteria by changing the value of the mixture concentration and perform parametric studies.

In MAAP, the flame temperature criterion is used to determine the potential of a global burn; the critical temperature is set at 983 K. Figure 4 illustrates the calculated adiabatic flame temperature as a function of hydrogen concentration for the VGES fans-off experiments. Applying the flame temperature criterion, it predicts that a global burn will occur at a hydrogen concentration of 7.3%. In MAAP, the specific heat at constant pressure is used to calculate the adiabatic flame temperature. However the specific heat used in this calculation does not consider the effect of temperature. In reality, the specific heat is temperature-dependent. In Figure

Table 3. Parameters Used for Case Study of the MAAP
Combustion Model

(1) VGES Fans-Off and Fans-On Cases

Burning Velocity Multiplier	=	1.0
Drag Coefficient	=	100.0
Characteristic Length	=	3.680 m
Height of the Vessel	=	4.267 m
Radius of the Vessel	=	0.610 m

(2) NTS Fans and Sprays Off Cases

Burning Velocity Multiplier	=	1.0
Drag Coefficient	=	100.0
Characteristic Length	=	14.02 m
Use Cylindrical Geometry		
Height of the Vessel	=	15.85 m
Radius of the Vessel	=	6.471 m

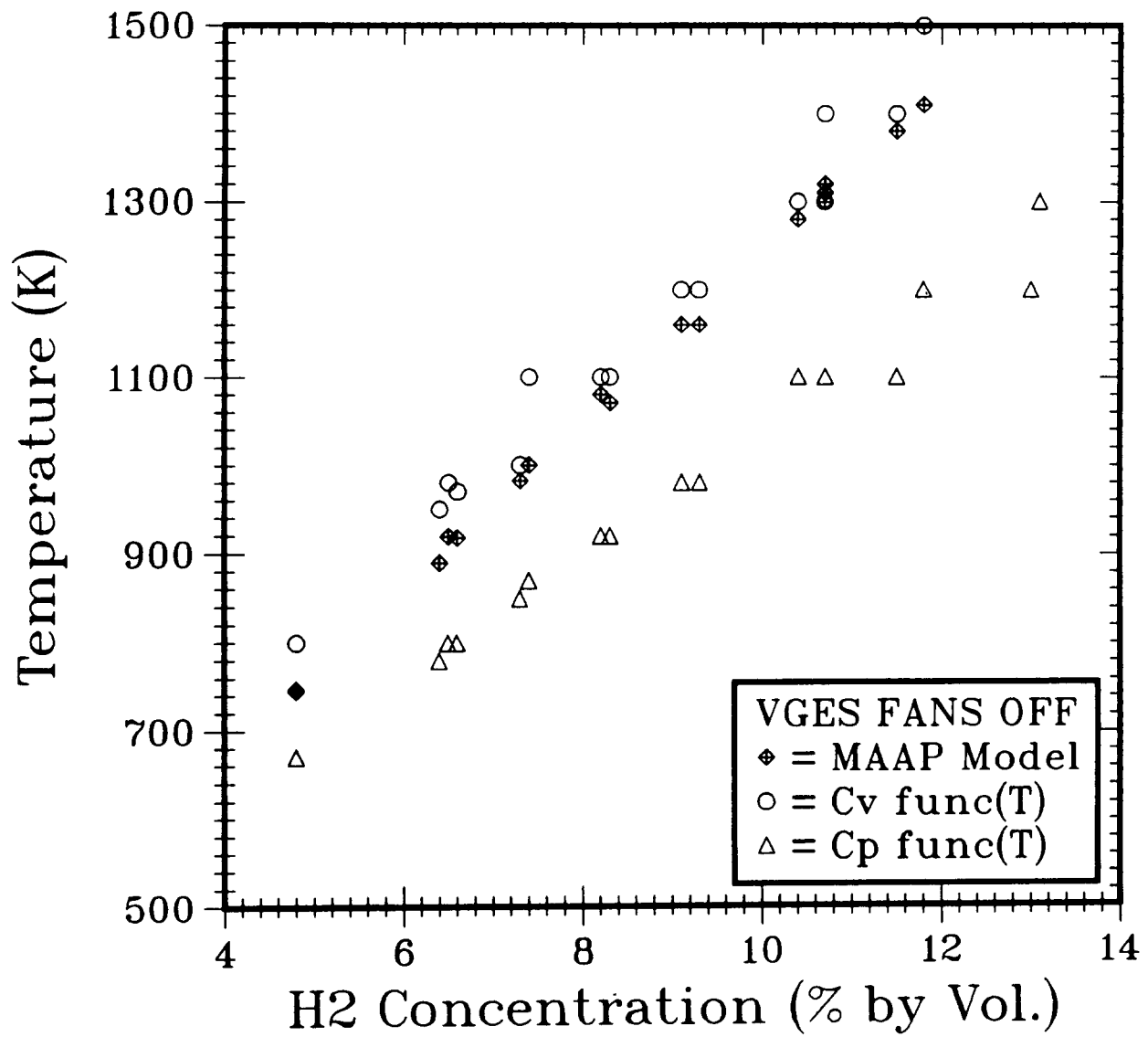


Figure 4. Adiabatic Flame Temperature as a Function of Hydrogen Concentration

4, two more curves are also included to show how the flame temperature criterion will change if the specific heat at constant volume and specific heat at constant pressure are calculated accounting for the actual temperature dependence [13]. If a temperature-dependent specific heat at constant pressure is used, it predicts that a global burn will occur at hydrogen concentration of 8.7%; this is quite similar to the findings in Reference 14.

To determine whether an incomplete burn will take place, MAAP will check (1) if the calculated burning velocity is greater than 1 cm/s, and (2) if igniters are functioning. This 1 cm/s burning velocity condition implies that an incomplete burn occurs at a hydrogen concentration of about 4.8 to 5.0%, depending upon the steam mole fraction (Figure 5). Here, as shown in Figure 5, the steam inerting effect on initiation of an incomplete burn is rather small. Hydrogen will still combust at a concentration of 5.5% even though there is substantial amount of steam in an environment ($> 55\%$ steam). However experiments which studied flammability of hydrogen-air-steam mixtures [15, 16, 17] have shown that combustion will be precluded if the steam mole fraction is greater than 55% or at even lower steam concentrations if the hydrogen concentration is 4-6%.

In Figure 6, the ignition criteria used in HECTR and in MAAP for both global and incomplete burns are compiled and plotted against data obtained from FITS combustion experiments [15] to study flammability of hydrogen-air-steam mixtures in a quiescent environment. The ignition criteria in HECTR will prevent any combustion if steam concentration is too high ($> 55\%$); on the contrary, the MAAP criteria do not consider any steam inerting effect. Neglecting the steam inerting effect may give a very different result when analyzing containment responses during a severe nuclear reactor accident. For example, in Reference 6, during a S_2D accident with 75% zirconium-water reaction, HECTR predicted that a substantial amount of steam had already built up in the lower compartment of an ice-condenser containment when the hydrogen was released. Even though igniters were working, combustion in the lower compartment did not occur because of the steam inerting environment. Eventually, combustion took place in the dome and generated a peak pressure of 343 kPa (50 psia). If combustion were allowed in the lower compartment, neglecting the steam inerting effect, an earlier and more moderate burn leading to a much lower peak pressure (less than 200 kPa or 28 psia) would be predicted.

A newly generated flammability correlation [15] based on the FITS experiments is also plotted in Figure 6. This correlation is better than the existing criteria used in HECTR and in MAAP to account for the steam inerting effect. Incorporation of this flammability correlation is recommended for any code to perform containment analysis.

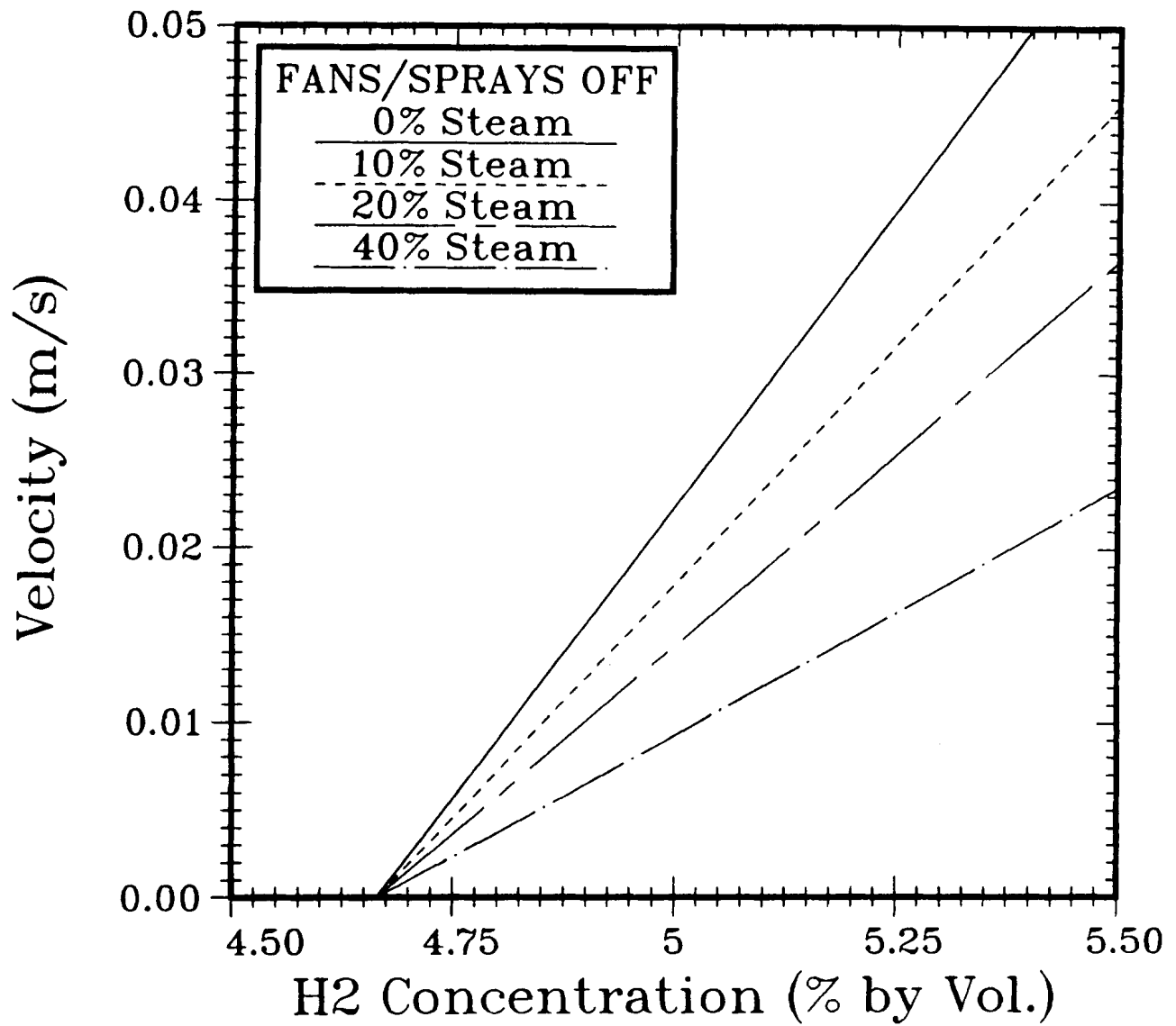


Figure 5. Burning Velocity as a Function of Hydrogen and Steam Concentrations

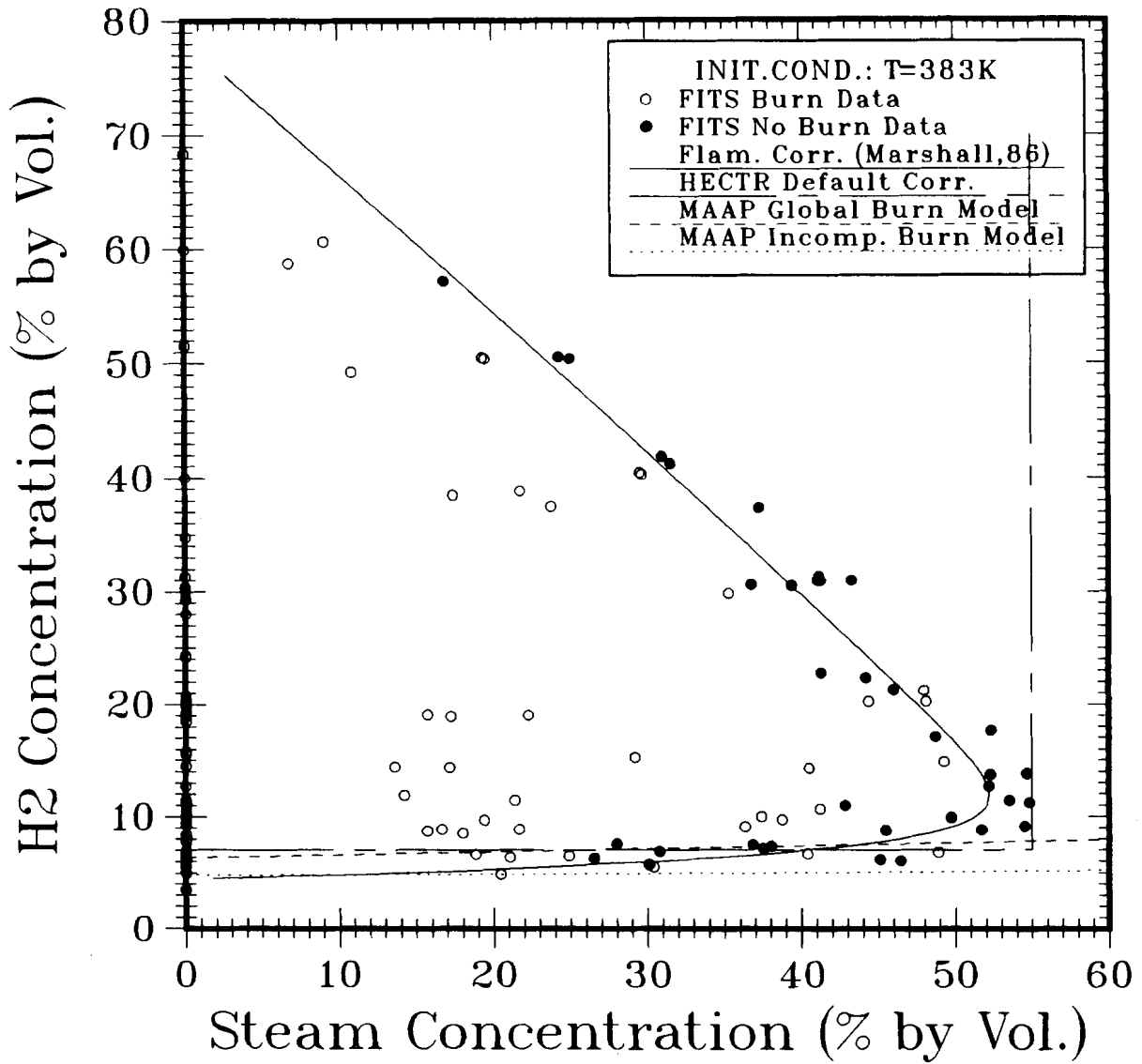


Figure 6. Flammability of Hydrogen:Air:Steam Mixture in a Quiescent Environment [15]

3.3.2 Combustion Completeness

At the beginning of a burn, HECTR will determine the amount of hydrogen left when combustion is complete, based upon an empirical formula that depends on the pre-burn hydrogen concentration. The influence of steam concentration and vessel geometry on combustion completeness is minimal. The results of VGES and NTS experiments (Figures 7 to 10) show that the measured combustion completeness data can be correlated in this way. Combustion completeness of 100% occurs at a hydrogen concentration of about 8%, while minimum burn (less than 1%) occurs at a hydrogen concentration of about 3.7%. The HECTR predictions of combustion completeness for VGES and NTS experiments using this empirical formula are shown in Figures 7 to 10.

Unlike HECTR, MAAP relies on the flame temperature criterion to determine whether a burn in a compartment is complete or incomplete. The default critical flame temperature is 983 K. For an incomplete burn, the burnt volume of the mixture is calculated by an analytical expression, which depends upon burning velocity, drag coefficient, ignition location, and regional radius of the characteristic cylindrical volume [3].

Based upon this analytical expression, I first calculated the burned volume, then divided by the total volume of the vessel to obtain the combustion completeness for VGES, NTS experiments (Figures 7 to 10). Since the combustion chamber in NTS experiments was spherical rather than cylindrical, as suggested in Reference 3, analyses were performed by transforming the spherical vessel into an equivalent cylindrical geometry with an equal height and an equal volume.

Overall, both the empirical formulas (as in HECTR) and analytical expression (as in MAAP) predict the region of complete burn reasonably well. For an incomplete burn, the analytical expression generally underpredicts the combustion completeness, except in VGES fans-on and fans-off experiments when hydrogen concentration is about 5% to 7%. Figures 7 to 10 show that it overpredicts the completeness if the propagating flame front hits the wall before reaching the top of the vessel; otherwise, it underpredicts the completeness. In VGES experiments, where the vessel is smaller, the burning radius will intersect the wall before the flame reaches the top. Thus, the analytical expression overpredicts the combustion completeness. However, for a very lean hydrogen combustion case (less than 5%), the burning velocity is so small that the flame hits the top of the vessel before it reaches the wall. It underpredicts the combustion completeness. Similarly, in NTS experiments, where the vessel is bigger and the region radius of the characteristic cylindrical volume is larger, the flame never hits the side wall

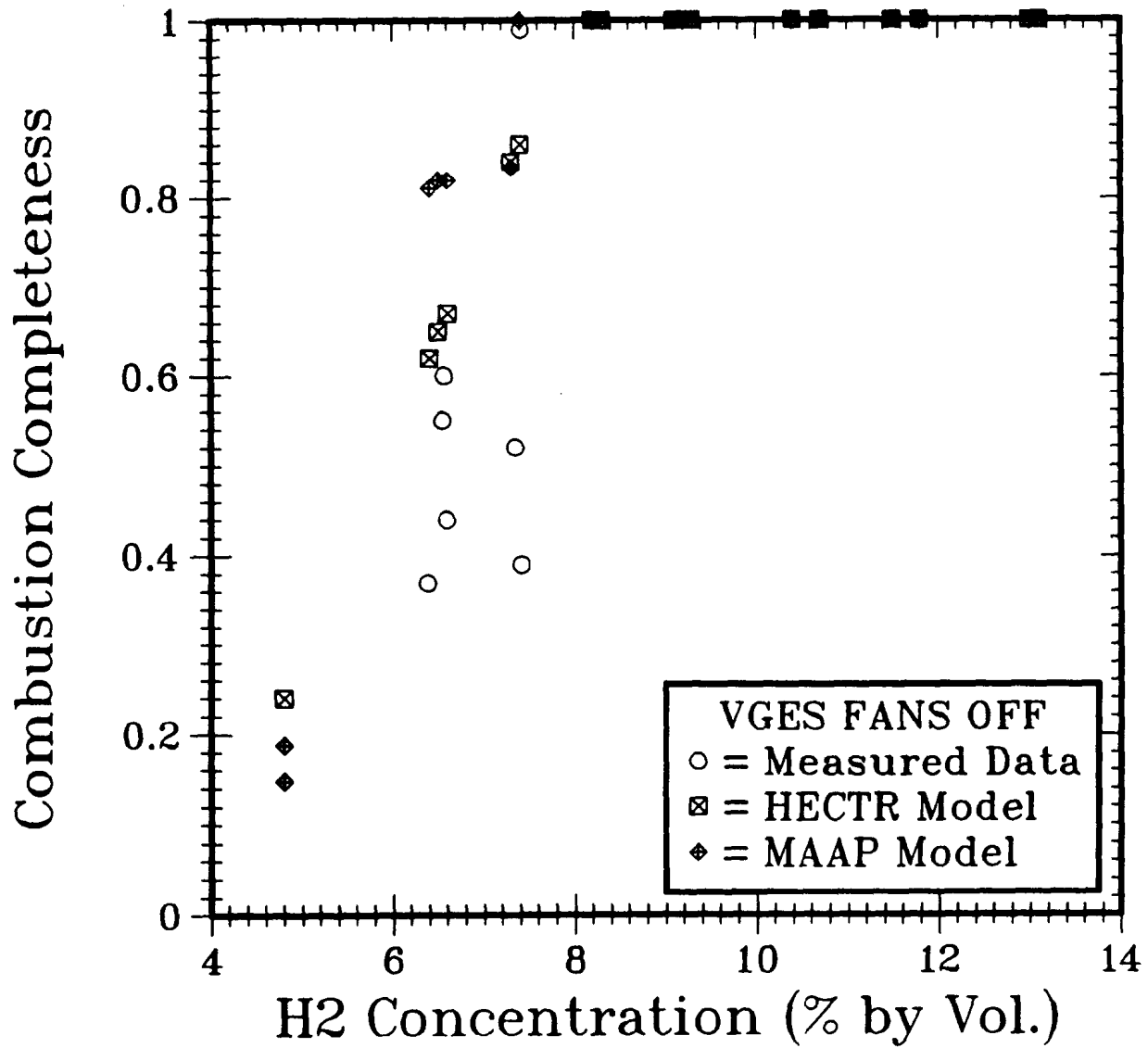


Figure 7. Comparison of Combustion Completeness Between Measured Data and Predictions by the HECTR and MAAP Models for VGES Fans-off Experiments

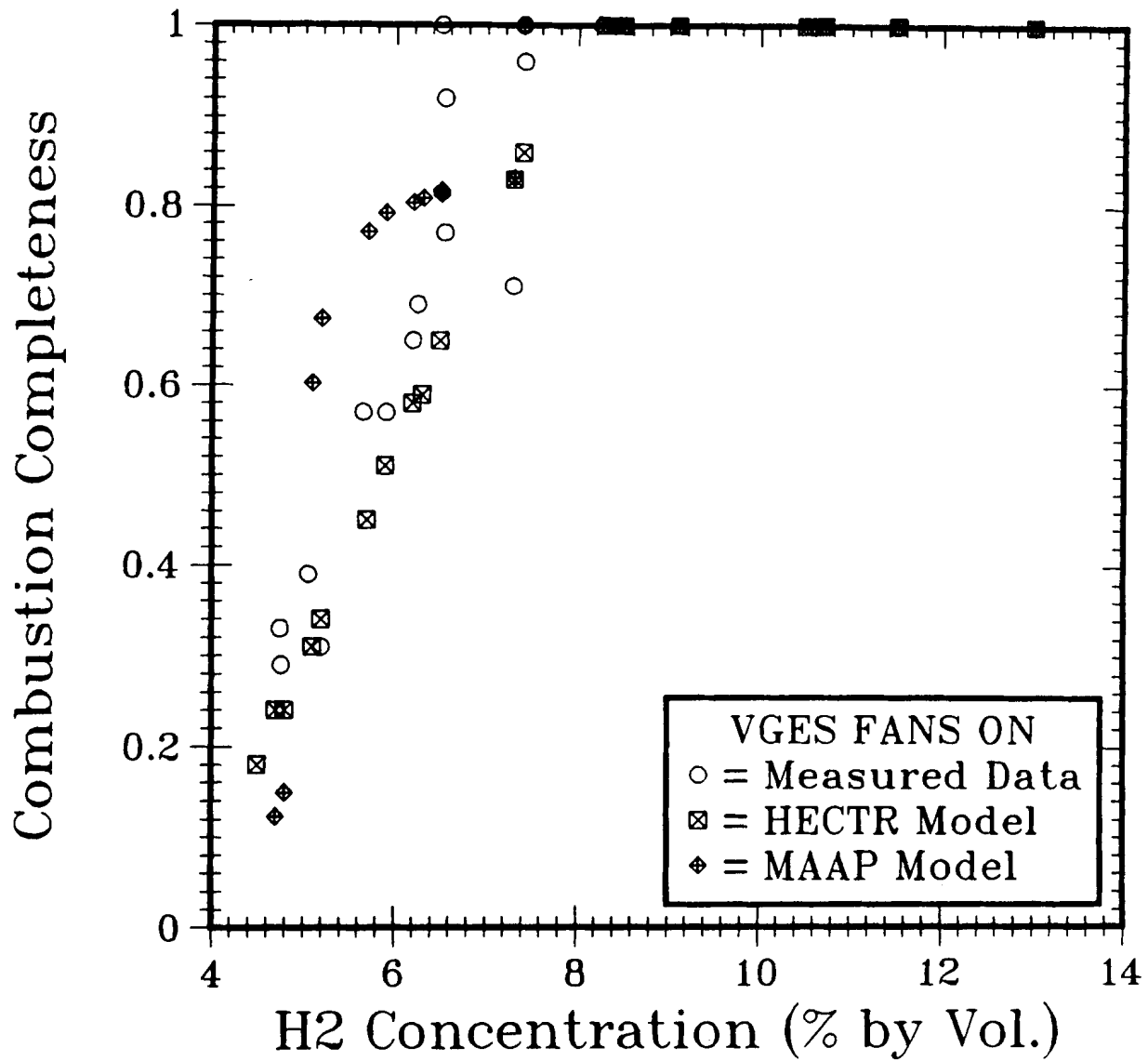


Figure 8. Comparison of Combustion Completeness Between Measured Data and Predictions by the HECTR and MAAP Models for VGES Fans-on Experiments

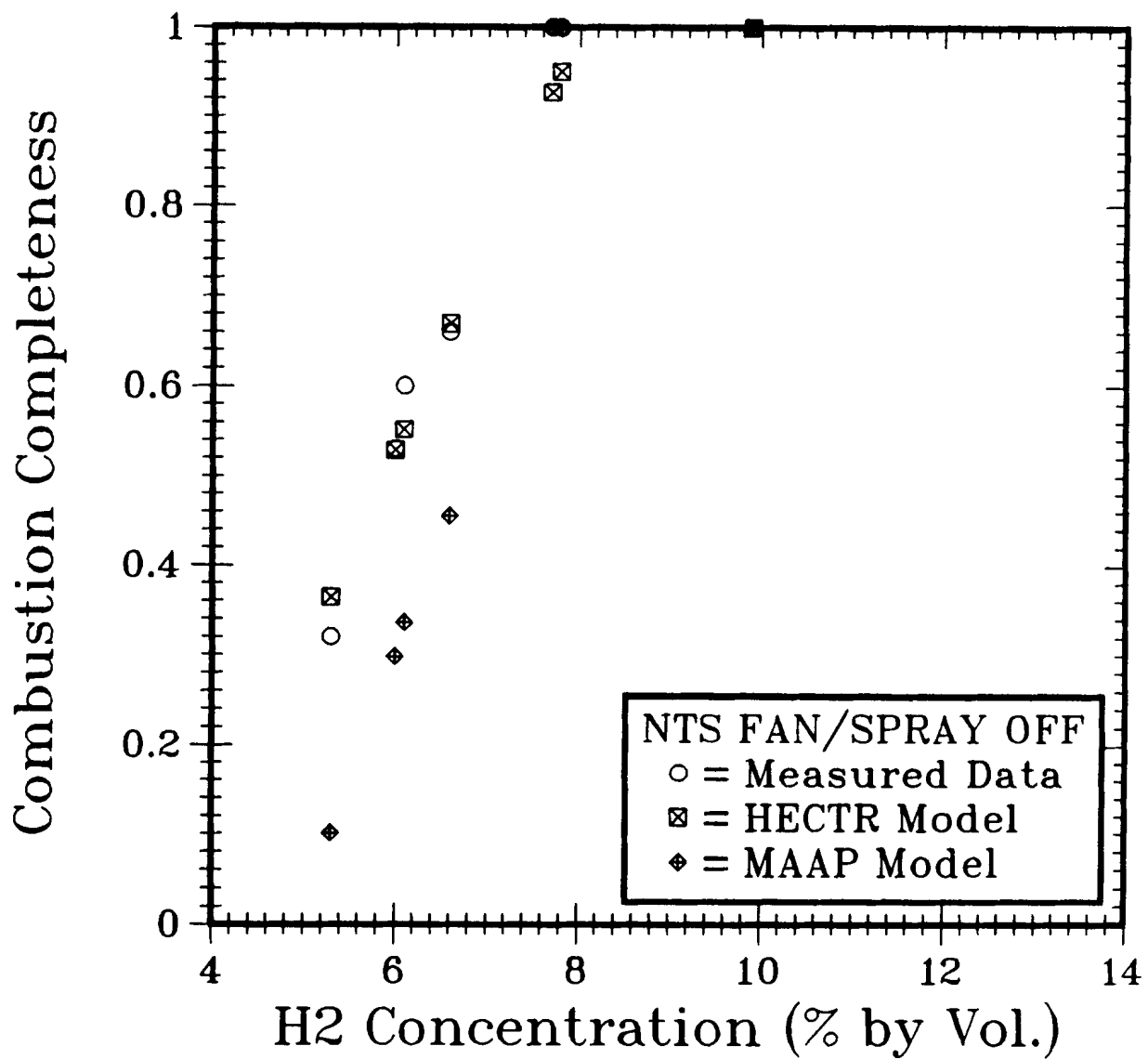


Figure 9. Comparison of Combustion Completeness Between Measured Data and Predictions by the HECTR and MAAP Models for NTS Low-Steam Experiments

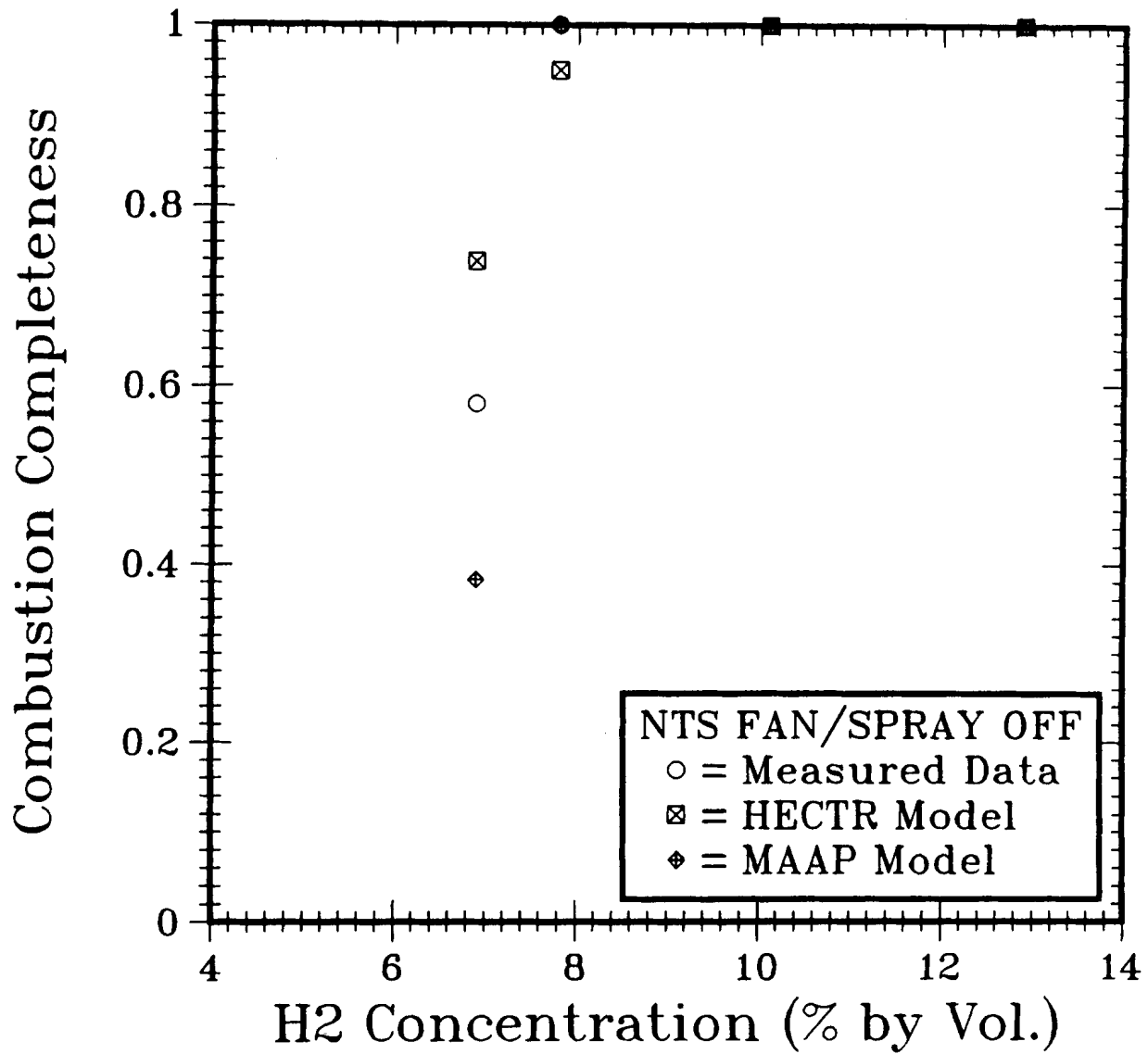


Figure 10. Comparison of Combustion Completeness Between Measured Data and Predictions by the HECTR and MAAP Models for NTS High-Steam Experiments

as it is propagating upward to the top. Hence, it underpredicts the completeness. Readjusting the values of drag coefficient and burning velocity multiplier may improve the prediction by the incomplete burn model. However, resetting these values for every containment analysis would be difficult, if not impractical.

3.3.3 Flame Speed and Burn Time

As discussed in Section 2.1, HECTR uses an "effective" flame speed to calculate the burn time, which in turn determines the burn rate at every time step. Flame speed is defined as the velocity of the propagating flame front in the laboratory frame. The default flame speed correlation is a function of hydrogen and steam concentrations. The burn time is calculated as a user-specified burn characteristic length divided by the flame speed.

The model in MAAP relies upon the burning velocity to estimate the burn time. Burning velocity is defined as the velocity of the propagating flame front relative to the gas motion downstream from the flame front. For a global burn, burn time is predicted by dividing the regional radius of a characteristic cylindrical volume by the flame velocity. Burn time for an incomplete burn is expressed as a function of burning velocity, drag coefficient, mixture density, and a characteristic length.

In order to compare the calculated flame speed with the existing experimental data (VGES and NTS) for lean hydrogen combustion (less than 15% H_2 concentration), I used the burn time calculated by the MAAP model to generate the "effective" flame speed for these experiments. (The "effective" flame speed can be obtained by dividing the characteristic length by the burn time. Burn time is the duration of time between ignition and extinction. Pressure-rise time is the duration of time between ignition and the compartment pressure at its maximum value. Pressure-rise time is not necessarily equal to the burn time because pressure may start to fall before the flame will be extinguish if there is more heat lost to environment than heat generated from chemical reaction.) The results of the flame speed comparison can be found in Figures 11 to 14, and the results of the burn time comparison are shown in Figures 15 to 18. Since our interest is the burn time, not the pressure-rise time, its values can easily be calculated by either an empirical formula (as in HECTR) or an analytical expression (as in MAAP).

Because the default flame speed correlation in HECTR is based upon the VGES fans-on experiments, HECTR overpredicts the flame speed when compared to the observed values in the VGES fans-off and NTS fans/sprays-off experiments. Obviously, a prediction of a larger flame speed will result in a shorter burn time and a smaller flame speed will lead to a longer burn time

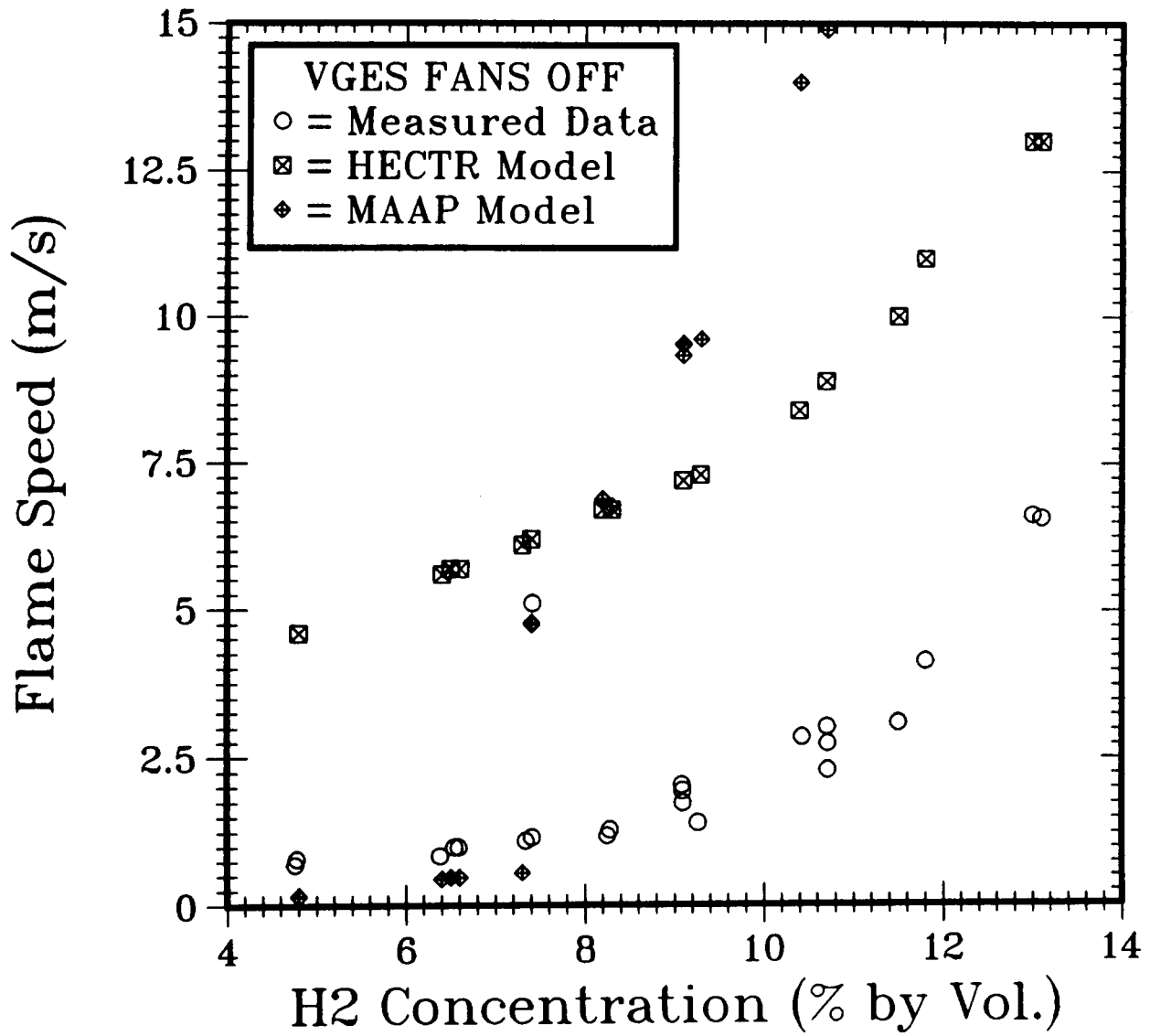


Figure 11. Comparison of Upward Flame Speed Between Measured Data and Predictions by the HECTR and MAAP Models for VGES Fans-off Experiments

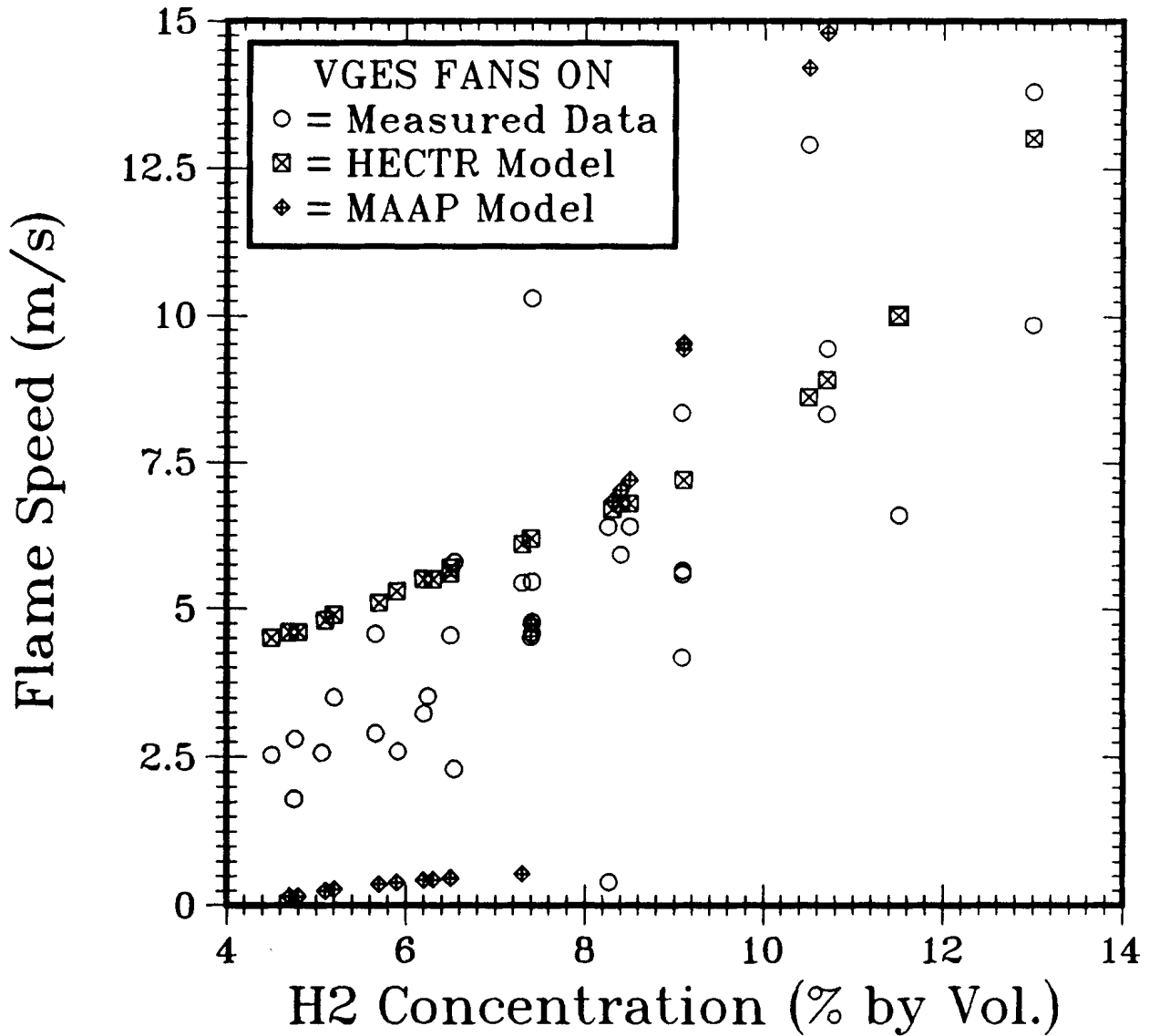


Figure 12. Comparison of Upward Flame Speed Between Measured Data and Predictions by the HECTR and MAAP Models for VGES Fans-on Experiments

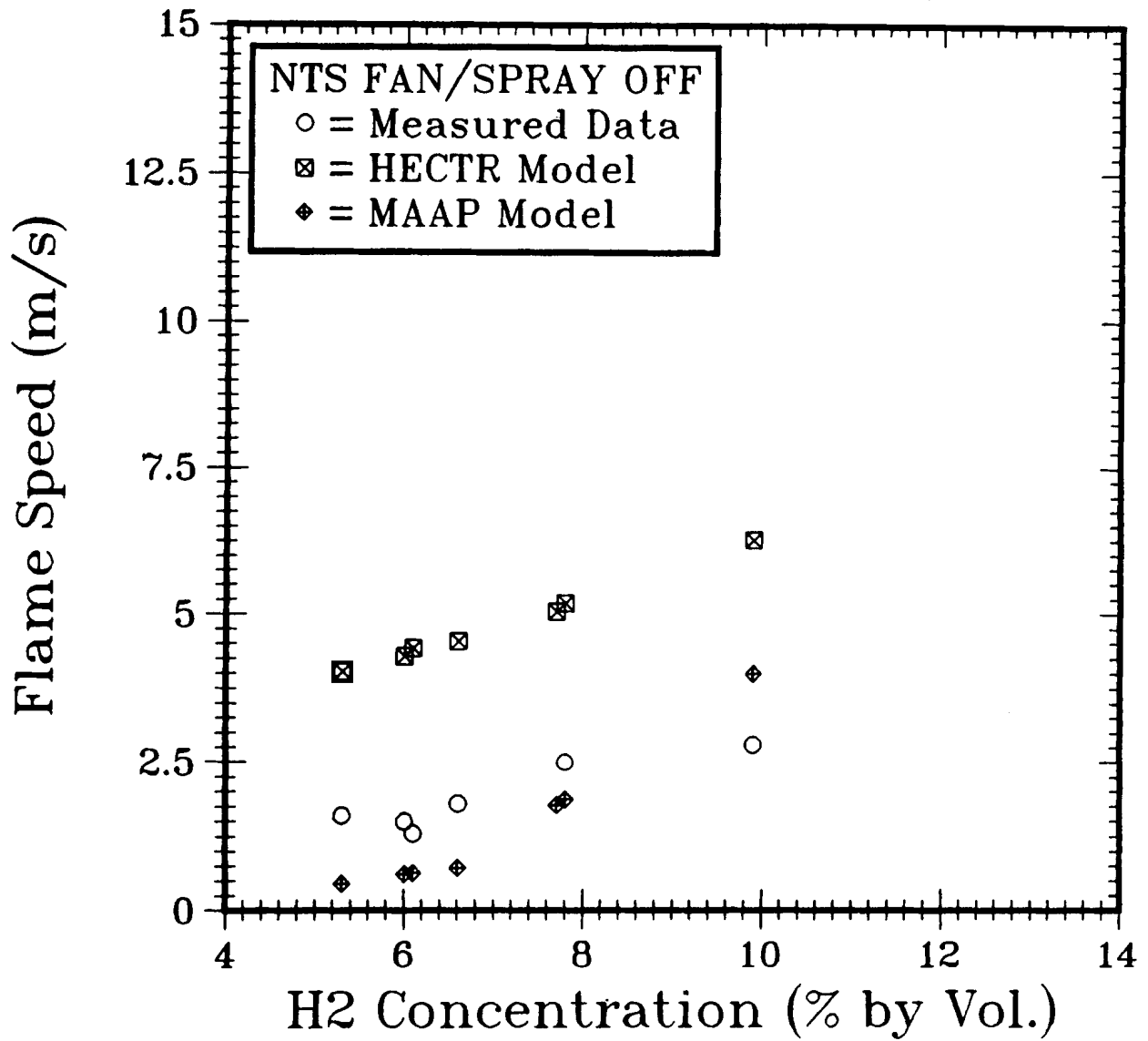


Figure 13. Comparison of Upward Flame Speed Between Measured Data and Predictions by the HECTR and MAAP Models for NTS Low-Steam Experiments

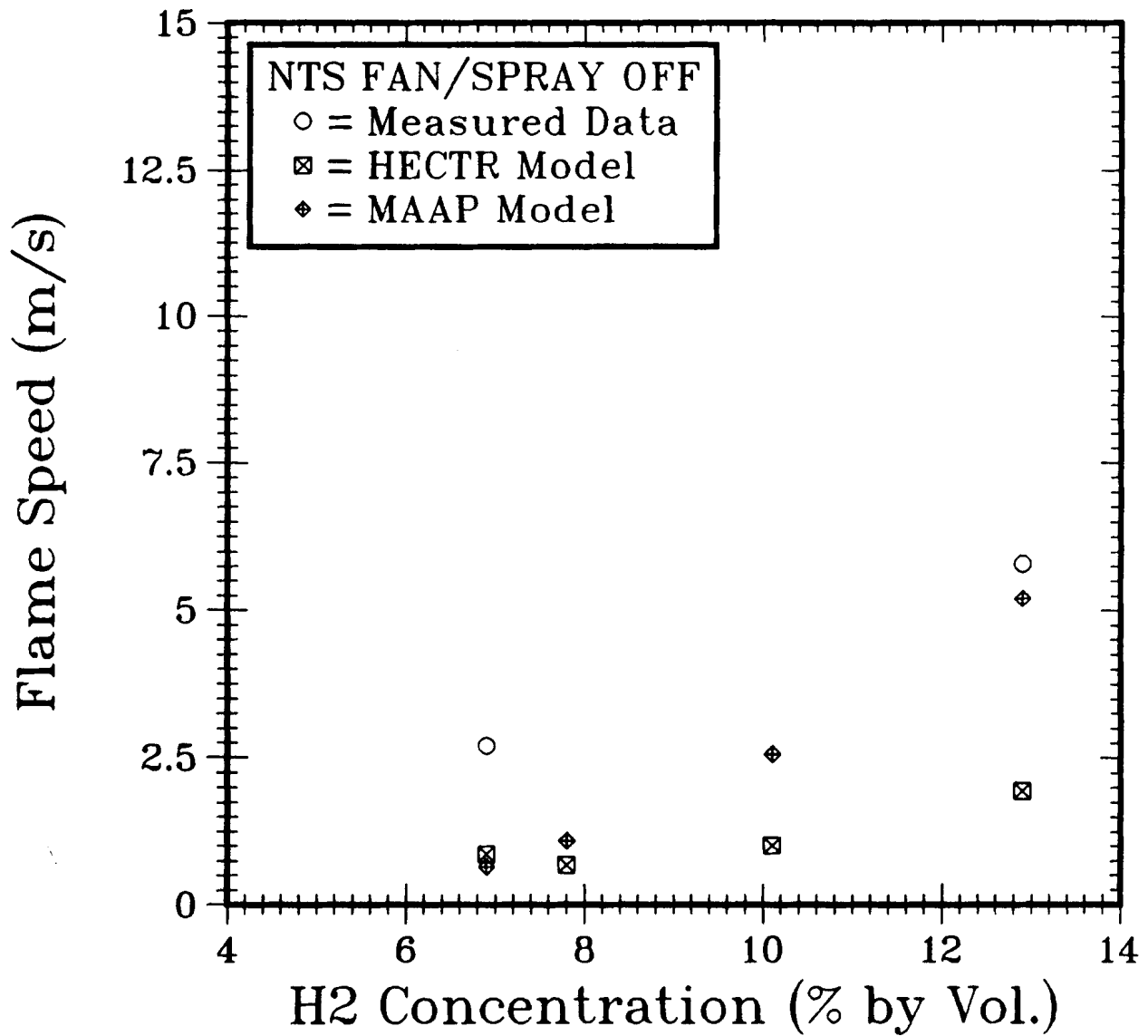


Figure 14. Comparison of Upward Flame Speed Between Measured Data and Predictions by the HECTR and MAAP Models for NTS High-Steam Experiments

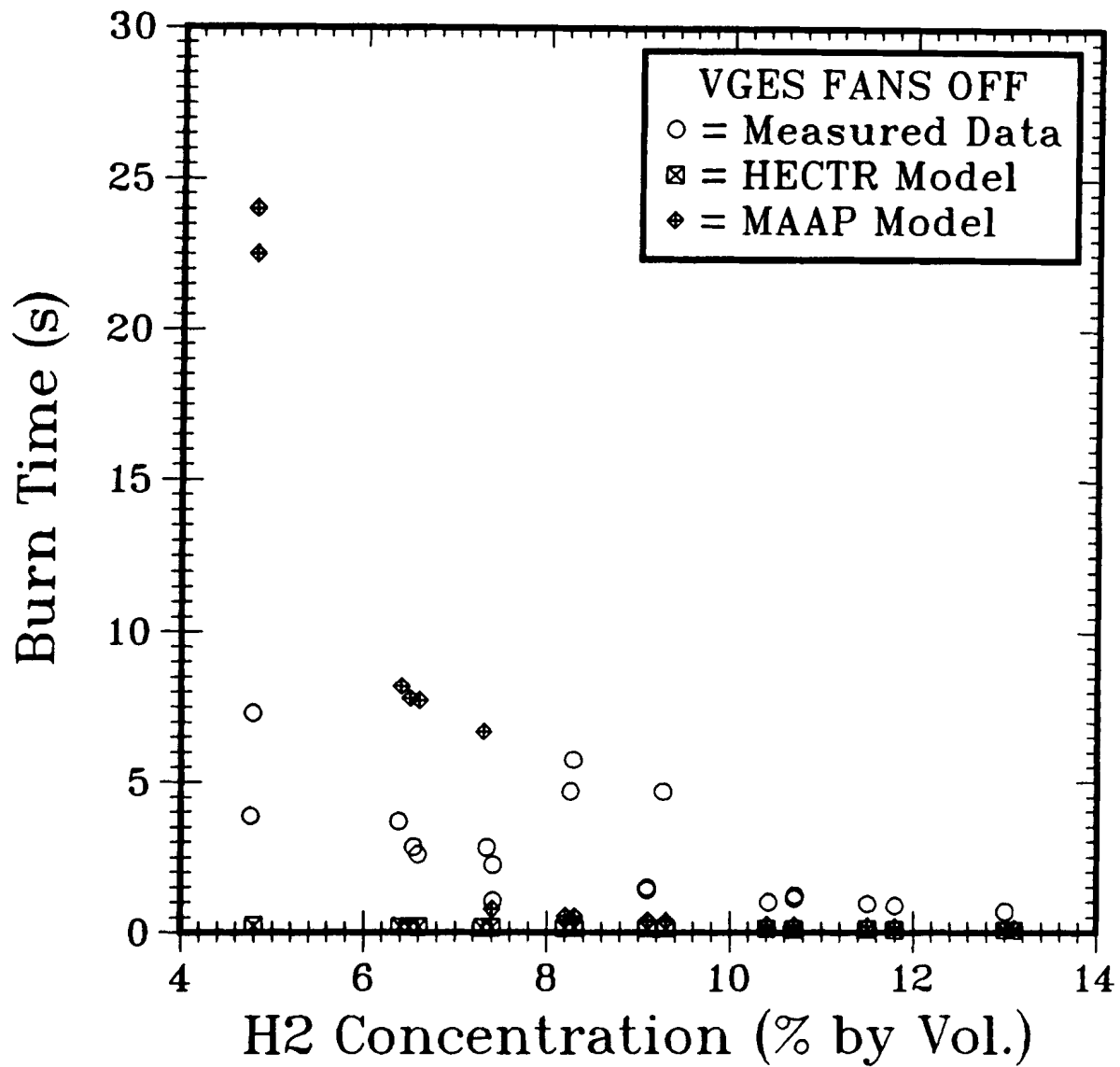


Figure 15. Comparison of Burn Time Between Measured Data and Predictions by the HECTR and MAAP Models for VGES Fans-off Experiments

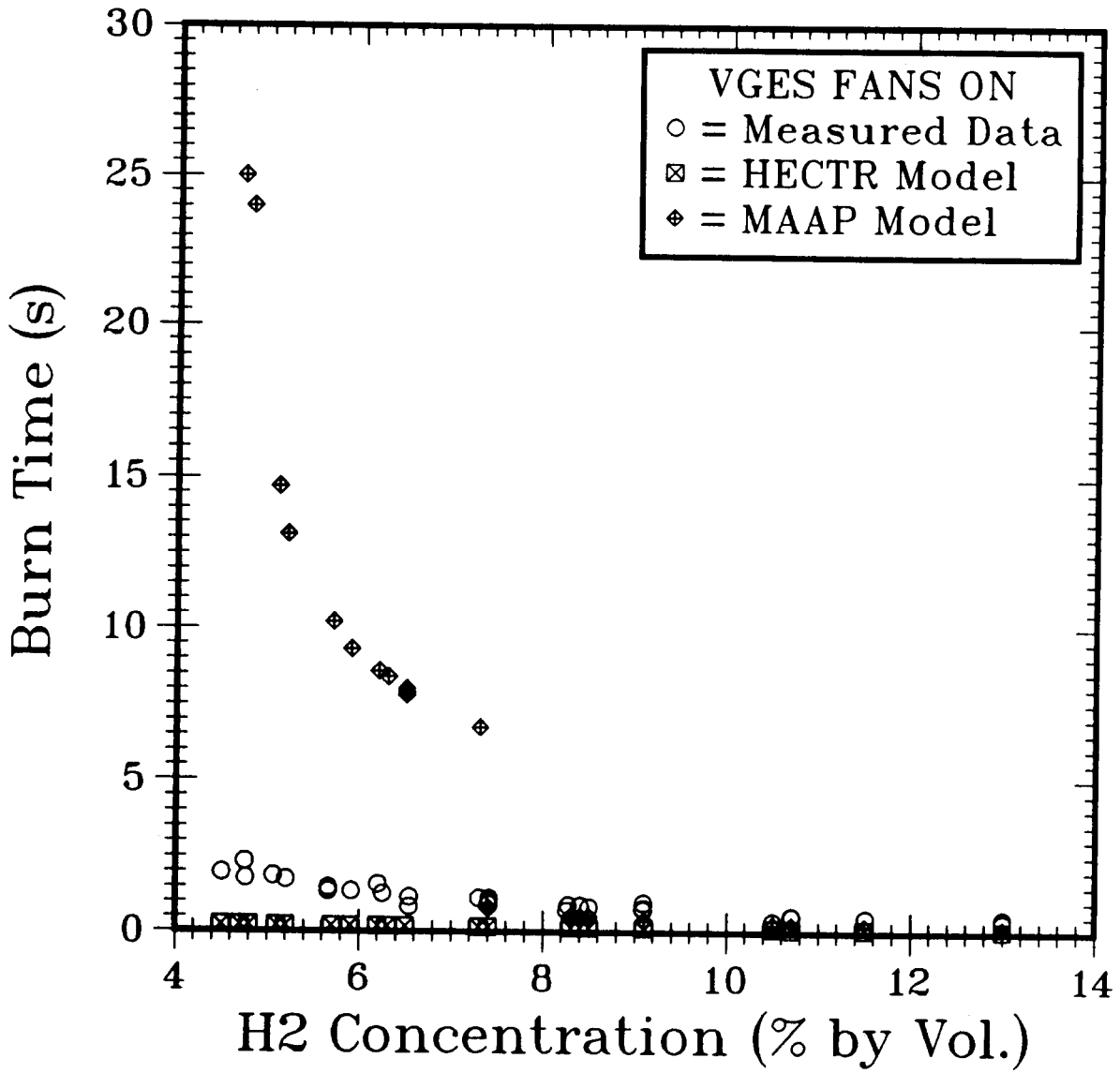


Figure 16. Comparison of Burn Time Between Measured Data and Predictions by the HECTR and MAAP Models for VGES Fans-on Experiments

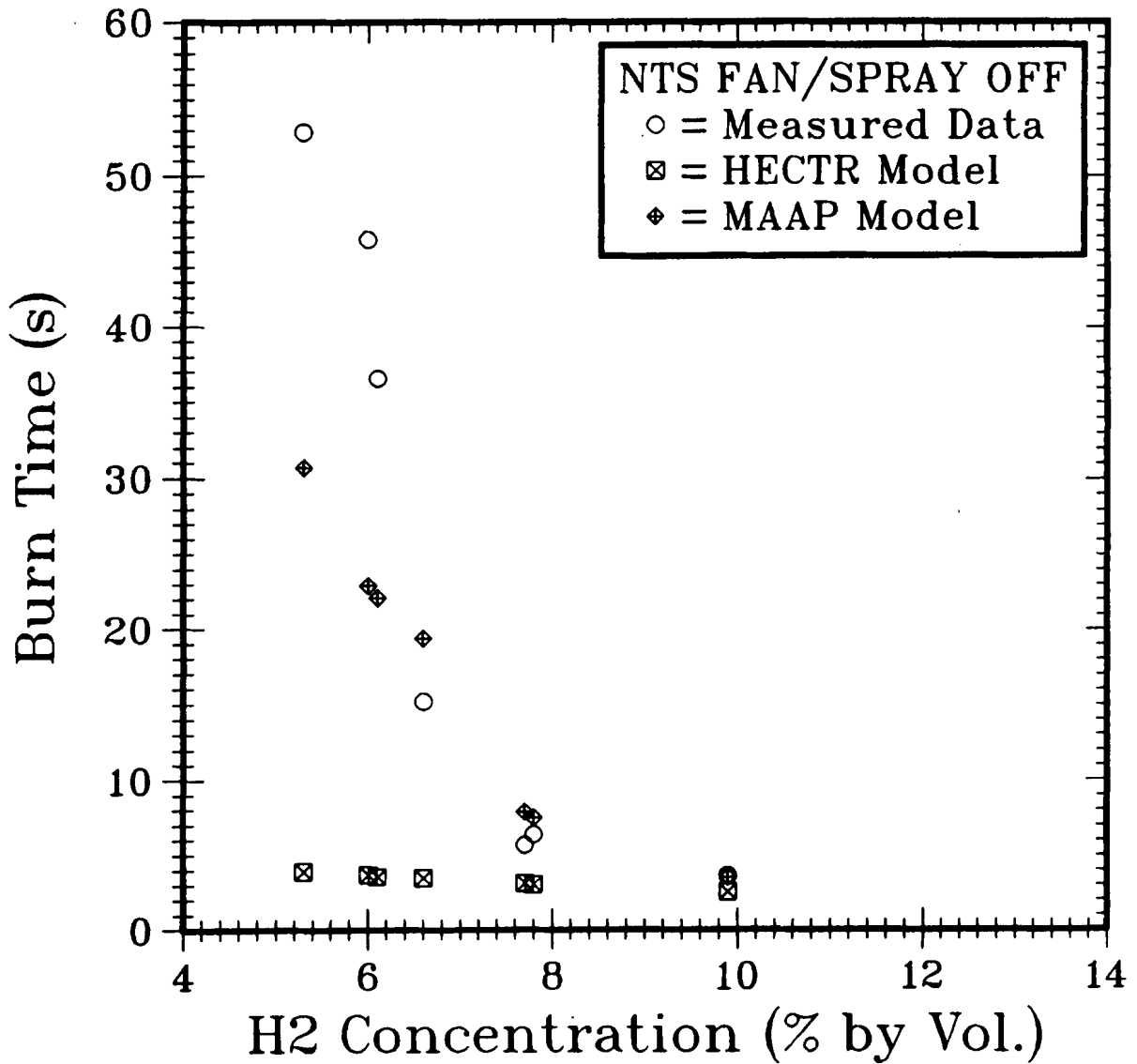


Figure 17. Comparison of Burn Time Between Measured Data and Predictions by the HECTR and MAAP Models for NTS Low-Steam Experiments

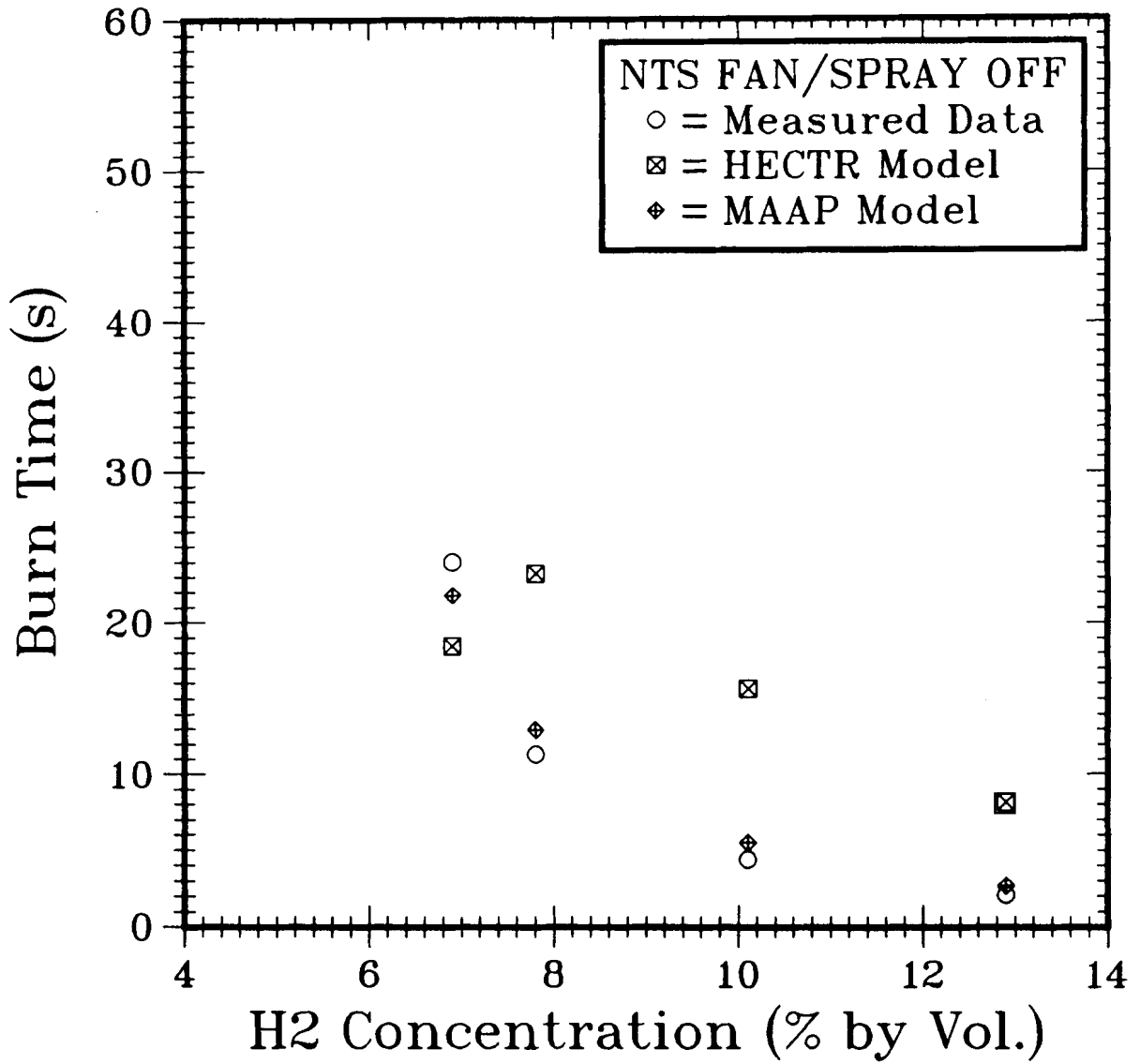


Figure 18. Comparison of Burn Time Between Measured Data and Predictions by the HECTR and MAAP Models for NTS High-Steam Experiments

(Figures 11 to 18). For those cases with high steam concentration, HECTR underpredicts the flame speed (Figure 14), which leads to a longer burn time. Hence, the influence of steam on flame speed appears to not be well modeled in the present correlation in HECTR. Moreover, from References 18 and 19, when comparing the measured flame speed data from NTS experiments with data from VGES experiments, it has been found that there may be a scaling dependence on the flame speed. The existing flame speed correlation in HECTR does not depend upon vessel geometry.

In general, the MAAP burn model underpredicts flame speed and overpredicts burn time when compared with the NTS experimental data; however, for the VGES fans-on and fans-off experiments, the global burn model overpredicts the flame speed when hydrogen concentration is more than 8%. The flame speed is overpredicted in VGES experiments, but not in NTS experiments, because the geometry of the two test vessels is different. The ratio of vessel height to regional radius used in VGES calculations is larger than in NTS, therefore, it gives a larger value for the flame speed. (The effective flame speed predicted by the MAAP global burn model depends directly on the ratio of vessel height to regional radius.) This comparison shows that even though the flame speed expression derived from the MAAP model has an implicit scaling dependence, it appears to be not well correlated.

For those cases with fans or sprays on, the completed calculations neglect the effect of turbulence on combustion generated by fans and sprays because a burning velocity multiplier of 1 is used. If a larger value of burning velocity multiplier (> 10) is used, this would improve the comparison of the analytical results with the the experimental data. The combustion model in MAAP relies heavily on the laminar burning velocity correlation developed in Reference 10; at present, the experimental data-base to support this correlation in the lean hydrogen combustion region (less than 15%) is not well established. Substantial uncertainty exists when apply this correlation to predict the burning velocity at hydrogen concentration below 15%. This leads to more uncertainty in predicting flame speed and burn time.

3.3.4 Flame Propagation

A flame is allowed to propagate into any adjacent compartments in HECTR as long as the propagation criteria are satisfied (Table 2). In MAAP, a flame is only allowed to propagate upward into the adjacent compartment, as long as the calculated burning velocity is greater than 1 cm/s, which is about 5% H_2 concentration. No horizontal or downward propagation is permitted. This restriction is contradictory to the test results of the VGES and NTS experiments where downward propagation of flames was observed.

When burning occurs within a compartment, neither model explicitly tracks the flame front. Hence, a mixture of both burned and unburned gases will be convected out of the compartment through junctions, even though a junction may be downstream from the flame front. Consider a case with gas flowing from a larger burning compartment to a smaller neighboring compartment with the connecting flow-junction downstream from the flame; the present models will allow for both burned and unburned gases instead of only the unburned gases to convect into the smaller compartment. The burned gases convected from the burning compartment may inert the smaller compartment and prevent any flame propagation. This may alter the combustion event and result in a lower peak combustion pressure.

In both models, when combustion occurs in a specific compartment, the final mole fraction of hydrogen at the completion of burn is predetermined at the initiation of burn. During the combustion process, if any combustible gases are convected into the burning compartment, the burn rate will be adjusted at every time step so that the final mole fraction of the combustible gases will be consistent with the predicted value. By setting the ignition criterion at a low hydrogen concentration and with a long burn time (usually this is predicted to be the case by the MAAP incomplete burn model), the combustion process will behave like a standing flame rather than a deflagration. This type of burning will not produce a very high peak pressure and temperature.

3.4 Summary of Modeling Differences

In terms of the prediction of the consequences of hydrogen combustion during reactor accidents, the most important differences between HECTR and MAAP are:

- I. Steam Inerting: MAAP does not allow for the inerting of hydrogen mixtures due to excess steam; HECTR uses experimentally determined flammability limits which include the steam inerting effect.
- II. Ignition Criteria:
 - (a) Global Burns: MAAP specifies that ignition will occur when the hydrogen concentration exceeds a threshold determined by a "flame temperature criterion;" this corresponds to about 7.3% hydrogen in air. HECTR can model ignition for any user-specified concentration or time into the accident;
 - (b) "Incomplete" Burns: If igniters are available, MAAP initiates burns at concentrations corresponding to about

4.8% hydrogen in dry air. HECTR allows continuous burning as well as deliberate burning initiated at any hydrogen concentration specified by the user.

Neither of the models currently is capable of accurately calculating a standing flame, because flashback, and flame stability for steam-hydrogen-air mixtures are not adequately modelled. Flashback and standing flames were observed in all of the Nevada Test Site (NTS) tests involving continuous injection [18 and 20]. In these tests, hydrogen release rates are relatively high, above 1.6 kg/min. As a result of high injection rate, the flames, regardless of where they were initially ignited, tended to burn back to the hydrogen-steam source and anchor there as standing flames.

In a sense, the MAAP "incomplete burn" model resembles diffusion flames anchored on the igniters (rather than at the hydrogen source), slowly burning the hydrogen and/or carbon monoxide in bunsen-burner fashion. Such burns would be unable to threaten containment integrity, although the survival of nearby equipment might be threatened due to high thermal loads.

HECTR has been used in the past to model diffusion-flame scenarios for BWR Mark IIIs [21]. The current release version of the code contains a simple model for continuous burning [2].

If propagating flames occur, MAAP and HECTR will approximately agree if the burn is assumed to occur in HECTR at about 7-8% hydrogen in dry air (or its equivalent with steam present). For burns at lower or higher equivalent concentrations, HECTR will predict thermal and mechanical loads lower or higher, respectively, than the MAAP predictions.

4. HECTR RESULTS OF THE STANDARD PROBLEM

Seventeen HECTR calculations were performed to understand the differences between these two codes and their impact on risk assessment. These calculations can be divided into three different sets. The characteristics of each set are:

1. HECTR default calculations.
2. Modified HECTR calculations for matching MAAP results.
3. Sensitivity studies.

In the first set of calculations, HECTR analyses of the problem were performed using the default setup in the code. The results of these calculations show that there are differences between HECTR and MAAP predictions. In order to match the results predicted by the MAAP code, a modified HECTR calculation was made using the 6-compartment model with the MAAP geometrical data. This calculation involved tuning the HECTR code by changing certain parameters, for example, ignition criterion, combustion completeness, and burn time. Sensitivity studies were also performed to evaluate the importance of sensitive parameters to better understand HECTR predictions. The results of these calculations are summarized in Table 4.

4.1 Modeling of the Reactor Containment

Three different nodding systems were used to model the reactor containment (see Appendix B). They are:

1. 6-compartment model with MAAP geometrical data.
2. 6-compartment model with Sandia geometrical data.
3. 16-compartment model with Sandia geometrical data.

Both 6-compartment models have the same nodding as in the MAAP code for the Sequoyah Ice-Condenser Containment [3 and 4]. The differences between these two 6-compartment models are the geometrical data used in these calculations (Table 5). The MAAP geometrical data are those used in the MAAP analysis [22]. The Sandia geometrical data are obtained either from the Final Safety Analysis Report of the Sequoyah Nuclear Power Plant [23] or from Reference 6. The major differences between these two data sets are the total free volume in the lower compartment, the total surface area, and the time delay for the air-return fans to be activated after the set-point is satisfied.

The 16-compartment model is extracted from the 40-compartment model used in Reference 24. Since we are not concerned with the recirculation loop in the ice bed region in this problem, the 16-compartment model, which has a one-dimensional ice-condenser model, is sufficient for this standard

Table 4. Summary of HECTR Analyses of the Standard Problem

	P_{\max} (kPa)	T_{\max} (K)	T_w^a (K)	T_w^b (K)
MAAP Code	142.7	423.1	-	-
<u>Default Calculations</u>				
HECTR/MAAP-6	162.2	820.4	348.2	375.9
HECTR-6	150.6	788.0	348.5	369.0
HECTR-15	142.9	808.5	351.7	370.5
<u>Modified Calculations</u>				
HECTR/MAAP-6	151.1	539.1	353.3	383.4
<u>Sensitivity Studies</u>				
HECTR-15 ^c	133.1	682.4	351.5	370.1
HECTR-15 ^d	172.5	962.7	348.8	352.9
HECTR-15 ^e	299.7	1049.3	348.8	352.9

^a Steel equipment in the lower compartment

^b Concrete in the lower compartment

^c Ignition Criterion = 6% hydrogen concentration

^d Ignition Criterion = 8% hydrogen concentration

^e 8% hydrogen combustion in the dome region

Table 5. Major Differences between HECTR and MAAP
Input Data

	HECTR	MAAP
1. Reactor Cavity:		
Total Volume	396.0	419.09 m ³
2. Lower Compartment:		
Total Volume	6334 m ³	8184 m ³
Sump Area	59.2 m ²	502.6 m ²
Steel Area	5940 m ²	2780 m ²
Concrete Area	3569 m ²	1796 m ²
3. Annular Region:		
Sump Area	0	446.8 m ²
Steel Area	1834 m ²	0
Concrete Area	3257 m ²	1027 m ²
4. Upper Plenum:		
Steel Area	1000 m ²	0
5. Upper Compartment:		
Concrete Area	4085 m ²	3760 m ²
Steel Area	2000 m ²	1065 m ²
6. Ice Condenser:		
Wall Structure - Wt.	2.0x10 ⁵ kg	-
- Area	2058 m ²	-
Baskets - Wt.	1.47x10 ⁵ kg ²	-
- Area	9920 m ²	-
7. Air-Return Fans:		
Delay time	600 s	0.167 s
LC to Annular Region		
Vol. flow rate	1.17 m ³ /s	0

problem. However, in the second part of this standard problem, because we intend to study the natural circulation loop between the lower compartment and the reactor cavity, it will be necessary to refine the noding in the lower compartment so that more detailed information can be obtained.

In HECTR analyses, the first part of the standard problem begins at the time when core uncovering occurs (1.3 hours or 4705 seconds) and ends at the time when the reactor vessel fails (2.34 hours or 8418 seconds). At 1.3 hours, the air-return fans have been on for a period of time and the containment spray system fails because switching over to the recirculation mode is unsuccessful. Hence, the discrepancy with respect to the time delay for fan activation does not affect the outcome of this standard problem. However, since the containment spray system is working in the injection mode before it fails to switch over to the recirculation mode, water will accumulate in various locations including the reactor refilling area. The HECTR input deck has been modified to reflect the water accumulated in the sumps, which, in turn, decreases the gas-free volume of those compartments involved. In the 16-compartment model, the compartment that models the reactor refilling area will be deleted because it is filled with water and becomes useless in our calculations. Therefore, there are only 15 compartments used in the present calculations.

In the following discussion, the HECTR 6-compartment model using the MAAP geometrical data will be referred to as the HECTR/MAAP 6-compartment model, while the HECTR 6-compartment and the HECTR 15-compartment model, respectively, will represent the 6-compartment and 15-compartment models using the Sandia geometrical data.

4.2 HECTR Default Calculations

Calculations using the default values in HECTR were performed. In HECTR version 1.5 [2], the default criterion for hydrogen ignition had been changed such that combustion would occur if the hydrogen mole fraction within a compartment was above 7 percent instead of 8%.

The HECTR 15-compartment model predicted that six sequential burns occurred in the reactor containment, with the burns initiated in the lower compartment where hydrogen and steam sources were located. Each burn propagated into the lower plenum, the ice bed, and eventually into the upper plenum, except one burn that stopped at the top of the ice bed.

The HECTR 6-compartment and HECTR/MAAP 6-compartment models predicted that four and three sequential burns would

occur, respectively, with the flame propagation similar to the prediction of the HECTR 15-compartment model. All the burns were initiated in the lower compartment and completed in the upper plenum above the ice-condenser region. The total burn times (the time between ignition in the lower compartment to extinguishing in the upper plenum) calculated by each model for each sequential burn are quite similar. They are 8.54, 7.79 and 4.15 s for the HECTR 15-compartment, HECTR 6-compartment and HECTR/MAAP 6-compartment models, respectively. In the HECTR 15-compartment model, the steam generator (SG) housing was modeled as a separate compartment. This allowed the flame to propagate into the SG housing compartment and resulted in an additional 17.14 s of burning in the SG housing compartment. In the HECTR/MAAP 6-compartment model, the characteristic length for flame propagation in the lower compartment is relatively shorter than the other two cases; hence the burn time is relatively shorter. As a result, among these three calculations, the HECTR/MAAP 6-compartment model predicted the highest peak pressure and temperature with respect to hydrogen combustion (Table 4 and Figures 19 to 21).

The differences between these HECTR results can be explained by the way these three compartment models were set up. The lower compartment in the HECTR 6-compartment model has a smaller free volume and more total surface area than in the HECTR/MAAP 6-compartment model (Table 5). Given that the same amount of hydrogen and steam were injected into the lower compartment, the HECTR 6-compartment model, as expected, calculated a higher hydrogen concentration. Since the ignition criterion depended on the hydrogen concentration, the HECTR 6-compartment model predicted an earlier burn and an additional sequential burn. Larger total surface area would allow more heat loss and condense more steam, which, in turn, would increase the hydrogen mole fraction. The result of an earlier, less severe burn decreased the peak combustion pressure and temperature.

The argument discussed in the previous paragraph can also be applied when comparing the results between the HECTR 15-compartment and HECTR 6-compartment model. The HECTR 15-compartment model had a more refined noding in the lower compartment region. Thus it calculated a higher hydrogen concentration in the source compartment, which led to an earlier burn and an additional sequential burn. This resulted in a lower peak combustion pressure. However, the finer noding system in the lower compartment also produced higher gas and wall temperatures because it calculated the temperature distribution within the lower compartment region and identified the local hot spot. The coarse-noding system had only one control volume which averaged out the temperature distribution by assuming uniform mixing within a compartment.

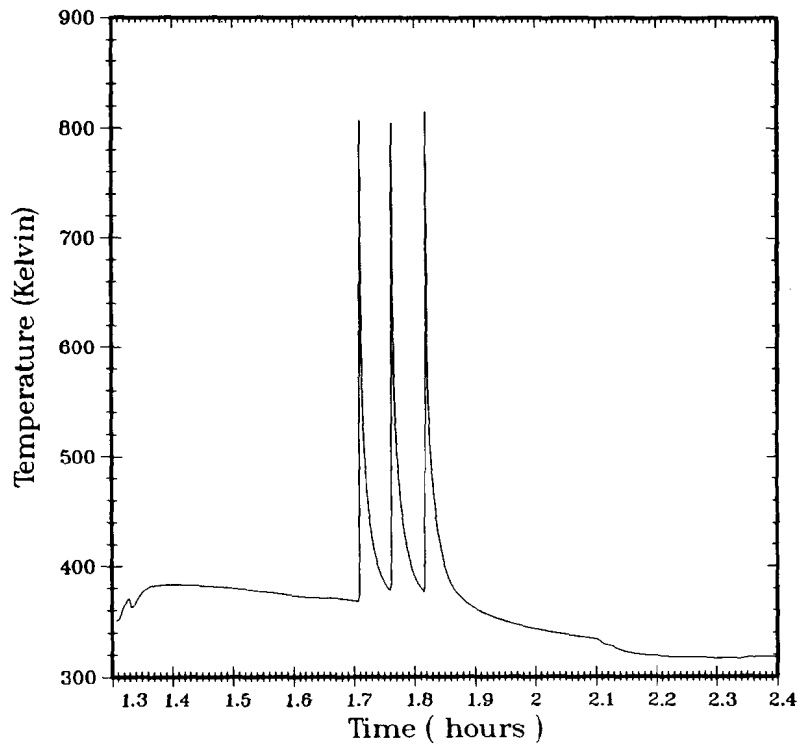
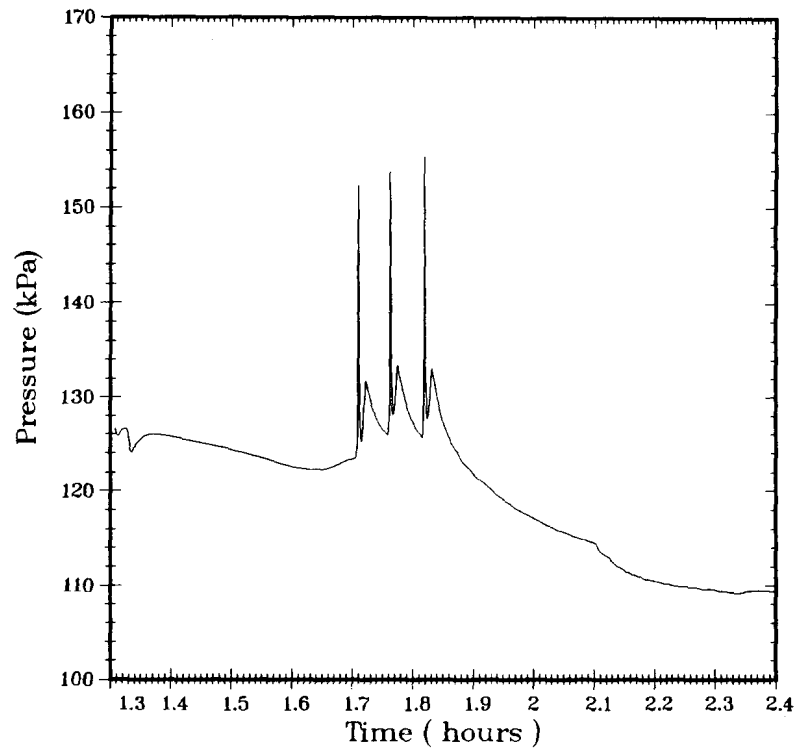


Figure 19. Pressure and Temperature Responses in the Lower Compartment Predicted by HECTR Using the HECTR/MAAP 6-Compartment Model (Default Calculation)

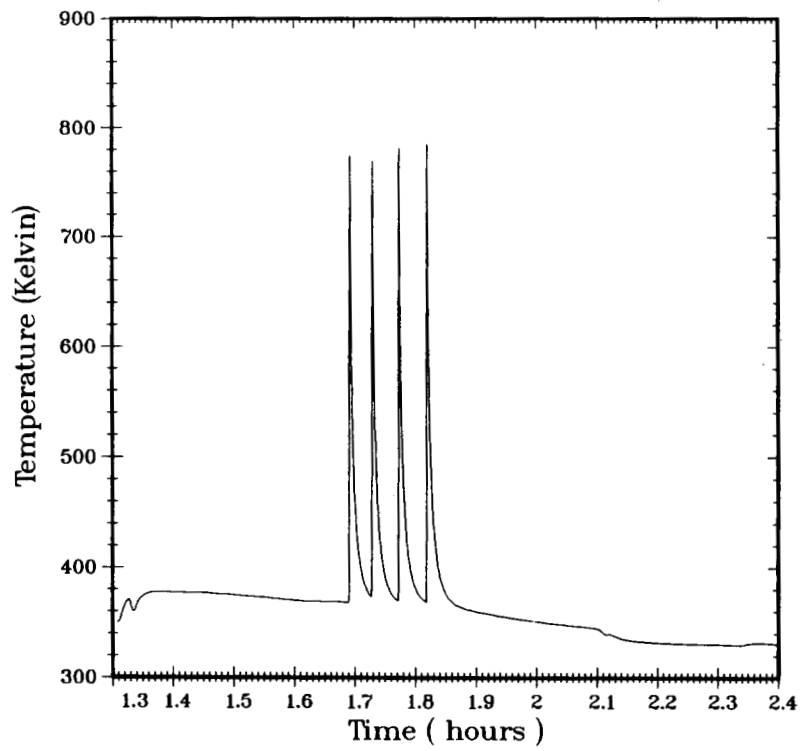
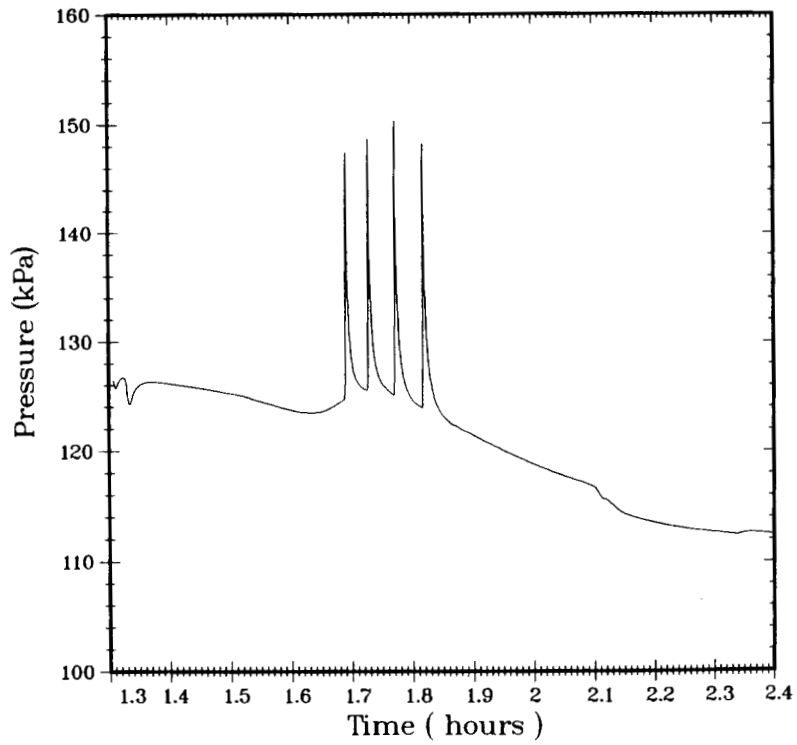


Figure 20. Pressure and Temperature Responses in the Lower Compartment Predicted by HECTR Using the HECTR 6-Compartment Model (Default Calculation)

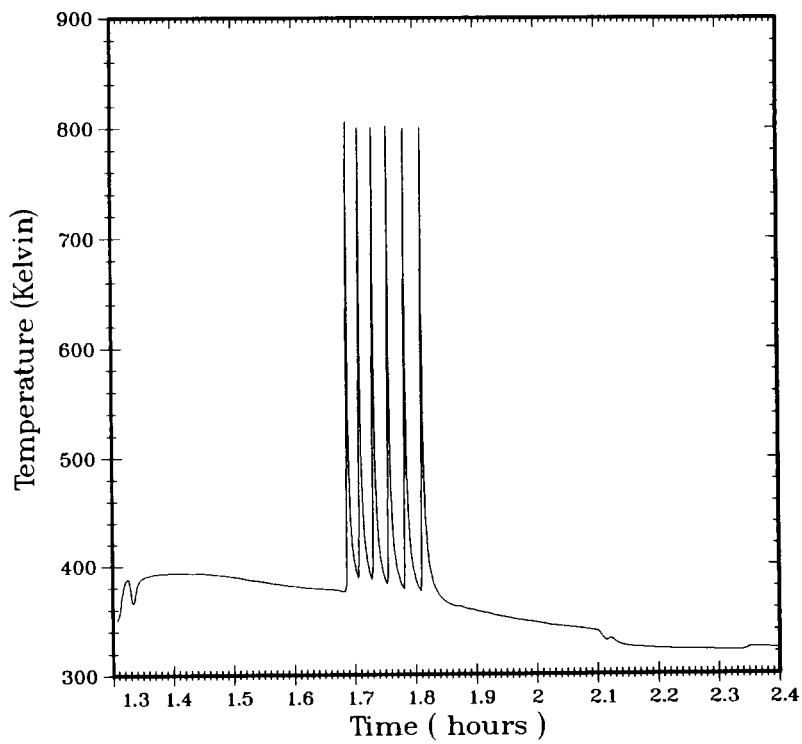
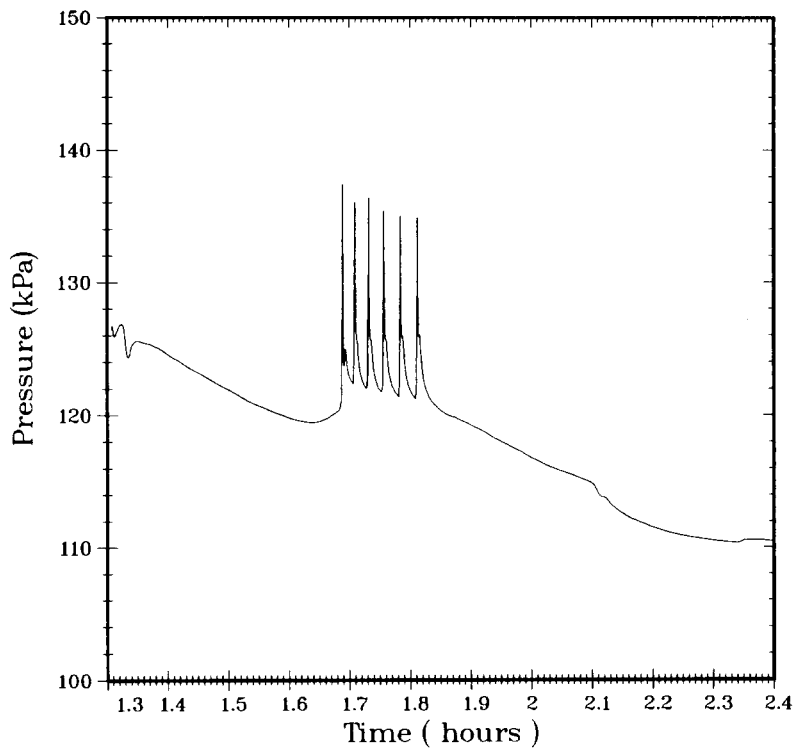


Figure 21. Pressure and Temperature Responses in the Lower Compartment Predicted by HECTR Using the HECTR 15-Compartment Model (Default Calculation)

To summarize the HECTR default calculations, all three compartment models predicted similar magnitudes of pressure and temperature rises with respect to hydrogen combustion. They all predicted a series of moderate burns.

4.3 Modified HECTR Calculations to Match MAAP Results

A set of HECTR calculations using the HECTR/MAAP 6-compartment model was performed in an attempt to match MAAP results given in Reference 25. A few changes were made in HECTR before any calculations were completed. First, several FORTRAN statements were added to the HECTR code so that the ignition would occur at the exact times and locations as they were specified in Reference 25. Burn time for each discrete burn occurring in the corresponding compartment was also adjusted so that it matched the value given in Reference 25. The value of the combustion completeness for each burn was estimated by assuming that only that portion of the hydrogen between igniters and the top of the compartment would combust. As in MAAP, I did not allow any flame propagation into the neighboring compartment. The selected combustion parameters I used for this part of the calculations are listed in Table 6.

The results of this modified HECTR calculation and its comparison with MAAP predictions [24] are shown in Figure 22. HECTR predicts a peak pressure and gas temperature of 151 kPa (21.9 psia) and 539 K, respectively while MAAP predicts a value of about 143 kPa (20.7 psia) and 423 K, respectively. The cause of these differences is unknown. Several calculations with different combustion completeness and convective heat transfer coefficients were performed in an attempt to match the pressure and gas temperature in the lower compartment predicted by the MAAP code. The pressure and gas temperature in the lower compartment calculated by HECTR did decrease as a result of less complete burns or larger heat transfer coefficient, but the changes were insignificant. Hence by adjusting the combustion process to be less complete and last much longer, we can qualitatively match the MAAP prediction of the containment responses for this standard problem.

Next, I will compare the results of these modified HECTR calculations with the results of the 15-compartment model. The pressure rises with respect to hydrogen combustion for both cases compare well. However, the calculated peak temperatures in the lower compartment are far apart: the 15-compartment model predicts a peak value of 808 K while the new HECTR/MAAP 6-compartment model and MAAP code show the peak temperature to be 539 K and 366 K, respectively. The substantial difference in the lower compartment temperature may be important for studying the survivability of equipment.

Table 6. Combustion Parameters Used in the Modified HECTR Calculations

	Ignition Time (sec.)	Time (hrs.)	Burn Time (seconds)	Combustion Completeness
Lower Compartment	6070	1.69	842	42.12%
Upper Plenum	6113	1.70	2051	19.18%
	8180	2.27	20	19.18%
	8220	2.28	20	19.18%
	8260	2.29	20	19.18%
	8300	2.31	20	19.18%
Upper Compartment	6647	1.85	626	84.40%
	7279	2.02	69	84.40%
	7368	2.05	65	84.40%
	7467	2.07	63	84.40%
	7588	2.11	60	84.40%
	7756	2.15	63	84.40%
Annular Region	6491	1.80	7299	53.72%
	7004	1.95	28	53.72%
	7043	1.96	26	53.72%
	7090	1.97	35	53.72%
	7179	1.99	35	53.72%

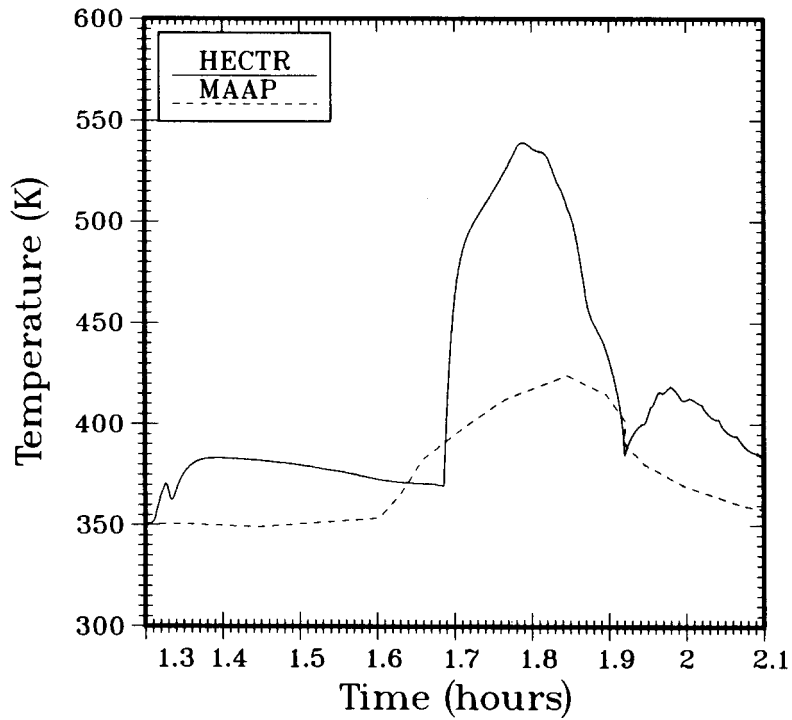
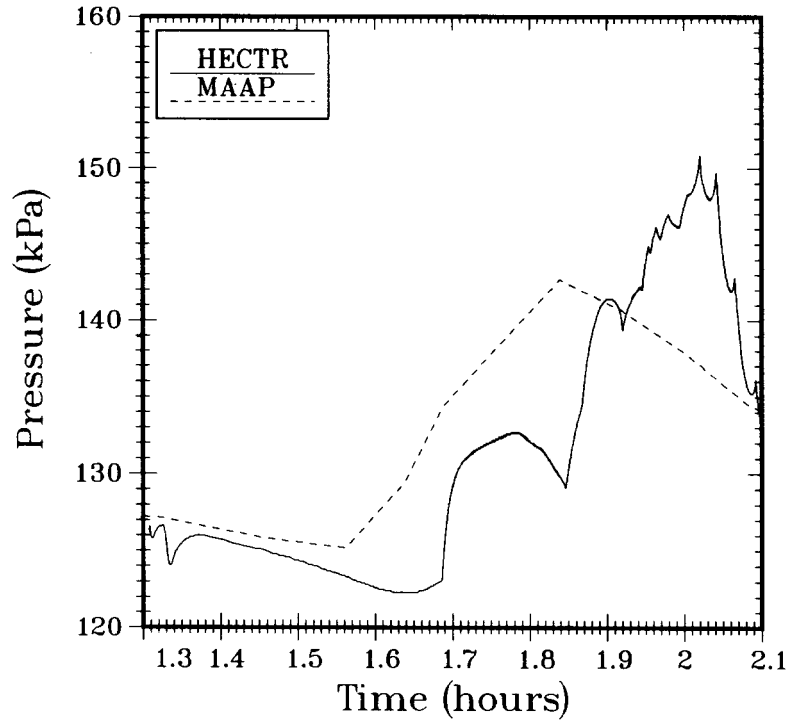


Figure 22. Pressure and Temperature Responses in the Lower Compartment Predicted by HECTR Using the HECTR/MAAP 6-Compartment Model (MAAP Ignition Time, Burn Time, and Combustion Completeness)

For equipment survival, energy deposition (the integral of total heat flux over time) is an important parameter to calculate the thermal loading. Figures 23 to 26 plot the surface temperature and total heat flux for two kinds of surfaces in the lower compartment (steel and concrete) as predicted by HECTR using two different compartment models. In the 15-compartment model, as a result of a finer noding in the lower compartment, HECTR predicted a higher peak surface temperature and larger heat flux for each discrete burn. However, for the modified HECTR calculation using the HECTR/MAAP 6-compartment model, the total heat flux on the surface behaved like the response to a diffusion flame rather than to a discrete burn. It seems that the 15-compartment model predicts a much bigger energy deposition rate than the revised HECTR/MAAP 6-compartment model.

4.4 Sensitivity Studies

Several sensitivity studies were performed to evaluate the importance of parameters to better understand the HECTR predictions. Three such studies are discussed in this report. Two involved changing the ignition criterion to either 6% or 8% hydrogen mole fraction using the 15-compartment model. These two ignition criteria were used because as shown in Fig. 6, the uncertainty of the flammability limits for the hydrogen:air:steam mixture is about 1%.

For ignition occurred at 6% hydrogen, HECTR predicted an earlier, more moderate burn and more sequential burns in the reactor containment. These burns were all initiated in the lower compartment, then propagated into the ice bed and upper plenum. The result of these burns gave a peak pressure of 133 kPa (19.3 psia) and peak temperature of 682 K (Figure 27).

When the ignition criterion was increased to 8% hydrogen concentration, the flame propagation pattern was quite different. In this case, the flame was initiated in the upper plenum and propagated downward into the ice bed twice and upward into the dome twice. Not a single burn sequence propagated back into the lower compartment in this calculation. In HECTR, the downward flame propagation limit is set at 9% hydrogen. Throughout the transient, the hydrogen concentration in the lower compartment never reached 8% because of the high steam content. Hence ignition could not occur or flame could not propagate down into the lower compartment. Besides two sequential burns, there were also three local regional burns in the upper plenum predicted by HECTR. Since the burning was at the higher hydrogen mole fraction and at a later time, it was more severe. However, even though the flame from the regional burn did propagate into the dome, only a small fraction of hydrogen present in the dome was combusted. Therefore, the calculated peak pressure and

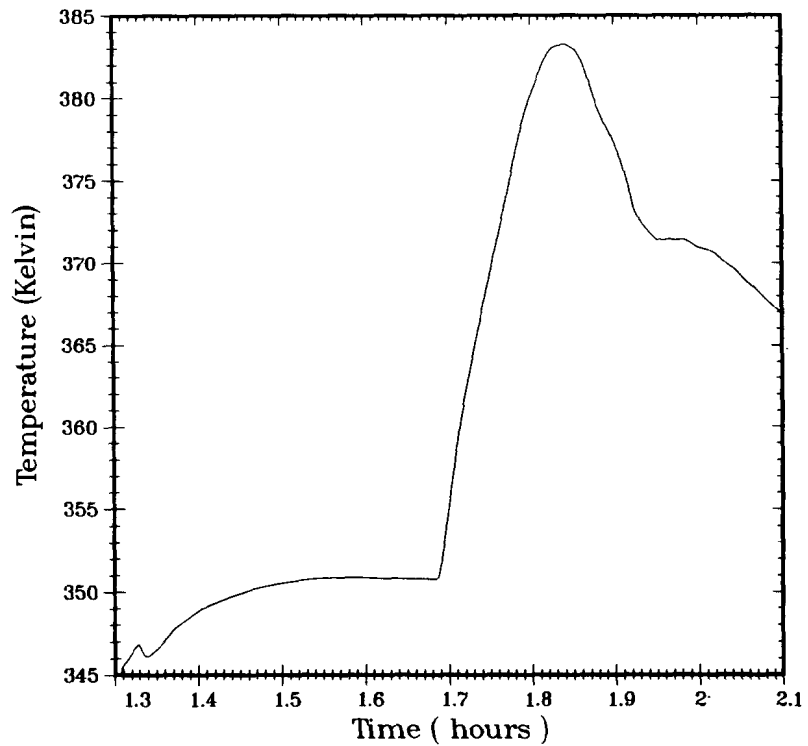
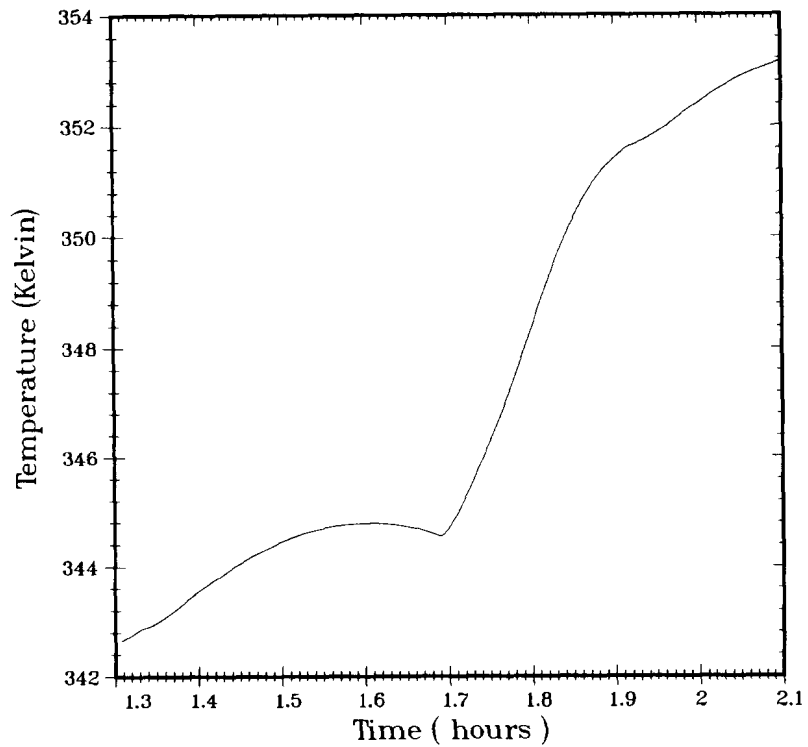


Figure 23. Surface Temperature Responses of Steel Equipment (Top) and Concrete (Bottom) in the Lower Compartment Predicted by HECTR Using the HECTR/MAAP 6-Compartment Model (MAAP Ignition Time, Burn Time, and Combustion Completeness)

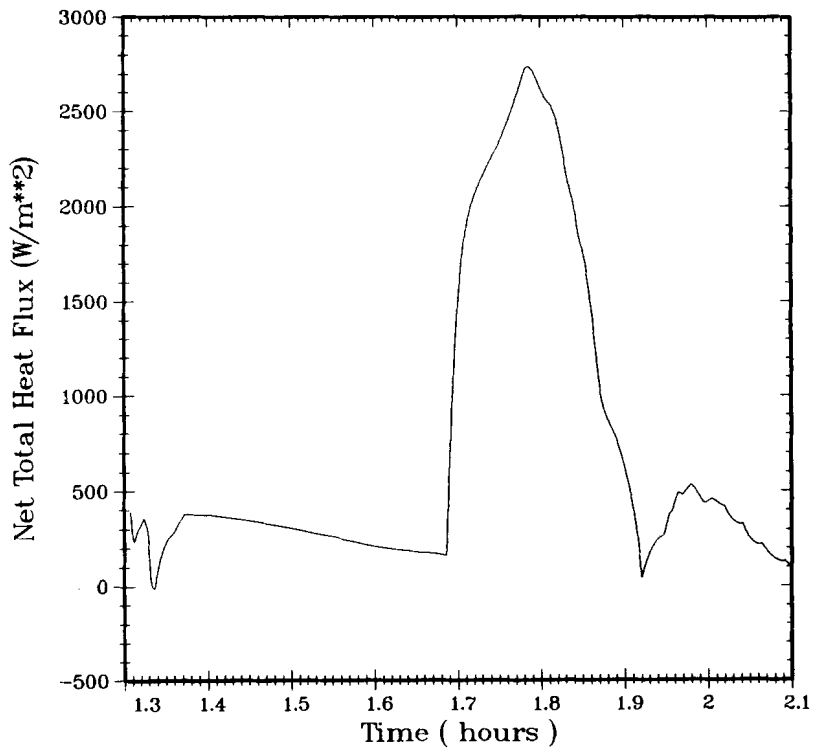
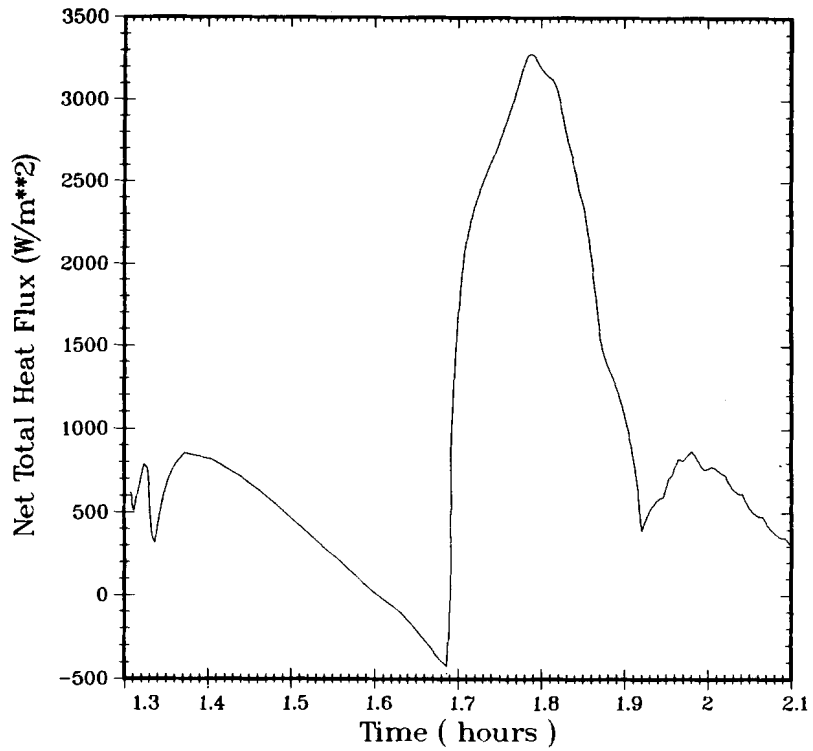


Figure 24. Total Heat Flux to the Surface of Steel Equipment (Top) and Concrete (Bottom) in the Lower Compartment Predicted by HECTR Using the HECTR/MAAP 6-Compartment Model (MAAP Ignition Time, Burn Time, and Combustion Completeness)

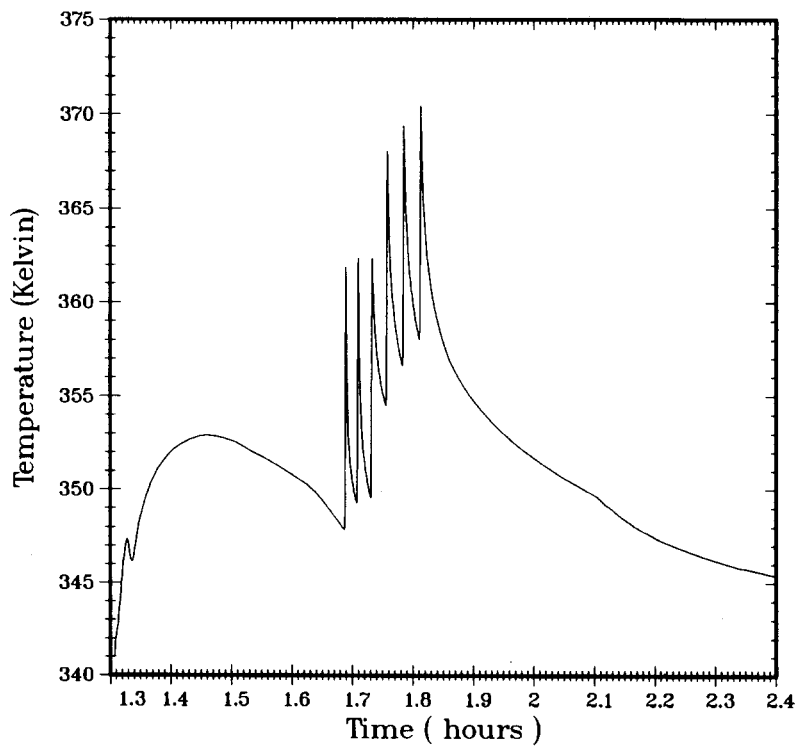
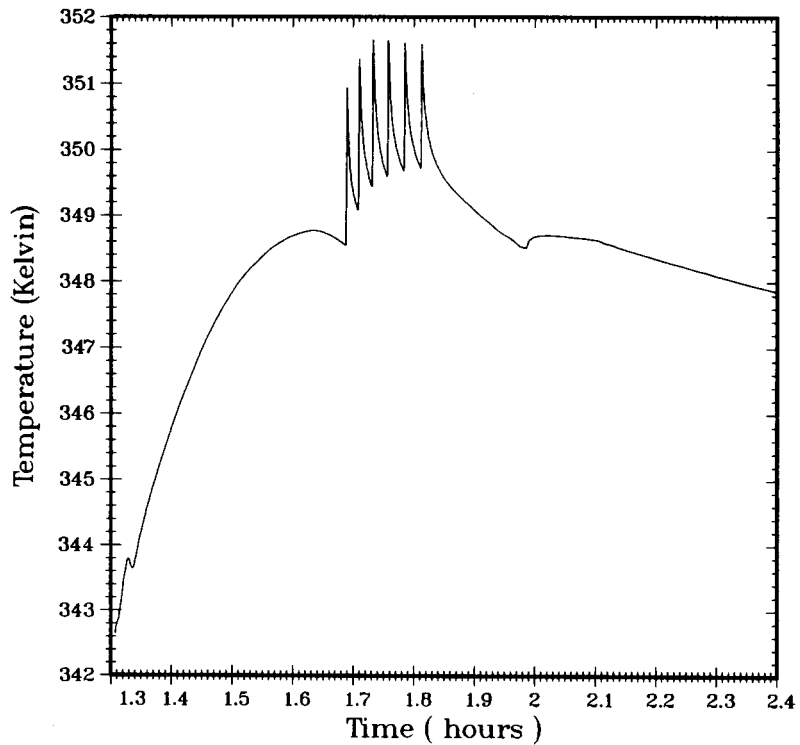


Figure 25. Surface Temperature Responses of Steel Equipment (Top) and Concrete (Bottom) in the Lower Compartment Predicted by HECTR Using the HECTR 15-Compartment Model (Default Calculation)

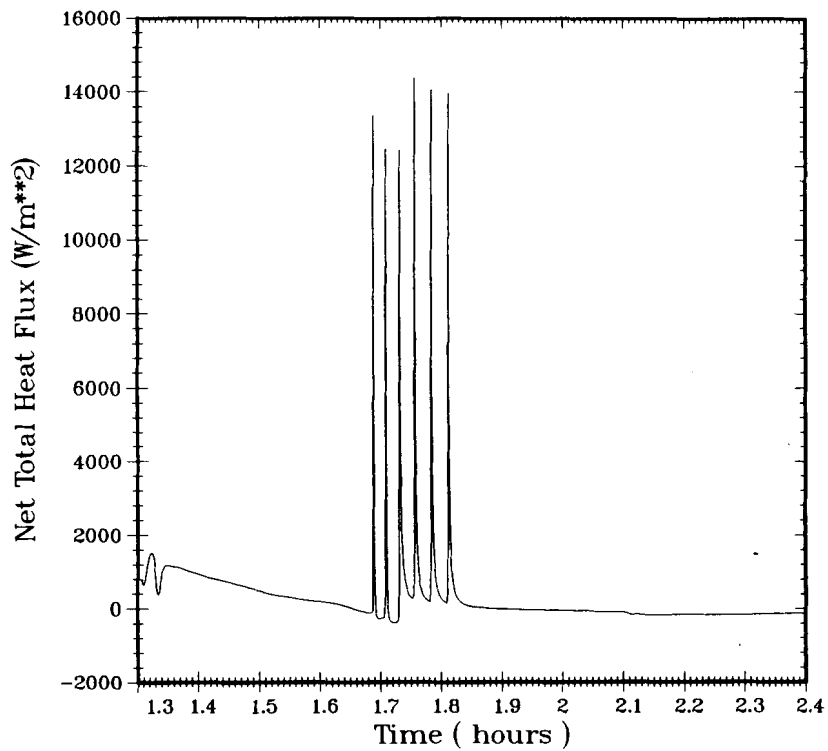
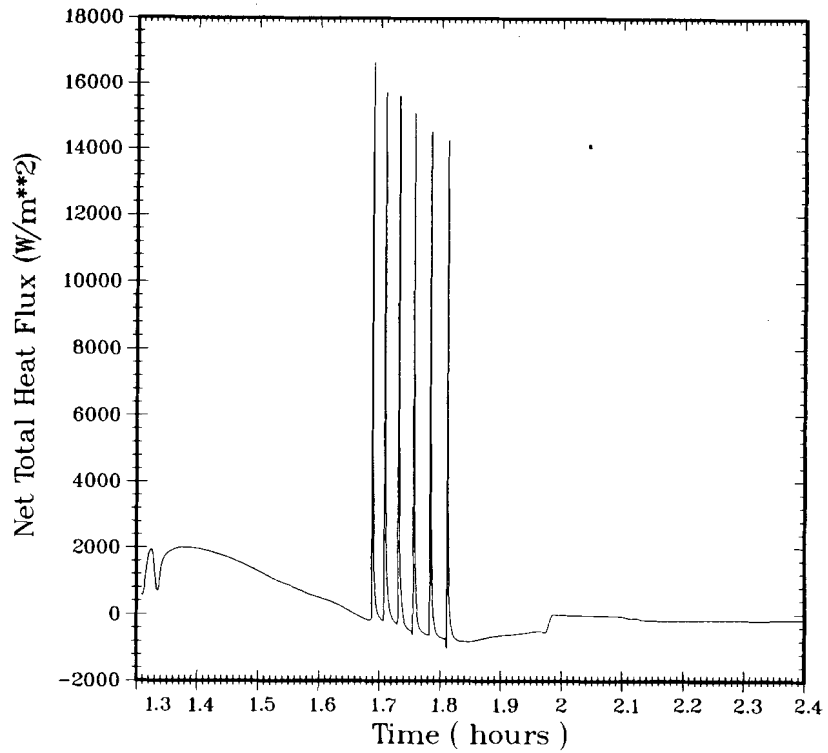


Figure 26. Total Heat Flux to the Surface of Steel Equipment (Top) and Concrete (Bottom) in the Lower Compartment Predicted by HECTR Using the HECTR 15-Compartment Model (Default Calculation)

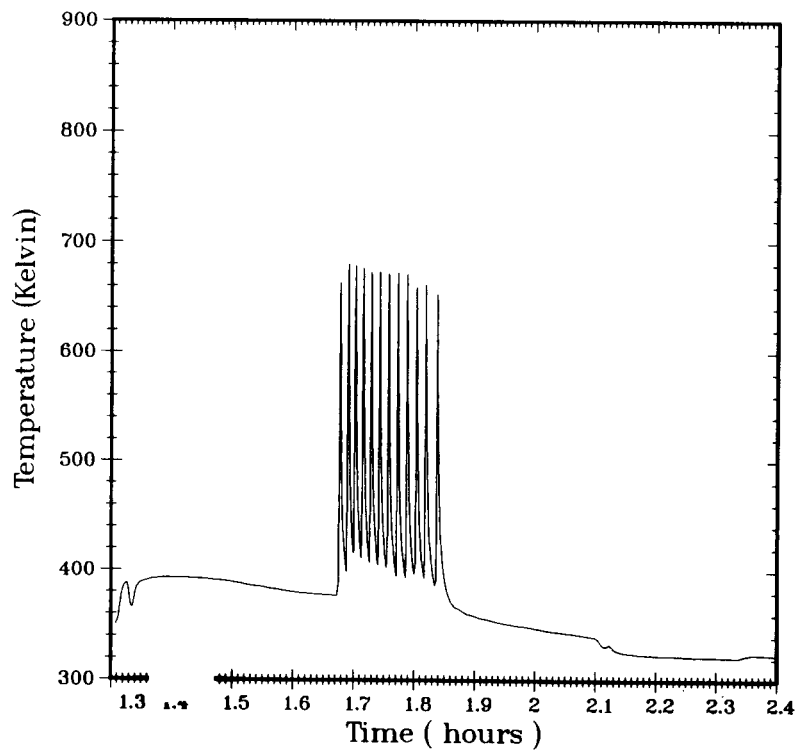
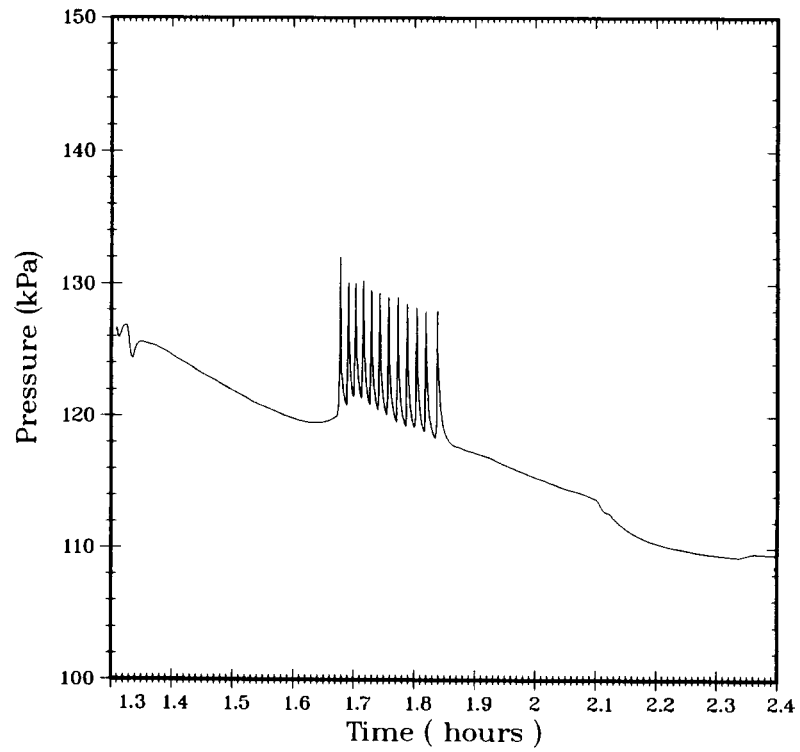


Figure 27. Pressure and Temperature Responses in the Lower Compartment Predicted by HECTR Using the HECTR 15-Compartment Model (Ignition Criterion: 6% of H₂)

temperature were slightly higher than other cases: 172.5 kPa (25 psia) and 962.7 K (Figure 28). For the study of equipment survival, there was not much heating of the surface in the upper plenum and in the dome region because the burn time was short and the degree of burning was minimal. For a different reason, the surfaces in the lower compartment did not heat up substantially either because no combustion took place in that region.

Another sensitivity study was performed to analyze 8% hydrogen combustion in the dome. Suppose that igniters in the upper plenum and in the lower compartment were not functioning or igniters did not come on until 6800 s; then 8% hydrogen would accumulate in the dome. If ignition occurred in the dome at that time, it would generate pressure and temperature spikes of 299.7 kPa (43.5 psia) and 1049.3 K, respectively (Figure 29). However, this global burn happened only in the dome and there was no flame propagation into either the lower region of the upper compartment or into the upper plenum because neither compartments never reached 9% hydrogen concentration. (Using the generation rates given by MAAP in a well-mixed environment without any combustion, HECTR predicted a hydrogen concentration of 8.4% in a dry mixture within the ice-condenser containment.)

More sensitivity studies are recommended because very large differences between HECTR and MAAP predictions could occur for other accident scenarios, especially whenever the following conditions were involved: steam inerting of one or more compartments in containment, ignition at concentrations corresponding to flame temperatures significantly higher or lower than 983 K, and combustion in plants equipped with deliberate ignition systems. Smaller differences would also result from the different models for combustion completeness and flame speeds, and for sideways and downward flame propagation. Another sensitivity studies to investigate the effect of the noding system (coarse versus fine and 1 versus 4 control volumes in the ice bed) on the hydrogen transport in reactor containment, is also important.

4.5 Summary of Findings

Overall the differences between HECTR and MAAP results can be best illustrated by comparing the HECTR calculation using a HECTR/MAAP 6-compartment model with the MAAP prediction. Both the source release rate and geometrical data are identical. The pressures predicted by the two codes are shown in Figure 30. The characteristics of the predicted combustion are very different. HECTR predicts three global deflagrations with very sharp, but brief pressure peaks. MAAP predicts a much more gradual increase in pressure, characteristics of diffusion flames rather than propagating deflagrations. In spite of the different combustion

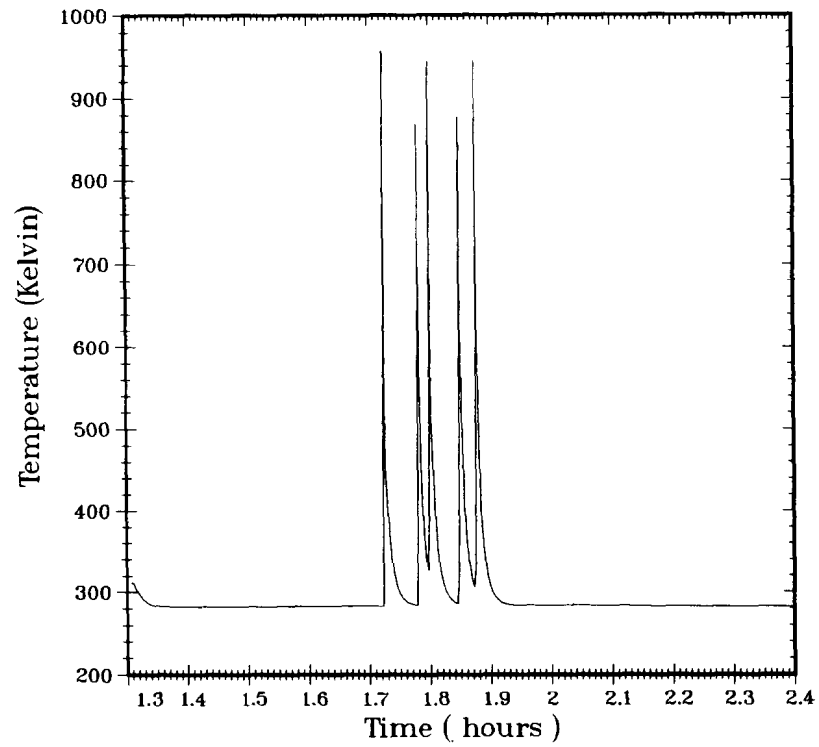
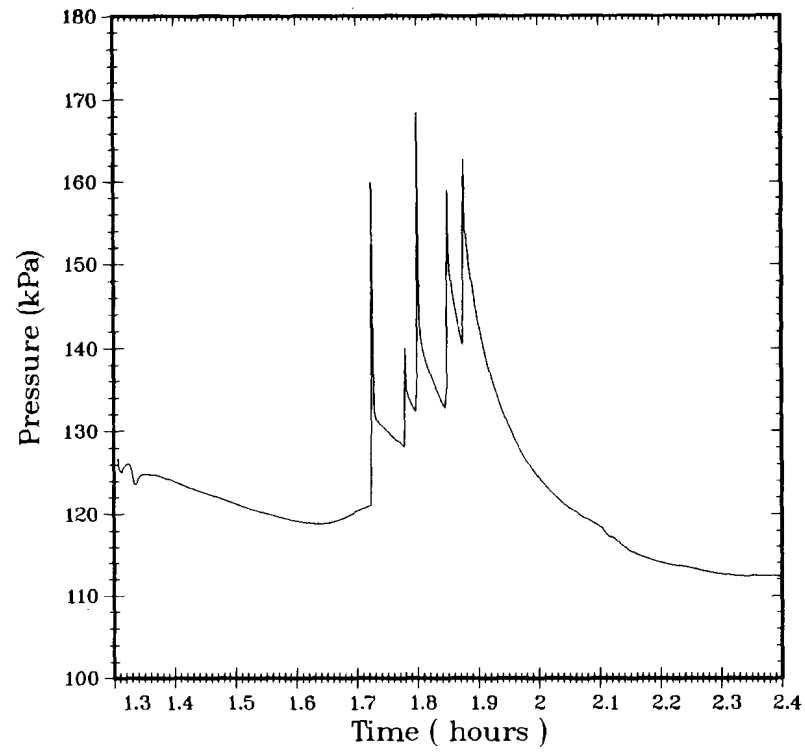


Figure 28. Pressure and Temperature Responses in the Upper Plenum Predicted by HECTR Using the HECTR 15-Compartment Model (Ignition Criterion: 8% of H₂)

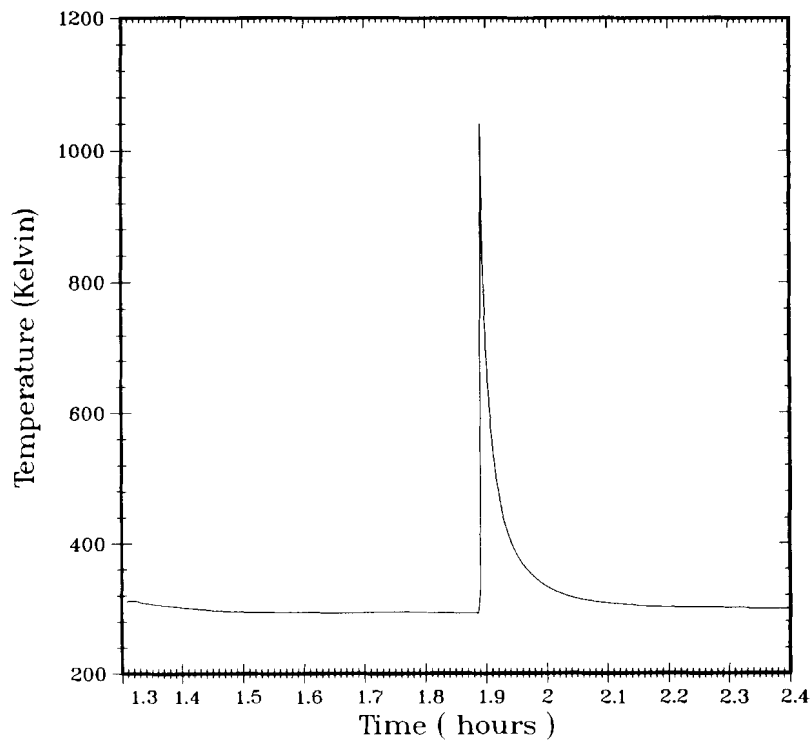
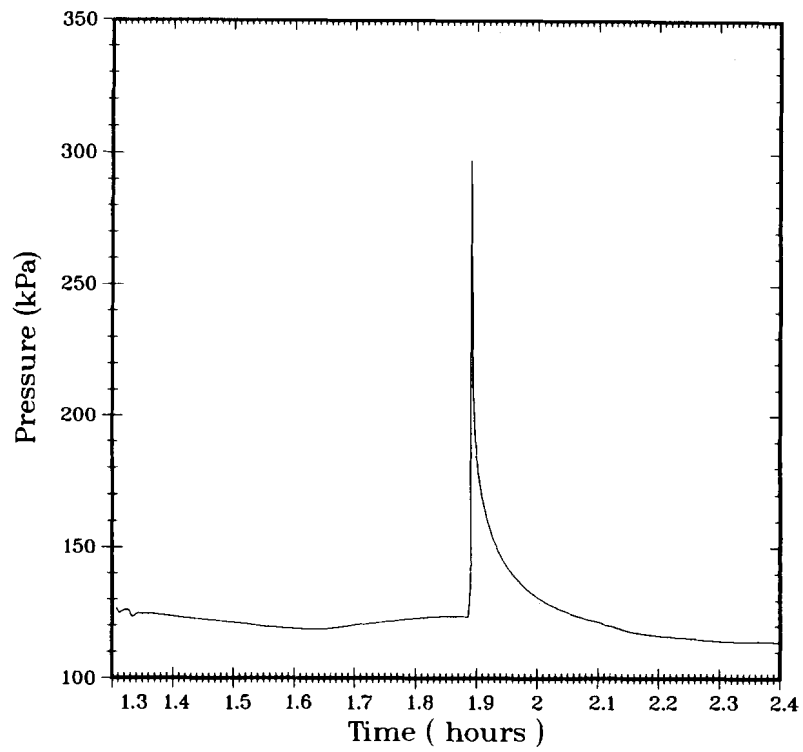


Figure 29. Pressure and Temperature Responses in the Dome Predicted by HECTR Using the HECTR 15-Compartment Model (Combustion Occurred at 8% H₂ Concentration in the Dome)

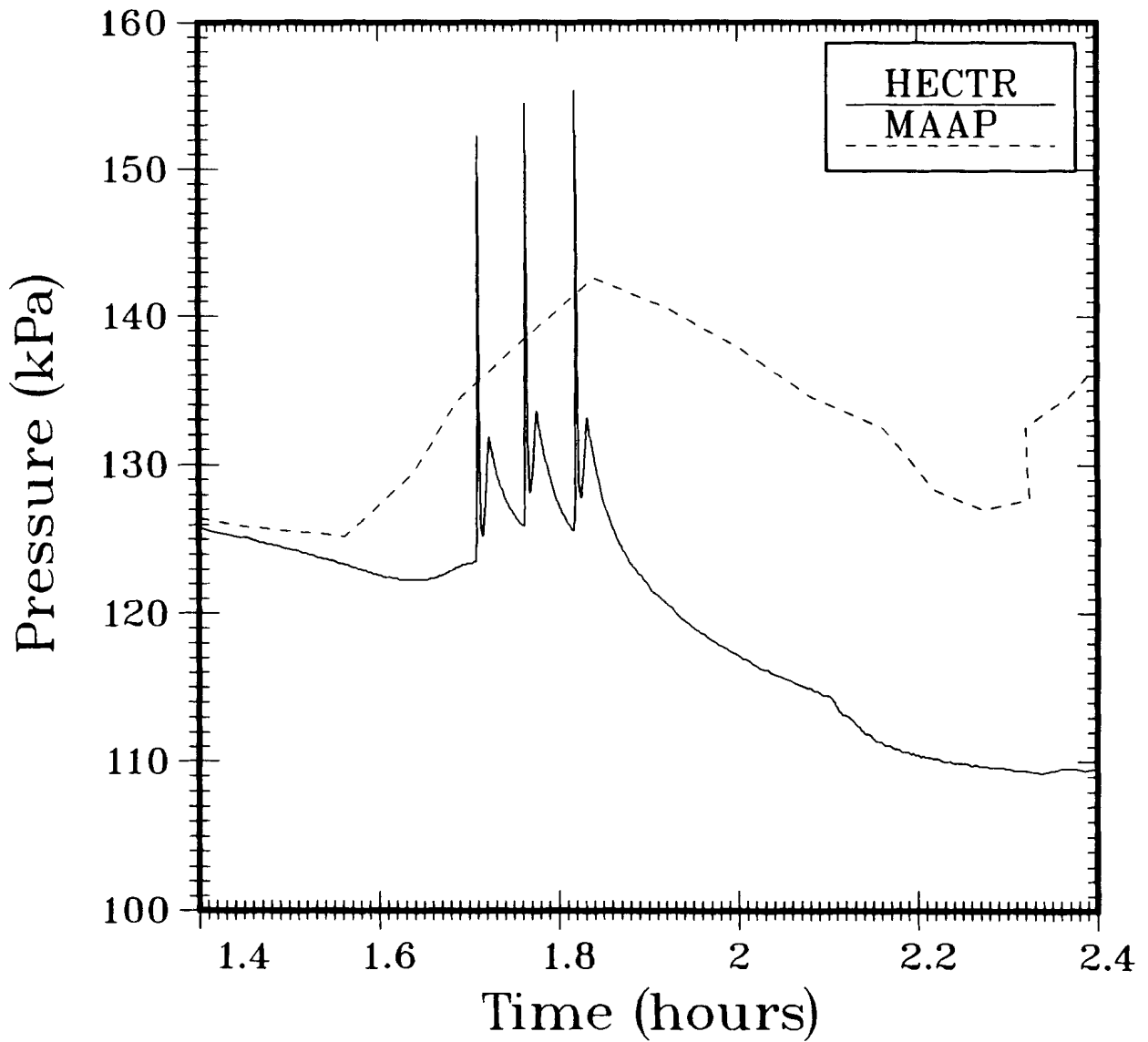


Figure 30. Pressure Comparison Between HECTR and MAAP Predictions

characteristics, the calculated peak pressures do not differ greatly: 162 kPa (23.5 psia) for HECTR versus 141 kPa (20.5 psia) for MAAP.

Temperature histories computed by the two codes are shown in Figure 31. Again, the different combustion modes lead to very different containment temperatures. However, although the differences in predicted pressure are not great, the peak temperatures computed by the two codes are very different: 821 K for HECTR versus 460 K for MAAP.

A comment on the completed HECTR analyses is that the probability of the flame at a point flashing back to the source location and burning as a diffusion flame has not been studied thoroughly. It is possible that this can happen [18 and 20], even though my first analysis shows that the flame may be unstable because of the high predicted steam-to-hydrogen mixture ratio at the break (Figure 32). More work on diffusion flame stability is recommended.

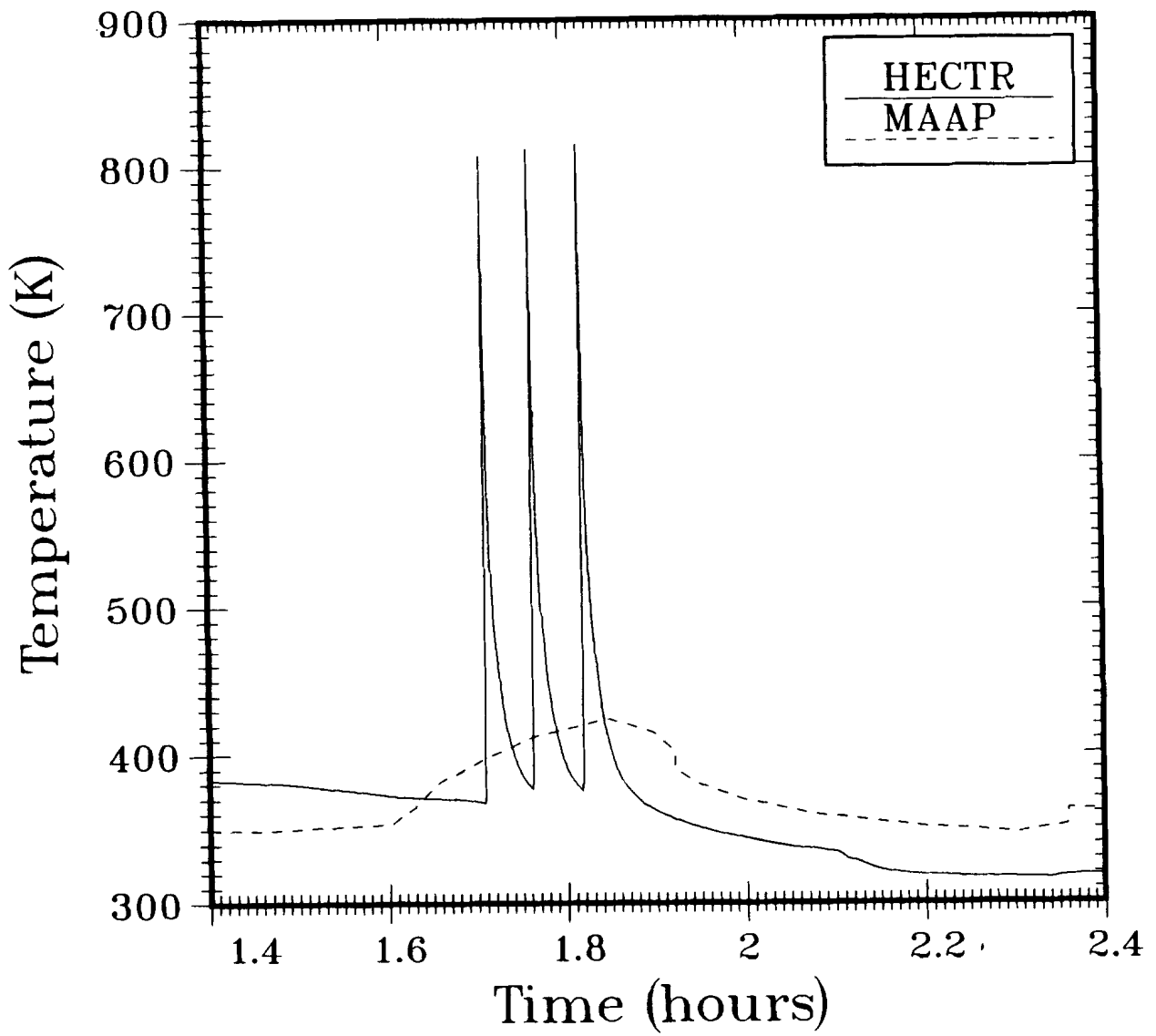


Figure 31. Temperature Comparison Between HECTR and MAAP Predictions

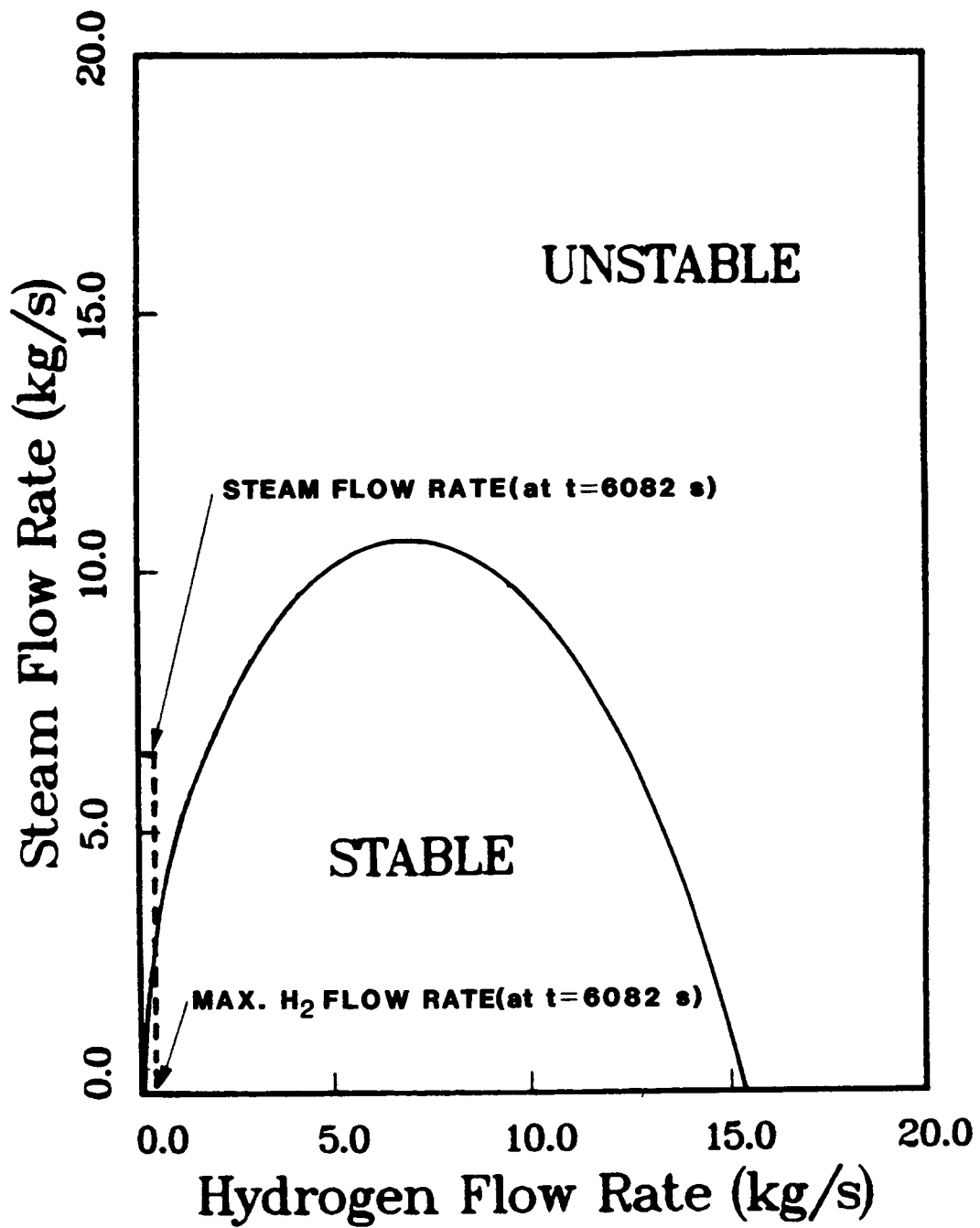


Figure 32. Calculated Stability Boundaries for a 5 cm. Diameter Jet as a Function of Hydrogen and Steam Flow Rates. Jet Fluid is at 200°C, the atmosphere is air at room temperature (p. 60 in 25).

5. CONCLUSION

The most important differences between the HECTR and MAAP calculations involve the assessment of the threat to containment integrity. MAAP does not distinguish between the clearly separate processes of flame ignition and flame propagation - ignition is defined to occur immediately upon the achievement of a particular hydrogen concentration. Global burns in MAAP can never yield pressures in excess of that corresponding to 7.3% hydrogen in dry air, because a "flame temperature criterion" is used instead of experimentally determined flammability limits and ignition thresholds. Since essentially all containments can survive combustion under these conditions, MAAP never predicts any threat. However, since ignition may be random if igniters are not operating, burns at concentrations much higher than 7.3% are possible. Furthermore, a plant may be steam inerted, which would prevent combustion at high concentrations of hydrogen developed. When the steam condensed (by natural condensation or by spray initiation), deflagrations could take place at high hydrogen concentrations. MAAP does not account for the possibility of steam inerting.

"Incomplete burns" calculated by MAAP are always inconsequential. The concentration of hydrogen is so low, and the burning rate so slow, that containment integrity is never threatened. Such predictions are not unreasonable for some accidents in IC plants. However, there are accident scenarios in which the lower compartment is steam inerted. High concentrations of hydrogen could develop, and high pressures could result from burns taking place in the dome. The MAAP predictions would be non-conservative for these scenarios.

Although HECTR relies on many empirical correlations, it allows more flexibility in examining different accident scenarios. Where processes might be random, such as ignition, HECTR permits the analyst to parametrically investigate different assumptions.

Neither HECTR nor MAAP allows for the possibility of flame acceleration or transition to detonation.

6. REFERENCES

1. A. Camp, M. Wester, and S. Dingman, HECTR Version 1.0 User's Manual, Sandia National Laboratories, Albuquerque, N.M., NUREG/CR-3913, SAND84-1522, February 1985.
2. S. Dingman, A. Camp, C.C. Wong, D. King, and R. Gasser, HECTR Version 1.5 User's Manual, Sandia National Laboratories, Albuquerque, N.M., NUREG/CR-4507, SAND86-0101, April 1986.
3. MAAP, Modular Accident Analysis Program, User's Manual - Volume II, IDCOR Technical Report 16.2-3, August 1983.
4. Sequoyah Nuclear Plant - Integrated Containment Analysis, IDCOR Task 23.1 Final Report, December 1984.
5. Letter from Marty Plys, Fauske & Associates, Inc., to C. Channy Wong, Sandia National Laboratories, Albuquerque, October 8, 1985.
6. A. Camp, V. Behr, and F. Haskin, MARCH-HECTR Analysis of Selected Accidents in an Ice-Condenser Containment, Sandia National Laboratories, Albuquerque, N.M., NUREG/CR-3912, SAND83-0501, December 1984.
7. J. O. Henrie and A. K. Postma, "Analysis of the Three Mile Island (TMI-2) Hydrogen Burn," Proceedings of the 2nd Int. Topical Meeting on Nuclear Reactor Thermal Hydraulics, Santa Barbara, CA, p. 1157, January 1983.
8. W.B. Benedick, J.C. Cummings, and P.G. Prassinis, "Experimental Results from Combustion of Hydrogen:Air Mixtures in an Intermediate-Scale Tank," in Proceedings of the Second International Conference on the Impact of Hydrogen Water Reactor Safety, NUREG/CP-0038, EPRI RP1932-35, SAND82-2456, P. 665-680, October 1982.
9. B. Lewis and G. von Elbe, Combustion, Flames and Explosions of Gases, 2nd ed., Academic Press, Inc., New York, 1961.
10. D.D. Liu, and R. MacFarlane, "Laminar Burning Velocities of Hydrogen-Air and Hydrogen-Air-Steam Flames," Combustion and Flame, Volume 49, P.59-71, 1983.
11. W.B. Benedick, J.C. Cummings, and P.G. Prassinis, Combustion of Hydrogen:Air Mixtures in the VGES Cylindrical Tank, Sandia National Laboratories, Albuquerque, N.M., NUREG/CR-3273, SAND83-1022, May 1984.
12. A.C. Ratzel, Data Analyses for Nevada Test Site (NTS) Premixed Combustion Tests, Sandia National Laboratories, Albuquerque, N.M., NUREG/CR-4138, SAND85-0135, May, 1985.

13. J.P. Holman, Thermodynamics, McGraw-Hill Book Company, Tables 2-3 and 2-3M, P. 64-65, 1980.
14. S.S. Tsai, N.J. Liparulo, J.E. Olhoeft, and D.F. Paddleford, "Flame Temperature Criteria Tests," in Proceedings of the Second International Conference on the Impact of Hydrogen Water Reactor Safety, NUREG/CP-0038, EPRI RP1932-35, SAND82-2456, P. 609-632, October 1982.
15. B.W. Marshall, Hydrogen:Air:Steam Flammability Limits and Combustion Characteristics in the FITS Vessel, Sandia National Laboratories, Albuquerque, N.M., NUREG/CR-3468, SAND84-0383, December 1986.
16. M.G. Zabetakis, Research on the Combustion and Explosion Hazards of Hydrogen-Water Vapor-Air Mixtures, Bureau of Mines, Division of Explosives Technology, Pittsburgh, PA., NTIS, USAEC Report AECU-3327, September 1957.
17. H. Tamm, R.K. Kumar, W.C. Harrison, "A Review of Recent Experiments at WNRE on Hydrogen Combustion," in Proceedings of the Second International Conference on the Impact of Hydrogen Water Reactor Safety, NUREG/CP-0038, EPRI RP1932-35, SAND82-2456, P. 633-650, October 1982.
18. L.B. Thompson, et al., Large-Scale Hydrogen Combustion Experiments, Electric Power Research Institute, Palo Alto, CA, EPRI NP-3878, Research Project 1932-11, (to be published).
19. C.C. Wong, "HECTR Analyses of Large-Scale Premixed Hydrogen Combustion Experiments," Proceedings of the International ANS/ENS Topical Meeting on Thermal Reactor Safety, San Diego, CA, Volume 2, Section XI.4, February 1986.
20. J.E. Shepherd, Analysis of Diffusion Flame Tests, Sandia National Laboratories, Albuquerque, N.M., to be published.
21. Letter Report from A.L. Camp, Sandia National Laboratories, Albuquerque, to J. Telford, U.S. Nuclear Regulatory Commission, Consensus Summary for Standard Problem 6 of the Containment Loads Working Group, June 5, 1984.
22. Letter from Marty Plys, Fauske & Associates, Inc., to C. Channy Wong, Sandia National Laboratories, Albuquerque, July 8, 1985.
23. Sequoyah Nuclear Plant, Units 1 and 2. License Application, Final Safety Analysis Report, Volume 5, Tennessee Valley Authority, DOCKET-50327-77, April, 1981.

24. S. Dingman, and A. Camp, "Pressure-Temperature Response in an Ice-Condenser Containment for Selected Accidents," Proceedings of the 13th Water Reactor Safety Research Information Meeting, Gaithersburg, Maryland, NUREG/CP-0072, Vol. 1, P. 223-243, October 22-25, 1985.
25. Letter from Marty Plys, Fauske & Associates, Inc., TO C. Channy Wong, Sandia National Laboratories, Albuquerque, July 2, 1986.
26. J.E. Shepherd, Hydrogen-Steam Jet-Flame Facility and Experiments, Sandia National Laboratories, Albuquerque, N.M., NUREG/CR-3638, SAND84-0060, February 1985.

APPENDIX A

COMPUTER PROGRAM TFLAME

A FORTRAN computer program TFLAME, which was written based on the MAAP's combustion model, was used to predict various combustion parameters for better comparison of modeling differences between HECTR and MAAP. The listing of the program is as follows:

```
PROGRAM TFLAME
C
C A FORTRAN PROGRAM TO CALCULATE FLAME TEMPERATURE
C AND EVALUATE STEAM INERTING EFFECT ACCORDING TO
C FLAME TEMPERATURE CRITERION.
C CALCULATE THE BURNING VELOCITY, FLAME SPEED,
C BURN TIME, COMBUSTION COMPLETENESS USING
C MAAP COMBUSTION MODEL
C
C INPUT: FOR005; OUTPUT: FOR006 & FOR010
C
PARAMETER (NH = 50, NS = 50)
COMMON /COMDAT/ QC, CS, CA, CH, CO, CN, XS, XH
COMMON /CONTRL/ ICPV, ITTL
DIMENSION XH2(NH), XST(NS)
REAL MWS, MWA, MWH, MWO, MWN
C
MWS = 18.016E-3
MWA = 28.966E-3
MWH = 2.0158E-3
MWO = 31.9988E-3
MWN = 28.0134E-3
RRR = 8.31434
GG = 9.80665
PI = 3.14159265
QC = 2.4181846E+5
TC = 983
C
C READ INPUT
C
WRITE(6,1000)
1000 FORMAT(' ENTER 1 FOR FLAME TEMPERATURE CALCULATION' /
*          ' ENTER 2 FOR STEAM CONCENTRATION CALCULATION' /
*          ' ENTER 3 FOR BURNING VELOCITY CALCULATION' /
*          ' ENTER 4 FOR COMBUSTION COMPLETENESS, ' /
*          ' BURN TIME, AND FLAME SPEED' /
*          ' ENTER 5 FOR BILLY FLAMMABILITY LIMIT')
READ(5,*) N
```

```

C
  WRITE(10,1100)
1100 FORMAT(' !'/' ! RESULTS FROM PROGRAM TFLAME (4/24/1986)'/
*          ' !')
C
  IF (N .EQ. 1 .OR. N .EQ. 2 .OR. N .EQ. 4) THEN
    WRITE(6,1200)
1200  FORMAT(' ENTER 0 FOR SPECIFIC HEAT AT CONSTANT'
*          ' PRESSURE'/' ENTER 1 FOR SPECIFIC HEAT AT'
*          ' CONSTANT VOLUME  ')
    READ(5,*) ICPV
    IF (ICPV .EQ. 0) THEN
      WRITE(10,1201)
1201  FORMAT(' USE SPECIFIC HEAT AT CONSTANT PRESSURE')
    ELSE
      WRITE(10,1202)
1202  FORMAT(' USE SPECIFIC HEAT AT CONSTANT VOLUME')
    END IF
C
  WRITE(6,1300)
1300  FORMAT(' ENTER 0 FOR TEMPERATURE INDEPENDENT PROPERTY'/
*          ' ENTER 1 FOR TEMPERATURE DEPENDENT PROPERTY')
  READ(5,*) ITTL
  IF (ITTL .EQ. 0) THEN
    WRITE(10,1301)
1301  FORMAT(' TEMPERATURE INDEPENDENT PROPERTY')
  ELSE
    WRITE(10,1302)
1302  FORMAT(' TEMPERATURE DEPENDENT PROPERTY')
  END IF
END IF
C
  WRITE(6,1400)
1400  FORMAT(' WHAT IS THE INITIAL TEMPERATURE (K) ?')
  READ(5,*) TI
  WRITE(10,1401) TI
1401  FORMAT(' THE INITIAL TEMPERATURE (K) = ',F8.3)
C
  WRITE(6,1500)
1500  FORMAT(' HOW MANY INPUT DATA FOR INITIAL H2'
*          ' CONCENTRATION?')
  READ(5,*) IH
  WRITE(6,1501)
1501  FORMAT(' WHAT ARE THE INITIAL H2 CONCENTRATIONS?')
  READ(5,*) (XH2(I),I=1,IH)
  WRITE(6,1502) (XH2(I),I=1,IH)
  WRITE(10,1502) (XH2(I),I=1,IH)
1502  FORMAT(' THE INITIAL H2 CONCENTRATIONS = '/10F8.3)
C
  IF (N .NE. 2 .AND. N .NE. 5) THEN

```

```

        WRITE(6,1600)
1600  FORMAT(' HOW MANY INPUT DATA FOR STEAM CONCENTRATION?')
        READ(5,*) JS
        WRITE(6,1601)
1601  FORMAT(' WHAT ARE THE INITIAL STEAM CONCENTRATIONS?')
        READ(5,*) (XST(I),I=1,JS)
        WRITE(6,1602) (XST(I),I=1,JS)
        WRITE(10,1602) (XST(I),I=1,JS)
1602  FORMAT(' THE INITIAL STEAM CONCENTRATIONS = '/10F8.3)
        END IF
C
        GO TO (100,200,300,400,500), N
100  CONTINUE
C
C CALCULATE THE FLAME TEMPERATURE
C
        WRITE(6,1610)
        WRITE(10,1610)
1610  FORMAT(3X,'H2 CONC      STEAM CONC      INIT TEMP      FLAME TEMP'/
*      ,3X,'                      (K)          (K)')
        DO 170 I = 1, IH
            XH = XH2(I)
            DO 170 J = 1, JS
                XS = XST(J)
                CALL SUB0(TI,TF)
                WRITE(6,1611) XH,XS,TI,TF
                WRITE(10,1611) XH,XS,TI,TF
1611  FORMAT(4F12.4)
170  CONTINUE
        STOP
C
200  CONTINUE
        WRITE(6,2200)
2200  FORMAT(' WHAT IS THE STEAM CORRECTION FACTOR?')
        READ(5,*) SCR
        WRITE(10,2201) SCR
2201  FORMAT(' THE STEAM CORRECTION FACTOR = ',F8.3)
        WRITE(6,2206)
        WRITE(10,2206)
2206  FORMAT(' H2 CONC.  REQUIRED STEAM CONC.  ')
C
C CALCULATE THE STEAM CONCENTRATION REQUIRED TO INERT
C
        DO 250 I=1,IH
            XH = XH2(I)
            X1 = -999.9
            X2 = -999.9
            CALL SUB0(TI,TF)
            CALL SUB1(AAO,AA1,BB1,TF)
            AA = AAO*SCR*100

```

```

        BB = AAO*TC + (BB1+AA1)*SCR*100
        CC = AA1*TC + BB1*TC
        CALL SUB1(AAO,AA1,BB1,TI)
        BB = BB - AAO*TI
        CC = CC - AA1*TI - XH*QC
        CALL SUB3(AA,BB,CC,X1,X2)
        WRITE(6,2207) XH,X1,X2
        WRITE(10,2207) XH,X1,X2
2207   FORMAT(3F10.4)
250    CONTINUE
        STOP
C
C   BURNING VELOCITY
C
300    CONTINUE
        WRITE(6,3100)
        WRITE(10,3100)
3100   FORMAT('   H2 CONC.   STEAM CONC.   BURNING VELOCITY '/
*
*                                     (M/S) ')
        DO 350 I=1,IH
            XH = XH2(I)
            DO 350 J=1,JS
                XS = XST(J)
                CALL SUB2(BURNV,TI)
                WRITE(6,3201) XH, XS, BURNV
                WRITE(10,3201) XH, XS, BURNV
3201   FORMAT(2F10.3,F15.6)
350    CONTINUE
        STOP
C
C   CALCULATE THE COMBUSTION COMPLETENESS, BURN TIME,
C   AND FLAME SPEED
C
400    CONTINUE
        WRITE(6,4100)
4100   FORMAT(' ENTER INITIAL PRESSURE (Pa) ')
        READ(5,*) P0
        WRITE(6,4101) P0
        WRITE(10,4101) P0
4101   FORMAT(' INITIAL PRESSURE (Pa) = ',E10.4)
C
        WRITE(6,4200)
4200   FORMAT(' ENTER FLAME DRAG COEFFICIENT ')
        READ(5,*) CD
        WRITE(6,4201) CD
        WRITE(10,4201) CD
4201   FORMAT(' FLAME DRAG COEFFICIENT = ',F10.4)
C
        WRITE(6,4210)
4210   FORMAT(' ENTER BURN VELOCITY MULTIPLIER ')

```

```

      READ(5,*) SCU
      WRITE(6,4211) SCU
      WRITE(10,4211) SCU
4211 FORMAT(' BURN VELOCITY MULTIPLIER =',F10.4)
C
      WRITE(6,4220)
4220 FORMAT(' ENTER THE CHARACTERISTIC LENGTH (M)')
      READ(5,*) CL
      WRITE(10,4221) CL
4221 FORMAT(' CHARACTERISTIC LENGTH (M) =',F8.3)
C
      WRITE(6,4300)
4300 FORMAT(' VESSEL GEOMETRY: ENTER 0 FOR SPHERICAL'/
*           ' 1 FOR CYLINDRICAL')
      READ(5,*) IG
      IF (IG .EQ. 0) THEN
        WRITE(10,4401)
4401  FORMAT(' VESSEL GEOMETRY : SPHERICAL')
        WRITE(6,4402)
4402  FORMAT(' WHAT IS THE DIAMETER OF THE VESSEL (m) ?')
        READ(5,*) DD
        WRITE(10,4403) DD
4403  FORMAT(' THE DIAMETER OF THE VESSEL (M) = ',F8.3)
        RR = DD/2
        VOLT = 4/3*PI*RR**3
      ELSE
        WRITE(10,4501)
4501  FORMAT(' VESSEL GEOMETRY : CYLINDRICAL')
        WRITE(6,4502)
4502  FORMAT(' WHAT IS THE CX DIAMETER OF THE VESSEL (M) ?')
        READ(5,*) DD
        WRITE(10,4503) DD
4503  FORMAT(' THE CX DIAMETER OF THE VESSEL (M) = ',F8.3)
        RR = DD/2
        WRITE(6,4504)
4504  FORMAT(' WHAT IS THE HEIGHT OF THE VESSEL (M) ?')
        READ(5,*) HT
        WRITE(10,4505) HT
4505  FORMAT(' THE HEIGHT OF THE VESSEL (M) = ',F8.3)
        VOLT = PI*RR*RR*HT
      END IF
      WRITE(6,4600)
      WRITE(10,4600)
4600 FORMAT(3X,'XH',5X,'XS',6X,'PI',7X,'TI',5X,'TFLAME',3X,
*          'B-VEL.',3X,'B-TIME',3X,'V-FLAME',2X,'COMBUSTION',
*          4X,'MAAP FV'/17X,'(Pa)',6X,'(K)',5X,'(K)',5X,
*          '(m/s)',5X,'(s)',6X,'(m/s)',3X,'COMPLETENESS',
*          4X,'(m/s)')
C
      IFLAG = ICPV

```

C

```
DO 490 I=1, IH
  XH = XH2(I)
  DO 490 J=1, JS
    XS = XST(J)
    XA = 1 - XS - XH
    CALL SUB2(BURNV, TI)
    IF (BURNV .LE. 0.0) GO TO 485
    TMW = XS*MWS + XA*MWA + XH*MWH
    RHOU = PO*TMW/(RRR*TI)
    CALL SUBO(TI, TF)
```

C

```
IF (TF .LT. 983) THEN
  TMW = (XS+XH)*MWS + XA*MWA - 0.5*XH*MWO
  RHOB = PO*TMW/(RRR*TF)
  FVEL = BURNV*RHO/RHOB
  DUM1 = (1 - RHOB/RHO)*FVEL*GG/CD
  A1 = 0.333333
  A2 = 0.666667
  A3 = 1.058267*DUM1
  DUM2 = A3**A1
  BURNT = CL**A2 / DUM2
  VFLAM = DUM2 * CL**A1
  IF (IG .EQ. 0) THEN
    ANGL = ATAN(FVEL/VFLAM)
    AA = 1
    BB = -2*(CL-RR)*COS(ANGL)
    CC = CL*CL - 2*CL*RR
    CALL SUB3(AA, BB, CC, X1, X2)
    XX = MAX(X1, X2)
    RB = XX*SIN(ANGL)
    TB = RB/FVEL
    YY = CL - XX*COS(ANGL)
    IF (YY .LE. RR) THEN
      VOLB1 = PI*YY*YY*(RR-YY/3)
    ELSE
      YZ = 2*RR - YY
      VOLB1 = PI*YZ*YZ*(RR-YZ/3)
      VOLB1 = 4*PI*RR**3 / 3 - VOLB1
    END IF
  ELSE
    TB = RR/FVEL
    If (TB .LT. BURNT) THEN
      YY = 1.088662*SQRT(DUM1)*TB**1.5
      VOLB1 = PI*RR*RR*(CL-YY)
    ELSE
      TB = BURNT
      VOLB1 = 0.0
    END IF
  END IF
```

```

VOLB2 = 0.46657*PI*SQRT(DUM1)*FVEL*FVEL*TB**3.5
VOLB = VOLB1+VOLB2
CC = VOLB/VOLT
ELSE
  ICPV = 1
  CALL SUBO(TI,TF)
  ICPV = IFLAG
  TMW = (XS+XH)*MWS + XA*MWA - 0.5*XH*MWO
  RHOB = PO*TMW/(RRR*TF)
  FVEL = BURNV*RHOH/RHOB
  DUM1 = (1 - RHOB/RHOH)*FVEL*GG/CD
  BURNT = RR/FVEL
  VFLAM = CL/BURNT
  CC = 1.0
END IF
WRITE(6,4601) *
XH,XS,PO,TI,TF,BURNV,BURNT,VFLAM,CC,FVEL
WRITE(10,4601) *
XH,XS,PO,TI,TF,BURNV,BURNT,VFLAM,CC,FVEL
4601  FORMAT(2F7.3,E10.3E1,6E9.3E1,E14.3E1)
GO TO 486
485  WRITE(6,4851) XH,XS,PO,TI,BURNV
4851  FORMAT(2F7.3,E10.2,E9.2/' BURNING VELOCITY (M/S)'
*      ' = ',E9.2)
      BURNV = 0.0
      BURNT = 9.99E+9
      VFLAM = 0.0
      CC = 0.0
      WRITE(10,4601) XH,XS,PO,TI,TF,BURNV,BURNT,VFLAM,CC
486  CONTINUE
490  CONTINUE
STOP
C
500  CONTINUE
      WRITE(6,5100)
      WRITE(10,5100)
5100  FORMAT(' BILLY FLAMMABILITY LIMIT DATA'/
*        ' XH XS')
      DO 560 I=1,IH
        XH = XH2(I)
        XHH = XH*100
        A1 = -0.007*XHH
        A2 = -0.488*XHH
        XSS = 100 - XHH - 37.3*EXP(A1) - 518.0*EXP(A2)
        XS = XSS/100
        WRITE(6,5101) XH,XS
        WRITE(10,5101) XH,XS
5101  FORMAT(2F8.4)
560  CONTINUE
      END

```

```

C
C SUBROUTINE SUBO
C
C     SUBROUTINE SUBO(TI,TF)
C     COMMON /COMDAT/ QC, CS, CA, CH, CO, CN, XS, XH
C     COMMON /CONTRL/ ICPV, ITTL
C
C     IMAX = ITTL*100
C     ICOUNT = 0
C     TM = TI
10  ICOUNT = ICOUNT + 1
C     CALL SUB1(AAO,AA1,BB1,TM)
C     A1 = AAO*XS + AA1
C     A2 = QC*XH + A1*TI
C     A3 = BB1 + A1
C     TF = A2/A3
C     CHECK = (TF-TM)/TF
C     IF (ABS(CHECK) .LE. 0.001 .OR. ICOUNT .GE. IMAX) RETURN
C     TM = 0.5*(TF+TM)
C     GO TO 10
C     END
C
C SUBROUTINE SUB1
C
C     SUBROUTINE SUB1(AAO,AA1,BB1,TM)
C     COMMON /COMDAT/ QC, CS, CA, CH, CO, CN, XS, XH
C     COMMON /CONTRL/ ICPV, ITTL
C     SRTM= SQRT(TM)
C     CS = 83.15 - 1863/SRTM + 17445/TM
C     CH = 24.12 + 4.356E-3*TM + 62.41/SRTM
C     CO = 48.212 - 536.8/SRTM + 3559/TM
C     CN = 39.65 - 8071/TM + 1.5E+6/(TM*TM)
C
C     IF (ICPV .EQ. 1) THEN
C         CS = CS/1.33
C         CH = CH/1.41
C         CO = CO/1.40
C         CN = CN/1.40
C     END IF
C
C     CA = 0.79*CN + 0.21*CO
C
C     AAO = CS - CA
C     AA1 = CA + XH*(CH-CA)
C     DUM = CS - 0.5*CO - CH
C     BB1 = XH*DUM
C     RETURN
C     END
C

```

```

C SUBROUTINE SUB2
C
SUBROUTINE SUB2(BURNV, TI)
COMMON /COMDAT/ QC, CS, CA, CH, CO, CN, XS, XH
COMMON /CONTRL/ ICPV, ITTL
A11 = 4.644E-4
A22 = -2.119E-3
A33 = 2.344E-3
A44 = 1.571
A55 = 3.839E-1
A66 = -2.21
DDO = 0.42-XH
DD1 = A44 + A55*DDO
BURNV = A11 + A22*DDO + A33*DDO*DDO
BURNV = BURNV * TI**DD1 * EXP(A66*XS)
RETURN
END

C
C SUBROUTINE SUB3 : SOLVE LINEAR OR QUADRATIC EQUATION
C
SUBROUTINE SUB3(AA, BB, CC, X1, X2)
COMMON /COMDAT/ QC, CS, CA, CH, CO, CN, XS, XH
COMMON /CONTRL/ ICPV, ITTL
C
IF (AA .EQ. 0.) THEN
  IF (BB .NE. 0.) X1 = -CC/BB
  X2 = X1
ELSE
  D1 = 0.5*BB/AA
  D2 = D1*D1 - CC/AA
  IF (D2 .GE. 0) THEN
    D3 = 0.5*BB/AA
    X1 = -D3 - SQRT(D2)
    X2 = -D3 + SQRT(D2)
  ELSE
    WRITE(6, 1000)
    WRITE(10, 1000)
    1000 FORMAT('NO REAL ROOT')
  END IF
END IF
RETURN
END

```


C6 - SG DOGHOUSE
 1450.0 26.95 13.58 2 2 2
 C7 - ANNULUS
 2662. 10.56 13.30 2 2 2
 C8 - LOWER PLENUM
 679.3 18.75 3.5 3 3 3
 C9 - UPPER PLENUM
 1330. 37.60 9.0 1 3 3
 C10 - UPPER COMPARTMENT - DOME
 12764.78 44.20 17.53 3 4 4
 C11 - LOWER DOME
 4593.07 27.71 13.89 2 4 4

! FOR EACH SUMP, SUMP NUMBER, MAXIMUM VOLUME, SUMP NUMBER THAT
 ! THIS SUMP OVERFLOWS TO

!
 1 396. 2 ! SUMP IN REACTOR CAVITY
 2 1450. 1 ! LOWER COMPARTMENT SUMP
 3 16.50 2 ! LOWER PLENUM SUMP (2 INCH DEPTH)
 4 1300. 0 ! REFUELING CANAL SUMP (2 INCH DEPTH - NO SPRAYS)

\$

!

! FOR EACH SURFACE: TYPE OF SURFACE, MASS OF SURFACE, AREA OF
 ! SURFACE, CHARACTERISTIC LENGTH, SPECIFIC HEAT, EMISSIVITY,
 ! INTEGER INDICATING WHICH SUMP THE CONDENSATE GOES INTO. FOR
 ! SLABS (STYPE = 1), THE NUMBER OF LAYERS IN THE SURFACE, AND FOR
 ! EACH, THE THICKNESS, THERMAL DIFFUSIVITY, AND THERMAL
 ! CONDUCTIVITY. FINALLY, THE NODING INFORMATION AND BOUNDARY
 ! CONDITIONS ARE SPECIFIED (O'S INDICATE THE CODE WILL DETERMINE
 ! THE VALUES INTERNALLY). NOTE THAT SOME OF THE NUMBERS SET TO 1.
 ! ARE NOT USED FOR THAT SURFACE TYPE.

!

! REACTOR CAVITY - C1 - SURFACE 1

!

SUMP 1

3 559.82 59.20 5.18 1.0 0.94 1

!

! REACTOR SPACE - C2 - SURFACES 2 - 3

!

RS STEEL

1 1. 207.93 1.83 1. 0.9 1

1

0.069 1.28E-5 47.25

0 0. 0. 0.

!

RS CONCRETE

1 1. 247.36 9.14 1. 0.9 1

1

1. 5.8E-7 1.454

0 0. 0. 0.

!

! LOWER COMPARTMENT- C3 - SURFACES 4 - 6

!

LC1 STEEL

1 1. 611. 2. 1. 0.9 2

1

0.069 1.28E-5 47.25

0 0. 0. 0.

!

LC1 CONCRETE

1 1. 726.87 2. 1. 0.9 2

1

0.1 5.8E-7 1.454

0 0. 0. 0.

!

LC1 SUMP

3 1.32E5 105.9 11. 1. 0.94 2

!

! PRESSURIZER - C4 - SURFACES 7 - 8

!

PR STEEL

1 1. 63.94 1. 1. 0.9 2

1

0.069 1.28E-5 47.25

0 0. 0. 0.

!

PR CONCRETE

1 1. 76.07 1. 1. 0.9 2

1

0.1 5.8E-7 1.454

0 0. 0. 0.

!

! LOWER COMPARTMENT- C5 - SURFACES 9 - 11

!

LC2 STEEL

1 1. 1430.37 2. 1. 0.9 2

1

0.069 1.28E-5 47.25

0 0. 0. 0.

!

LC2 CONCRETE

1 1. 1701. 2. 1. 0.9 2

1

0.1 5.8E-7 1.454

0 0. 0. 0.

!

LC2 SUMP

3 3.09E5 247. 10.67 1. 0.94 2

!

! STEAM GENERATOR ENCLOSURES (INSIDE) - C6 - SURFACES 12 - 13

!

SG STEEL

1 1. 686.77 1. 1. 0.9 2
1
.069 1.28E-5 47.25
0 0. 0. 0.

!

SG CONCRETE

1 1. 817.03 1. 1. 0.9 2
1
0.1 5.8E-7 1.454
0 0. 0. 0.

!

! ANNULUS AROUND LOWER COMPARTMENT - C7 - SURFACES 14 - 15

!

A STEEL

1 1. 1834. 4. 1. 0.9 2
1
0.031 1.28E-5 47.25
0 0. 0. 0.

!

A CONCRETE

1 1. 3257. 4. 1. 0.9 2
1
0.448 5.8E-7 1.454
0 0. 0. 0.

!

! LOWER PLENUM COMPARTMENTS - C8 - SURFACES - 16 - 18

!

LP SUMP

3 5719.0 310.0 4. 1. 0.94 3

!

LP WALL

1 1. 280. 3. 1. 0.9 3
1
0.013 1.28E-5 47.25
0 0. 0. 0.

!

LP IC SUPPORT

1 1. 2660. 0.2 1. 0.9 3
1
0.0081 1.28E-5 47.25
0 0. 0. 0.

!

! UPPER PLENUM COMPARTMENTS - C9 - SURFACES 19

!

UP STEEL

1 1. 1000. 5. 1. 0.9 3
1
0.013 1.28E-5 47.25
0 0. 0. 0.

!
! UPPER COMPARTMENTS - C10 - SURFACES 20 - 22
!

UC DOME

1	1.	1762.	8.	1.	0.9	4
1						
0.0127		1.28E-5	47.25			
0	0.	5.	300.			

!
UC CONCRETE

1	1.	648.73	5.	1.	0.9	4
1						
0.91		5.8E-7	1.454			
0	0.	0.	0.			

!
UC STEEL

1	1.	2000.	1.	1.	0.9	4
1						
0.013		1.28E-5	47.25			
0	0.	0.	0.			

!
! LOWER DOME REGION - C11 - SURFACE 23
!

LDR CONCRETE

1	1.	1822.14	14.	1.	0.9	4
1						
0.91		5.8E-7	1.454			
0	0.	0.	0.			

!
! REFUELING CANAL SPACE - C11 - SURFACES 24
!

RC SUMP

3	1.259E6	67.75	6.	1.	0.94	4
---	---------	-------	----	----	------	---

!
\$ NO CONTAINMENT LEAKS
!

!
! FLOW JUNCTION DATA: COMPARTMENT ID'S, TYPE OF CONNECTION, FLOW
! AREA, LOSS COEFFICIENT, L/A RATIO, RELATIVE POSITION OF
! COMPARTMENTS, AND JUNCTION ELEVATION. COMPARTMENT ID OF 0
! INDICATES THE ICE CONDENSER. JUNCTIONS WITHIN THE ICE
! CONDENSER ARE SET UP INTERNALLY. ADDITIONAL INFORMATION IS !
! PROVIDED FOR JUNCTION TYPES 3 AND 4.
!

1	3	1	3.34	3.	2.56	1	4.50
1	2	1	0.929	10.	13.12	1	6.00
2	3	1	7.45	4.	0.94	0	19.47
2	5	1	15.04	4.	0.47	0	19.47
3	7	1	8.80	4.2	0.68	0	10.60
3	8	3	29.64	1.	0.20	1	19.00
0.	0.		142.07	0.96			

3	4	1	4.30	1.0	3.42	1	20.00
3	4	1	4.30	1.0	3.42	1	20.32
3	5	1	93.50	5.	0.17	0	12.30
5	7	1	18.89	4.2	0.32	0	10.60
5	8	3	69.16	1.	0.087	1	19.00
0.	0.	142.	07	0.96			
5	6	1	31.72	1.1	0.46	1	20.00
5	6	1	31.71	1.1	0.46	1	20.32
8	-1	1	91.88	1.	0.038	1	20.42
-1	9	1	1.86	10.	2.30	1	35.05
-1	9	3	91.30	1.	0.047	1	35.05
0.	263.	4	37910.	1.55			
9	10	1	186.00	1.	0.035	1	40.16
10	11	1	363.12	1.	0.045	-1	34.65
11	5	4	0.204	1.5	10.00	1	7.86
2	750.						
10	7	1	0.0022	10.	2277.0	-1	10.60

\$

!

! ICE CONDENSER INPUT

!

! NUMBER OF LOWER PLENUM AND UPPER PLENUM COMPARTMENTS

1 1

! UPPER PLENUM COMPARTMENTS

9

! LOWER PLENUM COMPARTMENTS AND THE SUMPS THEY DRAIN INTO

8 3

! LOWER PLENUM COMPARTMENT THAT EACH STACK DRAINS INTO

8

! ICE DESCRIPTION: TOTAL MASS, AREA, TEMPERATURE, LENGTH,
! EMISSIVITY, VOLUME.

5.449E5 1.5433E4 263.56 14.63 .94 594.23

! WALL AND STRUCTURES IN ICE CONDENSER (EXCLUDING BASKETS): MASS,
! AREA, SPECIFIC HEAT, EMISSIVITY

2.0E5 2058. 485.7 .9

! MASS OF BASKETS, AREA OF BASKETS, DRAIN TEMPERATURE.

1.47E5 9.92E3 310.

! ELEVATION OF BOTTOM OF ICE, TOTAL FREE GAS VOLUME, INITIAL
! VERTICAL FLOW AREA, VERTICAL FLOW AREA WITH ICE GONE, LOSS
! COEFFICIENTS FOR VERTICAL FLOW WITH AND WITHOUT ICE, FLOW AREA
! WITH AND WITHOUT ICE FOR CROSS FLOW, LOSS COEFFICIENTS FOR
! CROSS FLOW WITH AND WITHOUT ICE, L/A FOR CROSS FLOW

19. 3060.2

167. 167. 1.0 1.0

7.9 7.9 3.0 3.0 0.4

!

\$ NO SUPPRESSION POOL

!

! FAN DATA

! TEMP. AND PRESS. SETPOINTS, DELAY TIME, AND TIME TO TURN OFF.

! HIGH VALUE FOR TEMP. SETPOINT INDICATES THAT VALUE WON'T BE
! USED.

10000. 121590. 600. 1.E10

! COMPARTMENT ID'S, FLOW RATE (- INDICATES USE OF HEAD CURVE),
! SHUTOFF

! HEAD (PA), EFFICIENCY, RELATIVE POSITION OF COMPARTMENTS.

11 7 -35.54 1327.3575 1. -1

10 7 0.9439 1327.3575 1. -1

6 7 0.1775 1327.3575 1. -1

4 7 0.7079 1327.3575 1. -1

2 7 0.2832 1327.3575 1. -1

! SHUTOFF

! HEAD (PA), EFFICIENCY, RELATIVE POSITION OF COMPARTMENTS.

\$ END OF FANS TABLE

\$ END OF FANS INPUT

\$ NO FAN COOLERS

! RADIATIVE BEAM LENGTHS - UPPER RIGHT HALF OF MATRIX IS INPUT.
! ICE SURFACES ARE NOT INCLUDED HERE. (THEY ARE DONE INTERNALLY)

! BEAM LENGTHS

24.08108	23*0.0		
3.471194	3.471194	21*0.0	
3.471194	21*0.0		
3.216579	3.216579	3.216579	18*0.0
3.216579	3.216579	18*0.0	
3.216579	18*0.0		
3.471181	3.471181	16*0.0	
3.471181	16*0.0		
3.218120	3.218120	3.218120	13*0.0
3.218120	3.218120	13*0.0	
3.218120	13*0.0		
3.471206	3.471206	11*0.0	
3.471206	11*0.0		
1.882381	1.882381	9*0.0	
1.882381	9*0.0		
0.7587692	0.7587692	0.7587692	6*0.0
0.7587692	0.7587692	6*0.0	
0.7587692	6*0.0		
4.788000	5*0.0		
10.41850	10.41850	10.41850	2*0.0
10.41850	10.41850	2*0.	
10.41850	2*0.0		
9.484990	9.484990		
9.484990			

! VIEW FACTORS

! 1.000000 23*0.0

0.4566979	0.5433021	21*0.0	
0.5433021	21*0.0		
0.4231976	0.5034528	7.3349632E-02	18*0.0
0.5034528	7.3349632E-02	18*0.0	
7.3349714E-02	18*0.0		
0.4566817	0.5433183	16*0.0	
0.5433183	16*0.0		
0.4233906	0.5034972	7.3112182E-02	13*0.0
0.5034972	7.3112175E-02	13*0.0	
7.3112249E-02	13*0.0		
0.4566897	0.5433103	11*0.0	
0.5433103	11*0.0		
0.3602436	0.6397564	9*0.0	
0.6397564	9*0.0		
9.5384613E-02	8.6153843E-02	0.8184615	6*0.0
8.6153850E-02	0.8184615	6*0.0	
0.8184615	6*0.0		
1.000000	5*0.0		
0.3994804	0.1470800	0.4534397	2*0.0
0.1470800	0.4534397	2*0.0	
0.4534397	2*0.0		
0.9641514	3.5848647E-02		
3.5848618E-02			

!

! SPRAY INPUT

! NUMBER OF COMPARTMENTS WITH SPRAYS, AND ID OF THOSE

! COMPARTMENTS. SPRAY TEMP DURING INJECTION PHASE, FLOW RATE

! (M**3/S), NUMBER OF DROP SIZES, FREQUENCY AND DIAMETER

! (MICRONS) FOR EACH DROP SIZE.

1

10 313.56 0.593 2

0.95 309.

0.05 810.

! SPRAY CARRYOVER

10 11 1.

11 12 0.13

\$

! COMPARTMENT ID AND SPRAY FALL HEIGHT FOR THAT COMPARTMENT.

10 14.72

11 13.88

12 12.87

\$

! TEMPERATURE AND PRESSURE SETPOINTS, DELAY TIME FOR SPRAYS,

! TIME THAT SPRAYS REMAIN OPERATIVE AFTER INITIATION.

! HIGH TEMPERATURE INDICATES THAT NUMBER WON'T BE USED.

10000. 121590. 30. 1.E10

! INJECTION TIME, RATED SPRAY FLOW RATE (KG/S), HEAT EXCHANGER

! RATED EFFECTIVENESS (W/K), SECONDARY SIDE INLET TEMP, RATED

! SECONDARY SIDE FLOW RATE (KG/S), SUMP THAT WATER IS DRAWN FROM.

! (FROM MARCH-HECTR REPORT) 2000. 587. 3.74E6 301.5

7.55E2 2

```

$ NO SPRAY RECIRCULATION (S2HF ACCIDENT SCENERIO)
$
! *****
! ENTER INITIAL CONDITIONS AND ACCIDENT SCENARIO INFORMATION
! *****
! SIMULATION TIME
4000.
!
! COMPARTMENT INITIAL CONDITIONS: TEMP; PARTIAL PRESSURES OF
! STEAM, NITROGEN, OXYGEN, HYDROGEN, CARBON MONOXIDE,
! CARBON DIOXIDE ; CONVECTIVE VELOCITY.
!
! C1 - CAVITY
348.83  40183.  69218.  17304.  0.  0.  0.  0.3
! C2 - REACTOR SPACE
349.98  42169.  67413.  16854.  0.  0.  0.  0.3
! C3 - LOWER COMP 1 (PRESSURIZER)
349.98  42169.  67413.  16854.  0.  0.  0.  0.3
! C4 - PRESSURIZER SPACE
349.98  42169.  67413.  16854.  0.  0.  0.  0.3
! C5 - LOWER COMP 2 (STEAM GENERATOR)
349.98  42169.  67413.  16854.  0.  0.  0.  0.3
! C6 - STEAM GEN DOGHOUSES
349.98  42169.  67413.  16854.  0.  0.  0.  0.3
! C7 - ANNULUS
310.92   6617.  96087.  24022.  0.  0.  0.  0.3
! C8 - LOWER PLENUM
349.98  42169.  67413.  16854.  0.  0.  0.  0.3
! C9 - UPPER PLENUM
310.94   6628.  96078.  24020.  0.  0.  0.  0.3
! C10 - UPPER COMPARTMENT
310.97   6631.  96080.  24021.  0.  0.  0.  0.3
! C11 - LOWER DOME REGION
310.97   6631.  96080.  24021.  0.  0.  0.  0.3
! ICE CONDENSER INITIAL CONDITIONS
310.84   6578.  95538.  23885.  0.  0.  0.
!
! SOURCE TERMS
!
$ STEAM SOURCE FROM EXTERNAL TABLE
$ NO NITROGEN SOURCES
$ NO OXYGEN SOURCES
$ HYDROGEN SOURCE FROM EXTERNAL TABLE
$ NO CO SOURCES
$ NO CO2 SOURCES
$ NO SUMP WATER REMOVAL
$ NO ENERGY SOURCES
$ NO CONTINUOUS BURNING
!

```

! INITIAL SURFACE TEMPERATURES

!

! C1 RC

350.39

! C2 RS

342.65

345.01

! C3 LC1

342.65

345.01

342.38

! C4 PR

342.65

345.01

! C5 LC2

342.65

340.97

342.38

! C6 SG

342.65

345.01

! C7 AN

310.51

310.51

! C8 LP

330.37

345.01

342.65

! C9 UP

312.59

! C10 UC

312.58

312.58

312.59

! C11

312.58

315.18

!

! NAMELIST INPUT

!

XHMNIG(8)=1.

XHMNIG(12)=1.

XHMNIG(13)=1.

XHMNIG(14)=1.

XHMNIG(15)=1.

DTHTMX = 1.0

DTFLMX = 1.0

SPRAYS = OFF

FANS = ON

MRCHSC=5

3 1797.52 2 ! ANNULUS SUMP (13.2 FT. DEPTH)
 4 1300.0 0 ! REFUELING CANAL SUMP

\$

!

! FOR EACH SURFACE: TYPE OF SURFACE, MASS OF SURFACE, AREA OF
 ! SURFACE, CHARACTERISTIC LENGTH, SPECIFIC HEAT, EMISSIVITY,
 ! INTEGER INDICATING WHICH SUMP THE CONDENSATE GOES INTO. FOR
 ! SLABS (STYPE = 1), THE NUMBER OF LAYERS IN THE SURFACE, AND FOR
 ! EACH, THE THICKNESS, THERMAL DIFFUSIVITY, AND THERMAL
 ! CONDUCTIVITY. FINALLY, THE NODING INFORMATION AND BOUNDARY
 ! CONDITIONS ARE SPECIFIED (O'S INDICATE THE CODE WILL DETERMINE
 ! THE VALUES INTERNALLY). NOTE THAT SOME OF THE NUMBERS SET TO 1.
 ! ARE NOT USED FOR THAT SURFACE TYPE.

!

! REACTOR CAVITY - C1 - SURFACE 1 - 2

!

SUMP 1

3 559.82 60.29 5.18 1.0 0.94 1

RC CONCRETE

1 1. 234.86 5.18 854.15 0.9 1

1

1.524 7.18E-7 1.453

0 0. 0. 0.

!

! LOWER COMPARTMENT- C2 - SURFACES 3 - 8

!

LC STEEL

2 1.60E6 2780.12 2. 460.5 0.9 2

!

LC OUTER WALL - CONCRETE

1 1. 962.20 4. 854.15 0.9 2

1

0.9144 7.18E-7 1.453

0 0. 0.0 0.0

!

LC INTERIOR WALL - CONCRETE

1 1. 330.90 4. 854.15 0.9 2

1

1.8166 7.18E-7 1.453

0 0. 0.0 0.0

!

LC FLOOR - CONCRETE

1 1. 502.66 4. 854.15 0.9 2

1

3.6576 7.18E-7 1.453

0 0. 0.0 0.0

LC SUMP

3 4.41E5 502.66 4. 1. 0.94 2

!

! ANNULUS AROUND LOWER COMPARTMENT - C3 - SURFACES 8 - 9

!

A LINER CONCRETE

1 1. 1027.14 4. 854.15 0.9 3

2

0.0296 1.28E-5 47.25

0.9144 7.18E-7 1.453

0 0. 3.5033 310.78

!

A SUMP

3 486.56 446.77 4. 1. 0.94 3

!

! UPPER COMPARTMENTS - C5 - SURFACES 10 - 13

!

UC OUTER WALL - LINER CONCRETE

1 1. 1929.97 5. 854.15 0.9 4

2

0.0124 1.28E-5 47.25

0.9144 7.18E-7 1.453

0 0. 3.5033 310.78

!

UC DECK - CONCRETE

1 1. 1830.19 5. 854.15 0.9 4

1

0.7620 7.18E-7 1.453

0 0. 0.0 0.0

!B

UC EQUIPMENT - STEEL

2 1.052E5 1064.13 5. 460.5 0.9 4

!

UC SUMP

3 1.259E6 51.8863 5. 1.0 0.94 4

!

\$ NO CONTAINMENT LEAKS

!

! FLOW JUNCTION DATA: COMPARTMENT ID'S, TYPE OF CONNECTION, FLOW
! AREA, LOSS COEFFICIENT, L/A RATIO, RELATIVE POSITION OF
! COMPARTMENTS, AND JUNCTION ELEVATION. COMPARTMENT ID OF 0
! INDICATES THE ICE CONDENSER. JUNCTIONS WITHIN THE ICE
! CONDENSER ARE SET UP INTERNALLY. ADDITIONAL INFORMATION IS
! PROVIDED FOR JUNCTION TYPES 3 AND 4.

!

1 2 1 4.952 3. 2.445 1 2.984

1 2 1 1.031 10. 11.74 1 0.6675

2 3 1 27.69 1.0 0.550 0 10.60

2 -1 1 101.08 1.0 0.151 1 20.50

-1 4 1 0.1011 10. 97.40 1 35.052

-1 4 3 186.09 1.0 0.053 1 35.052

0. 263.4 37910. 1.55

4 5 1 186.09 1. 0.095 1 40.12

```

5  2  4  0.223  10.  185.9  -1  7.864
2  750.
5  3  1  0.0022  10.  2277.  -1  10.60
$
!
! ICE CONDENSER INPUT
!
! NUMBER OF LOWER PLENUM AND UPPER PLENUM COMPARTMENTS
1  1
! UPPER PLENUM COMPARTMENTS
4
! LOWER PLENUM COMPARTMENTS AND THE SUMPS THEY DRAIN INTO
2  2
! LOWER PLENUM COMPARTMENT THAT EACH STACK DRAINS INTO
2
! ICE DESCRIPTION: TOTAL MASS, AREA, TEMPERATURE, LENGTH,
! EMISSIVITY, VOLUME.
5.4491E5  1.5433E4  263.56  14.63  .94  594.23
! WALL AND STRUCTURES IN ICE CONDENSER (EXCLUDING BASKETS): MASS,
! AREA, SPECIFIC HEAT, EMISSIVITY
! (USE OLD MARCH-HECTR DATA)
2.0E5  2058.  485.7  .9
! MASS OF BASKETS, AREA OF BASKETS, DRAIN TEMPERATURE.
! (USE OLD MARCH-HECTR DATA)
1.47E5  9.92E3  310.
! ELEVATION OF BOTTOM OF ICE, TOTAL FREE GAS VOLUME, INITIAL
! VERTICAL FLOW AREA, VERTICAL FLOW AREA WITH ICE GONE, LOSS
! COEFFICIENTS FOR VERTICAL FLOW WITH AND WITHOUT ICE, FLOW AREA
! WITH AND WITHOUT ICE FOR CROSS FLOW, LOSS COEFFICIENTS FOR
! CROSS FLOW WITH AND WITHOUT ICE, L/A FOR CROSS FLOW,
! (USE OLD MARCH-HECTR DATA)
20.42  3060.2
167.  167.  1.0  1.0
7.9  7.9  3.0  3.0  0.4
!
$ NO SUPPRESSION POOL
!
! FAN DATA
! TEMP. AND PRESS. SETPOINTS, DELAY TIME, AND TIME TO TURN OFF.
! HIGH VALUE FOR TEMP. SETPOINT INDICATES THAT VALUE WON'T BE
! USED.
10000.  0.0  0.167  1.E10
! COMPARTMENT ID'S, FLOW RATE (- INDICATES USE OF HEAD CURVE),
! SHUTOFF
! HEAD (PA), EFFICIENCY, RELATIVE POSITION OF COMPARTMENTS.
5  3  37.753  1327.3575  1.  -1
$ END OF FANS TABLE
$ END OF FANS INPUT
$ NO FAN COOLERS
!
```

! RADIATIVE BEAM LENGTHS - UPPER RIGHT HALF OF MATRIX IS INPUT.
 ! ICE SURFACES ARE NOT INCLUDED HERE. (THEY ARE DONE INTERNALLY)

! BEAM LENGTHS

	5.111720	5.111720	11*0.0	
	5.111720	11*0.0		
	5.801047	5.801047	5.801047	5.801047
5.801047	6*0.0			
	5.801047	5.801047	5.801047	5.801047
6*0.0	5.801047	5.801047	5.801047	6*0.0
	5.801047	5.801047	6*0.0	
	5.801047	6*0.0		
	6.501352	6.501352	4*0.0	
	6.501352	4*0.0		
	13.60971	13.60971	13.60971	13.60971
	13.60971	13.60971	13.60971	
	13.60971	13.60971		
	13.60971			

! VIEW FACTORS

	0.2042690	0.7957310	11*0.0	
	0.7957310	11*0.0		
	0.5474251	0.1894639	6.5156519E-02	9.8977268E-02
9.8977268E-02	6*0.0			
	0.1894639	6.5156512E-02	9.8977260E-02	9.8977260E-02
6*0.0	6.5156542E-02	9.8977298E-02	9.8977298E-02	6*0.0
	9.8977245E-02	9.8977245E-02	6*0.0	
	9.8977245E-02	6*0.0		
	0.6968811	0.3031189	4*0.0	
	0.3031189	4*0.0		
	0.3957958	0.3753330	0.2182304	1.0640776E-02
	0.3753330	0.2182304	1.0640777E-02	
	0.2182304	1.0640775E-02		
	1.0640800E-02			

! SPRAY INPUT
 ! NUMBER OF COMPARTMENTS WITH SPRAYS, AND ID OF THOSE
 ! COMPARTMENTS. SPRAY TEMP DURING INJECTION PHASE, FLOW RATE
 ! (M**3/S), NUMBER OF DROP SIZES, FREQUENCY AND DIAMETER
 ! (MICRONS) FOR EACH DROP SIZE.

1
 5 313.56 0.593 1
 1.00 700
 ! SPRAY CARRYOVER

```

$ NO CARRYOVER
! COMPARTMENT ID AND SPRAY FALL HEIGHT FOR THAT COMPARTMENT.
5 28.61
$
! TEMPERATURE AND PRESSURE SETPOINTS, DELAY TIME FOR SPRAYS,
! TIME THAT SPRAYS REMAIN OPERATIVE AFTER INITIATION.
! HIGH TEMPERATURE INDICATES THAT NUMBER WON'T BE USED.
10000. 120727.2 0.01611 1.E10
! INJECTION TIME, RATED SPRAY FLOW RATE (KG/S), HEAT EXCHANGER
! RATED EFFECTIVENESS (W/K), SECONDARY SIDE INLET TEMP, RATED
! SECONDARY SIDE FLOW RATE (KG/S), SUMP THAT WATER IS DRAWN FROM.
! (FROM MARCH-HECTR REPORT) 2000. 587. 3.74E6 301.5
7.55E2 2
$ NO SPRAY RECIRCULATION (S2HF ACCIDENT SCENERIO)
$
! *****
! ENTER INITIAL CONDITIONS AND ACCIDENT SCENARIO INFORMATION
! *****
! SIMULATION TIME
4000.
!
! COMPARTMENT INITIAL CONDITIONS: TEMP; PARTIAL PRESSURES OF
! STEAM, NITROGEN, OXYGEN, HYDROGEN, CARBON MONOXIDE,
! CARBON DIOXIDE ; CONVECTIVE VELOCITY.
!
! C1 - CAVITY
348.83 40183. 69218. 17304. 0. 0. 0. 0.3
! C2 - LOWER COMP
349.98 42169. 67413. 16854. 0. 0. 0. 0.3
! C3 - ANNULUS
310.92 6617. 96087. 24022. 0. 0. 0. 0.3
! C4 - UPPER PLENUM
310.94 6628. 96078. 24020. 0. 0. 0. 0.3
! C5 - UPPER COMPARTMENT
310.97 6631. 96080. 24021. 0. 0. 0. 0.3
! ICE CONDENSER INITIAL CONDITIONS
310.84 6578. 95538. 23885. 0. 0. 0.
!
! SOURCE TERMS
!
$ STEAM SOURCE FROM EXTERNAL TABLE
$ NO NITROGEN SOURCES
$ NO OXYGEN SOURCES
$ HYDROGEN SOURCE FROM EXTERNAL TABLE
$ NO CO SOURCES
$ NO CO2 SOURCES
$ NO SUMP WATER REMOVAL
$ NO ENERGY SOURCES
$ NO CONTINUOUS BURNING
!

```



```

5 ! NUMBER OF COMPARTMENTS EXCLUDING ICE REGION
!
! FOR EACH COMPARTMENT: THE VOLUME, ELEVATION, FLAME PROPAGATION
! LENGTH, NUMBER OF SURFACES, AND INTEGERS SPECIFYING WHICH SUMP
! TO DUMP EXCESS WATER (FROM SUPERSATURATION) INTO AND WHICH SUMP
! THE SPRAYS FALL INTO.
!
! WHERE SIMILAR NUMBERED COMPARTMENTS OCCUR ,E.G. C2 - C5,
! THEY ARE SPECIFIED BY COUNTING CLOCKWISE FROM THE REFUELING
! CANAL.
!
C1 - REACTOR CAVITY
396.00 0. 10.0 1 1 1
C2 - LOWER COMPARTMENT
5887.46 16.23 17.5 6 2 2
C3 - ANNULUS
2662.00 10.56 13.3 2 2 2
C4 - UPPER PLENUM
1330.00 37.60 9.00 1 3 3
C10 - UPPER COMPARTMENT
17357.85 38.39 17.5 4 4 4
! FOR EACH SUMP, SUMP NUMBER, MAXIMUM VOLUME, SUMP NUMBER THAT
! THIS SUMP OVERFLOWS TO
!
1 396.00 2 ! SUMP IN REACTOR CAVITY
2 1450.0 1 ! LOWER COMPARTMENT SUMP
3 16.493 2 ! LOWER PLENUM FLOOR (2 IN. DEPTH)
4 1300.0 0 ! REFUELING CANAL SUMP
$
!
! FOR EACH SURFACE: TYPE OF SURFACE, MASS OF SURFACE, AREA OF
! SURFACE, CHARACTERISTIC LENGTH, SPECIFIC HEAT, EMISSIVITY,
! INTEGER INDICATING WHICH SUMP THE CONDENSATE GOES INTO. FOR
! SLABS (STYPE = 1), THE NUMBER OF LAYERS IN THE SURFACE, AND FOR
! EACH, THE THICKNESS, THERMAL DIFFUSIVITY, AND THERMAL
! CONDUCTIVITY. FINALLY, THE NODING INFORMATION AND BOUNDARY
! CONDITIONS ARE SPECIFIED (O'S INDICATE THE CODE WILL DETERMINE
! THE VALUES INTERNALLY). NOTE THAT SOME OF THE NUMBERS SET TO 1.
! ARE NOT USED FOR THAT SURFACE TYPE.
!
! REACTOR CAVITY - C1 - SURFACE 1 - 2
!
SUMP 1
3 559.82 59.20 5.18 1.0 0.94 1
!
! LOWER COMPARTMENT- C2 - SURFACES 2 - 7
!

```

```

LC STEEL
1 1. 3000.0 2. 1.0 0.9 2
1
0.0690 1.28E-5 47.25
0 0. 0.0 0.0
!
LC CONCRETE
1 1. 3569.0 4. 1.0 0.9 2
1
0.10 5.8E-7 1.453
0 0. 0.0 0.0
!
LC SUMP
3 4.41E5 353.00 10.67 1. 0.94 2
!
LC - LP STEEL WALL
1 1. 280.00 3. 1.0 0.9 3
1
0.013 1.28E-5 47.25
0 0. 0.0 0.0
!
LC - IC SUPPORT STRUCTURE
1 1. 2660.0 0.2 1.0 0.9 3
1
0.0081 1.28E-5 47.25
0 0. 0.0 0.0
!
LC - LP FLOOR/SUMP
3 5719 310.00 4.0 1. 0.94 3
!
! ANNULUS AROUND LOWER COMPARTMENT - C3 - SURFACES 8 - 9
!
AN STEEL
1 1. 1834.0 4. 1. 0.9 2
1
0.0310 1.28E-5 47.25
0 0. 0.0 0.0
!
AN CONCRETE
1 1. 3257.0 4. 1. 0.9 2
1
0.4480 5.80E-7 1.454
0 0. 0.0 0.0
!
! UPPER PLENUM - C4 - SURFACE 10
!
UP - STEEL
1 1. 1000. 5. 1. 0.9 3
1
0.013 1.28E-5 47.25
0 0. 0.0 0.0

```

!JOBØØR COMPARTMENT - C5 - SURFACES 11 - 14

!

UC - DOME

1 1. 1762.0 8. 1. 0.9 4

1

0.0127 1.28E-5 47.25

0 0. 5.0 300.0

!

UC - CONCRETE

1 1. 2937.48 10. 1. 0.9 4

1

0.910 5.80E-7 1.454

0 0. 0.0 0.0

!

UC EQUIPMENT - STEEL

1 1. 2000. 1. 1. 0.9 4

1

0.013 1.28E-5 47.25

0 0. 0.0 0.0

!

UC - REFUELING CANAL SUMP

3 1.259E6 67.75 6. 1.0 0.94 4

!

\$ NO CONTAINMENT LEAKS

!

! FLOW JUNCTION DATA: COMPARTMENT ID'S, TYPE OF CONNECTION, FLOW
! AREA, LOSS COEFFICIENT, L/A RATIO, RELATIVE POSITION OF
! COMPARTMENTS, AND JUNCTION ELEVATION. COMPARTMENT ID OF 0
! INDICATES THE ICE CONDENSER. JUNCTIONS WITHIN THE ICE
! CONDENSER ARE SET UP INTERNALLY. ADDITIONAL INFORMATION IS
! PROVIDED FOR JUNCTION TYPES 3 AND 4.

!

1 2 1 3.345 3. 2.559 1 4.505

1 2 1 0.929 10. 13.12 1 6.00

2 3 1 27.70 10. 0.545 0 10.60

2 -1 1 91.88 1.0 0.164 1 20.42

-1 4 1 1.858 3.0 4.921 1 35.052

-1 4 3 91.30 1.0 0.100 1 35.052

0. 263.4 37910. 1.55

4 5 1 186.0 1. 0.081 1 40.16

5 2 4 0.204 10. 1.0 -1 7.864

2 750.

5 3 1 0.0022 10. 12690. -1 10.60

\$

!

! ICE CONDENSER INPUT

!

! NUMBER OF LOWER PLENUM AND UPPER PLENUM COMPARTMENTS

1 1

```

! UPPER PLENUM COMPARTMENTS
4
! LOWER PLENUM COMPARTMENTS AND THE SUMPS THEY DRAIN INTO
2 2
! LOWER PLENUM COMPARTMENT THAT EACH STACK DRAINS INTO
2
! ICE DESCRIPTION: TOTAL MASS, AREA, TEMPERATURE, LENGTH,
! EMISSIVITY, VOLUME.
5.4991E5 1.5433E4 263.56 14.63 .94 594.23
! WALL AND STRUCTURES IN ICE CONDENSER (EXCLUDING BASKETS): MASS,
! AREA, SPECIFIC HEAT, EMISSIVITY
! (USE OLD MARCH-HECTR DATA)
2.0E5 2058. 485.7 .9
! MASS OF BASKETS, AREA OF BASKETS, DRAIN TEMPERATURE.
! (USE OLD MARCH-HECTR DATA)
1.47E5 9.92E3 310.
! ELEVATION OF BOTTOM OF ICE, TOTAL FREE GAS VOLUME, INITIAL
! VERTICAL FLOW AREA, VERTICAL FLOW AREA WITH ICE GONE, LOSS
! COEFFICIENTS FOR VERTICAL FLOW WITH AND WITHOUT ICE, FLOW AREA
! WITH AND WITHOUT ICE FOR CROSS FLOW, LOSS COEFFICIENTS FOR
! CROSS FLOW WITH AND WITHOUT ICE, L/A FOR CROSS FLOW,
! (USE OLD MARCH-HECTR DATA)
19.0 3060.2
167. 167. 1.0 1.0
7.9 7.9 3.0 3.0 0.4
!
$ NO SUPPRESSION POOL
!
! FAN DATA
! TEMP. AND PRESS. SETPOINTS, DELAY TIME, AND TIME TO TURN OFF.
! HIGH VALUE FOR TEMP. SETPOINT INDICATES THAT VALUE WON'T BE !
USED.
10000. 121590.0 600.0 1.E10
! COMPARTMENT ID'S, FLOW RATE (- INDICATES USE OF HEAD CURVE),
! SHUTOFF
! HEAD (PA), EFFICIENCY, RELATIVE POSITION OF COMPARTMENTS.
5 3 -35.540 1327.3575 1. -1
2 3 1.1685 1327.3575 1. 0
5 3 0.9439 1327.3575 1. -1
$ END OF FANS TABLE
$ END OF FANS INPUT
$ NO FAN COOLERS
!
! RADIATIVE BEAM LENGTHS - UPPER RIGHT HALF OF MATRIX IS INPUT.
! ICE SURFACES ARE NOT INCLUDED HERE. (THEY ARE DONE INTERNALLY)
!
! BEAM LENGTHS
!
24.08108 13*0.0
6*2.241683 7*0.0

```

5*2.241683	7*0.0		
4*2.241683	7*0.0		
3*2.241683	7*0.0		
2*2.241683	7*0.0		
2.241683	7*0.0		
1.882381	1.882381	5*0.0	
1.882381	5*0.0		
4.788000	4*0.0		
9.903546	9.903546	9.903546	9.903546
9.903546	9.903546	9.903546	
9.903546	9.903546		
9.903546			

!

! VIEW FACTORS

!

1.000000	13*0.0		
0.2949272	0.3508651	3.4703106E-02	2.7526543E-02
0.2615022			
3.0475816E-02	7*0.0		
0.3508651	3.4703109E-02	2.7526544E-02	0.2615021
3.0475818E-02			
7*0.0			
3.4703109E-02	2.7526544E-02	0.2615022	3.0475816E-02
7*0.0			
2.7526543E-02	0.2615022	3.0475816E-02	7*0.0
0.2615022	3.0475819E-02	7*0.0	
3.0475795E-02	7*0.0		
0.3602436	0.6397564	5*0.0	
0.6397564	5*0.0		
1.000000	4*0.0		
0.2603724	0.4340742	0.2955419	1.0011482E-02
0.4340742	0.2955419	1.0011482E-02	
0.2955419	1.0011483E-02		
1.0011435E-02			

!

! SPRAY INPUT

! NUMBER OF COMPARTMENTS WITH SPRAYS, AND ID OF THOSE

! COMPARTMENTS. SPRAY TEMP DURING INJECTION PHASE, FLOW RATE

! (M**3/S), NUMBER OF DROP SIZES, FREQUENCY AND DIAMETER

! (MICRONS) FOR EACH DROP SIZE.

1

5 313.56 0.593 2

0.95 309

0.05 810

! SPRAY CARRYOVER

\$ NO CARRYOVER

! COMPARTMENT ID AND SPRAY FALL HEIGHT FOR THAT COMPARTMENT.

5 28.61

\$

! TEMPERATURE AND PRESSURE SETPOINTS, DELAY TIME FOR SPRAYS,

```

! TIME THAT SPRAYS REMAIN OPERATIVE AFTER INITIATION.
! HIGH TEMPERATURE INDICATES THAT NUMBER WON'T BE USED.
10000. 120727.2 30. 1.E10
! INJECTION TIME, RATED SPRAY FLOW RATE (KG/S), HEAT EXCHANGER
! RATED EFFECTIVENESS (W/K), SECONDARY SIDE INLET TEMP, RATED
! SECONDARY SIDE FLOW RATE (KG/S), SUMP THAT WATER IS DRAWN FROM.
! (FROM MARCH-HECTR REPORT) 2000. 587. 3.74E6 301.5
7.55E2 2
$ NO SPRAY RECIRCULATION (S2HF ACCIDENT SCENERIO)
$
! *****
! ENTER INITIAL CONDITIONS AND ACCIDENT SCENARIO INFORMATION
! *****
! SIMULATION TIME
4000.
!
! COMPARTMENT INITIAL CONDITIONS: TEMP; PARTIAL PRESSURES OF
! STEAM, NITROGEN, OXYGEN, HYDROGEN, CARBON MONOXIDE,
! CARBON DIOXIDE ; CONVECTIVE VELOCITY.
!
! C1 - CAVITY
348.83 40183. 69218. 17304. 0. 0. 0. 0.3
! C2 - LOWER COMP
349.98 42169. 67413. 16854. 0. 0. 0. 0.3
! C3 - ANNULUS
310.92 6617. 96087. 24022. 0. 0. 0. 0.3
! C4 - UPPER PLENUM
310.94 6628. 96078. 24020. 0. 0. 0. 0.3
! C5 - UPPER COMPARTMENT
310.97 6631. 96080. 24021. 0. 0. 0. 0.3
! ICE CONDENSER INITIAL CONDITIONS
310.84 6578. 95538. 23885. 0. 0. 0.
!
! SOURCE TERMS
!
$ STEAM SOURCE FROM EXTERNAL TABLE
$ NO NITROGEN SOURCES
$ NO OXYGEN SOURCES
$ HYDROGEN SOURCE FROM EXTERNAL TABLE
$ NO CO SOURCES
$ NO CO2 SOURCES
$ NO SUMP WATER REMOVAL
$ NO ENERGY SOURCES
$ NO CONTINUOUS BURNING
!
! INITIAL SURFACE TEMPERATURES
!
! C1 RC
1*350.39

```

```
! C2 LC
342.65
345.00
342.38
345.00
342.65
330.37
! C3 AN
2*310.51
! C4 UP
312.60
! C5 UC
308.12
312.60
312.60
315.18
!
! NAMELIST INPUT
!
DTHTMX = 1.0
DTFLMX = 1.0
SPRAYS = OFF
FANS = ON
MRCHSC=2
XHMNIG(6)=1.0
TIMZER=4706.6
COCO2=FALSE
$
```

DISTRIBUTION:

U.S. Government Printing Office
Receiving Branch (Attn: NRC Stock)
(250 Copies for R3)
8610 Cherry Lane
Laurel, MD 20707

U.S. Nuclear Regulatory Commission (11)
Division of Accident Evaluation
Office of Nuclear Regulatory Research
Washington, DC 20555

Attn: B. Burson R. Meyer
 W. S. Farmer J. Mitchell
 M. Fleischman C. W. Nilsen
 C. N. Kelber J. Telford
 T. Lee P. Worthington
 R. W. Wright

U.S. Nuclear Regulatory Commission (11)
Office of Nuclear Reactor Regulation
Washington, DC 20555

Attn: V. Benaroya K. I. Parczewski
 W. R. Butler Z. Rosctoczy
 G. W. Knighton T. M. Su
 J. T. Larkins C. G. Tinkler
 A. NotaFrancesco
 R. Palla D. D. Yue

U.S. Department of Energy
R. W. Barber
Office of Nuclear Safety Coordination
Washington, DC 20545

U. S. Department of Energy (2)
Albuquerque Operations Office
Attn: J. R. Roeder, Director
 Transportation Safeguards
 J. A. Morley, Director
 Energy Research Technology
For: R. N. Holton
 C. B. Quinn

P.O. Box 5400
Albuquerque, NM 87185

Acurex Corporation
485 Clyde Avenue
Mountain View, CA 94042

American Electric Power Service Corp.
Room 1158-D
Attn: K. Vehstedt
2 Broadway
New York, NY 10004

Applied Sciences Association, Inc.
Attn: D. Swanson
P. O. Box 2687
Palos Verdes Pen., CA 90274

Argonne National Laboratory (5)

Attn: R. Anderson
 D. Armstrong
 L. Baker, Jr.
 Dae Cho
 B. Spencer
9700 South Cass Avenue
Argonne, IL 60439

Prof. S. G. Bankoff
Northwestern University
Chemical Engineering Department
Evanston, IL 60201

Battelle Columbus Laboratory (2)

Attn: P. Cybulskis
 R. Denning
505 King Avenue
Columbus, OH 43201

Battelle Pacific Northwest Laboratory (2)

Attn: M. Freshley
 G. R. Bloom
P.O. Box 999
Richland, WA 99352

Bechtel Power Corporation (2)

Attn: D. Ashton
 D. Patton
15740 Shady Grove Road
Gaithersburg, MD 20877

Dr. Brinka, Director
Test Operations
D 9500/B 33008
P.O. Box 13222
Sacramento, CA 95813

Brookhaven National Laboratory (4)

Attn: R. A. Bari
T. Ginsburg
G. Greene
T. Pratt
Upton, NY 11973

Cleveland Electric Illuminating Co.

Perry Nuclear Plant
Attn: R. Stratman
10 Center Road
North Perry, OH 44081

Combustion Engineering Incorporated

Attn: J. D. Boyajian
1000 Prospect Hill Road
Windsor, CT 06095

Lynn Connor

Document Search NRC
P.O. Box 7
Cabin John, MD 20818

Dr. Michael Cook

Morton Thiokol
Ventron Group
150 Andover Street
Danvers, MA 01923

Donald C. Cook Nuclear Station

Indiana & Michigan Electric Company
Attn: D. Nelson
P.O. Box 458
Bridgman, MI 49106

Prof. M. L. Corradini

University of Wisconsin
Nuclear Engineering Department
1500 Johnson Drive
Madison, WI 53706

Duke Power Company (2)

Attn: F. G. Hudson
A. L. Sudduth
P.O. Box 3189
Charlotte, NC 28242

A. Pete Dzmura

NE 43
U.S. DOE
Washington, DC 20545

EG&G Idaho (3)

Willow Creek Building, W-3
Attn: D. Croucher
R. Hobbins
Server Sadik
P.O. Box 1625
Idaho Falls, ID 83415

Electric Power Research Institute (5)

Attn: J. Haugh
W. Loewenstein
B. R. Sehgal
G. Thomas
R. Vogel
3412 Hillview Avenue
Palo Alto, CA 94303

Factory Mutual Research Corporation

Attn: R. Zalosh
P.O. Box 688
Norwood, MA 02062

Fauske & Associates (2)

Attn: R. Henry
M. Plys
16W070 West 83rd Street
Burr Ridge, IL 60521

GPU Nuclear

Attn: J. E. Flaherty
100 Interpace Parkway
Parsippany, NJ 07054

General Electric Corporation

Attn: K. W. Holtzclaw
175 Curtner Avenue
Mail Code N 1C157
San Jose, CA 95125

General Electric Corporation

Advanced Reactor Systems Dept.
Attn: M. I. Temme, Manager
Probabilistic Risk Assessment
P.O. Box 3508
Sunnyvale, CA 94088

General Physics Corporation

Attn: C. Kupiec
1000 Century Plaza
Columbia, MD 21044

General Public Utilities
Three Mile Island Nuclear Station
Attn: N. Brown
P.O. Box 480
Middletown, PA 17057

Dr. Dennis Hacking
Enercon Services
520 West Broadway
P.O. Box 2050
Broken Arrow, OK 74013

Jim O. Henrie
Westinghouse Hanford Division
P.O. Box 1970
Richland, Washington 99352

Indiana and Michigan Electric Company
Attn: J. Dickson
P.O. Box 458
Bridgman, MI 49106

Institute of Nuclear Power Operation (3)
Attn: Henry Piper
S. Visner
E. Zebroski
1100 Circle 795 Parkway, Suite 1500
Atlanta, GA 30339

International Technology Corporation
Attn: Mario H. Fontana
575 Oak Ridge Turnpike
Oak Ridge, TN 37830

Lt. Kevin Klonoski
6595 Shuttle Test Group
Vandenberg Air Force Base
Vandenberg AFB, CA 93437

Knolls Atomic Power Lab (2)
Attn: Albert J. Kausch
R. L. Matthews
General Electric Company
Box 1072
Schnectady, NY 12301

Professor C. K. Law
Department of Mechanical Engineering
Davis, CA 95616

Robert Lipp
Westinghouse Hanford
838 West Octave
Pasco, WA 99301

Los Alamos National Laboratory (8)
Attn: W. R. Bohl
F. J. Edeskuty
R. Gido
J. Carson Mark
G. Schott
H. Sullivan
J. Travis
K. D. Willaimson, Jr.
P.O. Box 1663
Los Alamos, NM 87545

Massachusetts Institute of Technology
Attn: N. C. Rasmussen
Nuclear Engineering Department
Cambridge, MA 02139

University of Michigan
Attn: Prof. M. Sichel
Department of Aerospace Engineering
Ann Arbor, MI 47109

University of Michigan
Nuclear Engineering Department
Ann Arbor, MI 48104

Miller & White P.C.
Attn: John White, Patent Attorney
Anthony J. Zelano, Patent Attorney
503 Crystal Mall, Building 1
1911 Jefferson Davis Highway
Arlington, VA 22202

Mississippi Power & Light
Attn: S. H. Hobbs
P. O. Box 1640
Jackson, MS 39205

NUS Corporation
Attn: R. Sherry
4 Research Place
Rockville, MD 20850

Oak Ridge National Laboratory (2)
Attn: A. P. Malinauskas
T. Kress
NRC Programs
P.O. Box X, Bldg. 4500S
Oak Ridge, TN 37831

Pennsylvania Power & Light
Attn: R. DeVore
Susquehanna SES
P. O. Box 467
Berwick, PA 18603

Power Authority State of NY (2)
Attn: R. E. Deem
S. S. Iyer
10 Columbus Circle
New York, NY 10019

Dr. J. E. Shepherd
Rensselaer Polytechnic Institute
Troy, NY 12180-3590

Andrew F. Rutkiewicz
E. F. DuPont
Marshall Laboratory
P.O. Box 3886
Philadelphia, PA 19146

Sharon Sargent (15)
Sandia National Laboratories
P.O. Box 5800
Albuquerque, NM 87185

Bill Seddon
Atomic Energy of Canada
Research Company
Chalk River Nuclear Laboratories
KOJ 1JO CANADA

Dpak Shah, Sr. Dev. Eng.
Honeywell, Inc.
MN63-B170
Corporation Systems Dev. Division
1000 Boone Avenue North
Golden Valley, MN 55427

Stone & Webster Engineering Corp. (2)
Attn: G. Brown
E. A. Warman
245 Summer Street/9
Boston, MA 02143

Stratton & Associates, Inc.
Attn: W. Stratton
2 Acoma Lane
Los Alamos, NM 87544

Dr. Roger Strehlow
505 South Pine Street
Champaign, IL 61820

Steve Sweargin
Omaha Public Power District
Jones Street Station
O.H.P.D.
1623 Harney Street
Omaha, NE 68102

Technology for Energy Corporation (2)
Attn: J. Carter
E. L. Fuller
10770 Dutchtown Road
Knoxville, TN 37922

Texas A & M University
Nuclear Engineering Dept.
College Station, TX 77843

Prof. T. G. Theofanous
Chemical and Nuclear Engineering Dept.
University of California
Santa Barbara, CA 93106

Thompson Associates (2)
Attn: Timothy Woolf
639 Massachusetts Avenue
Third Floor
Cambridge, MA 02139

TVA
Attn: Wang Lau
400 Commerce
W9C157-CD
Knoxville, TN 37902

UCLA
Nuclear Energy Laboratory (2)
Attn: Prof. I. Catton
Prof. D. Okrent
405 Hilgard Avenue
Los Angeles, CA 90024

Virginia Electric & Power Company (3)
Attn: A. Hogg
E. L. Vilson
A. K. White
Northanna Power Station
P.O. Box 402
Mineral, VA 23117

Virginia Electric & Power Company
Attn: R. Garner
P.O. Box 26666
James River Plaza
Richmond, VA 23261

Danielle Weaver
Nucleonics Week
1120 Vermont Avenue N.W.
Suite 1200
Washington, DC 20005

Bill West
Bettis Atomic Power Laboratory
P.O. Box 79
West Mifflin, PA 15122

Westinghouse Corporation (3)
Attn: N. Liparulo
J. Olhoeft
V. Srinivas
P.O. Box 355
Pittsburgh, PA 15230

Westinghouse Electric Corporation (2)
Bettis Atomic Power Laboratory
Attn: Donald R. Connors
Charles Quinn
P.O. Box 79
West Mifflin, PA 15122

Westinghouse Electric Corporation
Attn: P. Lain
Monroeville Nuclear Center
Monroeville, PA 15146

Westinghouse Hanford Company (3)
Attn: G. R. Bloom
L. Mulstein
R. D. Peak
P.O. Box 1970
Richland, VA 99352

Lt. Sherman Westvig
Building 8500
Vandenberg Air Force Base
Vandenberg AFB, CA 93437

Keith Williams
Tayco Engineering, Inc.
P.O. Box 19
Long Beach, CA 90802

Zion Nuclear Power Station
Commonwealth Edison Company
Attn: C. Schultz
Shiloh Blvd. and Lake Michigan
Zion, IL 60099

Belgonucleaire S.A.
Attn: H. Bairiot
Rue de Champ de Mars 25
B-1050 Brussels
BELGIUM

Professor Lue Gillon
University of Louvain la
Neuve
Batiment Cyclotron
B1348 Louvain La Neuve
BELGIUM

Director of Research, Science &
Education
CEC
Attn: B. Tolley
Rue De La Loi 200
1049 Brussels
BELGIUM

Atomic Energy Ltd. (4)
Whiteshell Nuclear Research Establishment
Attn: D. Liu
C. Chan
K. Tennankore
D. Wren
Pinawa, Manitoba
CANADA

Atomic Energy Canada Ltd.
Attn: P. Fehrenbach
Chalk River, Ontario KOJ 1J0
CANADA

Defence Research Establishment Suffield
Attn: Dr. Ingar O. Moen
Ralston, Alberta TOJ 2N0
CANADA

McGill University (3)
Attn: Prof. John H. S. Lee
315 Querbes
Outremont, Quebec H2V 3W1
CANADA

Professor Karl T. Chuang
University of Alberta
Edmonton, Alberta, T6G 2E1
CANADA

CEA
Attn: M. Georges Berthoud
B.P. No. 85X-Centre de
F-38041 Grenoble Cedex
FRANCE

Battelle Institut E. V. (4)
Attn: Dr. Werner Baukal
Werner Geiger
Dr. Guenter Langer
Dr. Manfred Schildknecht
Am Roemerhof 35
6000 Frankfurt am Main 90
FEDERAL REPUBLIC OF GERMANY

Gesellschaft für Reaktorsicherheit (GRS)
Postfach 101650
Glockengasse 2
5000 Koeln 1
FEDERAL REPUBLIC OF GERMANY

Gesellschaft für Reaktorsicherheit (2)
Attn: Dr. E. F. Hicken
Dr. H. L. Jahn
8046 Garching
Forschungsgelände
FEDERAL REPUBLIC OF GERMANY

Universität Heidelberg
Attn: Juergen Warnatz
Heidelberg
FEDERAL REPUBLIC OF GERMANY

Institute für Kernenergetik und
Energiesysteme (2)
Attn: M. Buerger
G. Froehlich
H. Unger
University of Stuttgart
Stuttgart
FEDERAL REPUBLIC OF GERMANY

Kernforschungszentrum Karlsruhe (4)
Attn: Dr. S. Hagen
Dr. Heusener
Dr. Kessler
Dr. M. Reimann
Postfach 3640
7500 Karlsruhe
FEDERAL REPUBLIC OF GERMANY

Kraftwerk Union (2)
Attn: Dr. M. Peehs
Dr. K. Hassman
Hammerbacherstrasse 12 & 14
Postfach 3220
D-8520 Erlangen 2
FEDERAL REPUBLIC OF GERMANY

Lehrgebiet für Mechanik der
RWTH Aachen
Attn: Prof. Dr. Ing. N. Peters
Templergraben 55
D5100 Aachen
FEDERAL REPUBLIC OF GERMANY

Technische Universität München
Attn: Dr. H. Karwat
8046 Garching
FEDERAL REPUBLIC OF GERMANY

Propulsion and Combustion
Dept. of Aeronautical Engineering
Attn: Alon Gany, D.Sc.
Technion, Haifa 32000
ISRAEL

CNEN NUCLIT
Attn: A. Morici
Rome
ITALY

ENEA Nuclear Energy Alt Disp (2)

Attn: P. L. Ficara
G. Petrangeli

Via V. Brancati
00144 Roma
ITALY

ISPRA

Commission of the European Communities
Attn: Dr. Heinz Kottowski
C.P. No. 1, I-21020 Ispra (Varese)
ITALY

Universita Degli Studi Di Pisa

Dipartimento Di Costruzioni

Attn: M. Carcassi
Meccaniche E. Nucleari
Facolta Di Ingegneria
Via Diotisalvi 2
56100 Pisa
ITALY

Japan Atomic Energy Research Institute

Attn: Dr. K. Soda, Manager
Chemical Engineering Safety Laboratory
Dept. of Nuclear Fuel Safety
Tokai-mura, Naka-gun Ibaraki-ken
319-11
JAPAN

Japan Atomic Energy Research Institute

Attn: Dr. T. Fujishiro, Manager
Dept. of Fuel Safety Research
Tokai-mura, Naka-gun, Ibaraki-ken
319-11
JAPAN

Japan Atomic Energy Research Institute

Attn: Mr. Kazuo Sato, Director
Dept. of Reactor Safety Research
Tokai-mura, Naka-gun Ibaraki-ken
319-11
JAPAN

Power Reactor Nuclear Fuel

Development Corp. (PNC)
Attn: Dr. Watanabe
FBR Project
9-13, 1-Chome, Akasaka
Minato-ku, Tokyo
JAPAN

Korea Advanced Energy Research
Institute

Attn: H. R. Jun
P.O. Box 7
Daeduk Danji, Chungnam
KOREA

Netherlands Energy Research Foundation

Attn: K. J. Brinkmann
P.O. Box 1
1755ZG Petten NH
NETHERLANDS

Institute of Nuclear Energy Research

Attn: Sen-I-Chang
P.O. Box 3
Lungtan
Taiwan 325
REPUBLIC OF CHINA

Royal Institute of Technology

Attn: Prof. Kurt M. Becker
Dept. of Nuclear Reactor Engineering
Stockholm S-10044
SWEDEN

Statens Karnkraftinspektion

Attn: L. Hammer
P.O. Box 27106
S-10252 Stockholm
SWEDEN

Studsvik Energiteknik AB

Attn: K. Johansson
S-611 82 Nykoping
SWEDEN

Swedish State Power Board

Attn: Wiktor Frid
S-162 Fach 87 Vallingby
SWEDEN

Swedish State Power Board

Attn: Eric Ahlstrom
181-OCH Vaermeteknik
SWEDEN

D. Ulrich

SULZER Bros. Ltd.
TMV-0460
CH-8401 WINTERTHUR
SWITZERLAND

AERE Harwell
Attn: J. R. Matthews, TPD
Didcot
Oxfordshire OX11 0RA
UNITED KINGDOM

Berkeley Nuclear Laboratory (3)
Attn: J. E. Antill
S. J. Board
N. Buttery
Berkeley GL 139PB
Gloucestershire
UNITED KINGDOM

British Nuclear Fuels, Ltd.
Attn: W. G Cunliffe
Building 396
Springfield Works
Salwick, Preston
Lancs
UNITED KINGDOM

Imperial College of Science and
Technology
Attn: Dr. A. D. Gosman
Dept. of Mechanical Engineering
Exhibition Road
London SW7 2BX
UNITED KINGDOM

National Nuclear Corp. Ltd.
Attn: R. May
Cambridge Road
Whetstone, Leicester, LE8 3LH
UNITED KINGDOM

Simon Engineering Laboratory (2)
University of Manchester
Attn: Prof. W. B. Hall
S. Garnett
M139PL
UNITED KINGDOM

Anthony R. Taig
GDCD/CEGB
Barnwood, Gloucester
Gloucestershire
UNITED KINGDOM

UKAEA Safety & Reliability Directorate (4)
Attn: J. G. Collier
J. H. Gittus
S. F. Hall
M. R. Hayns
Wigshaw lane, Culcheth
Warrington WA3 4NE
Cheshire
UNITED KINGDOM

UKAEA, Culham Laboratory (4)
Attn: F. Briscoe
Ian Cook
D. Fletcher
B. D. Turland
Abingdon
Oxfordshire OX14 3DB
UNITED KINGDOM

UKAEA AEE Winfrith (4)
Attn: M. Bird
T. Butland
R. Potter
A. Wickett
Dorchester
Dorset DT2 8DH
UNITED KINGDOM

University of Aston in Birmingham (2)
Dept. of Chem.
Attn: A. T. Chamberlain
F. M. Page
Gosta Green, Birmingham B47ET
UNITED KINGDOM

Sandia Distribution:

1131 W. B. Benedick
1510 J. W. Nunziato
1512 J. C. Cummings
1530 L. W. Davison
3141 S. A. Landenberger (5)
3151 I. Klein
4030 J. D. Corey
4050 K. Olsen
6400 D. J. McCloskey
6412 A. L. Camp
6418 J. E. Kelly
6418 S. E. Dingman
6420 J. V. Walker
6422 D. A. Powers
6425 W. J. Camp
6427 M. Berman (5)
6427 D. F. Beck
6427 J. E. Dec
6427 L. S. Nelson
6427 M. P. Sherman
6427 S. E. Slezak
6427 D. W. Stamps
6427 S. R. Tieszen
6427 C. C. Wong (10)
6440 D. A. Dahlgren
8524 P. W. Dean

NRC FORM 335 (2-84) NRCM 1102, 3201, 3202		U.S. NUCLEAR REGULATORY COMMISSION		1 REPORT NUMBER (Assigned by TRD, add Vol. No., if any) NUREG/CR-4993 SAND87-1858	
BIBLIOGRAPHIC DATA SHEET					
SEE INSTRUCTIONS ON THE REVERSE					
2. TITLE AND SUBTITLE A Standard Problem for HECTR-MAAP Comparison: Incomplete Burning				3 LEAVE BLANK	
5 AUTHOR(S) C. Channy Wong				4 DATE REPORT COMPLETED MONTH YEAR April 1988	
				6 DATE REPORT ISSUED MONTH YEAR August 1988	
7 PERFORMING ORGANIZATION NAME AND MAILING ADDRESS (Include Zip Code) Sandia National Laboratories Albuquerque, New Mexico 87185				8 PROJECT/TASK/WORK UNIT NUMBER 9 FIN OR GRANT NUMBER A1246	
10 SPONSORING ORGANIZATION NAME AND MAILING ADDRESS (Include Zip Code) Division of Systems Research Office of Nuclear Regulatory Research U.S. Nuclear Regulatory Commission Washington, DC 20555				11a TYPE OF REPORT Final Report b PERIOD COVERED (Inclusive dates)	
12 SUPPLEMENTARY NOTES					
13. ABSTRACT (200 words or less) <p>To assist in the resolution of differences between the NRC and IDCOR on the hydrogen combustion issue, a standard problem has been defined to compare the results of HECTR and MAAP analyses of hydrogen transport and combustion in a nuclear reactor containment. The first part of this standard problem, which addresses incomplete burning of hydrogen in the lower and upper compartments, has been completed, and the results will be presented in this report. A critical review and comparison of the combustion models in HECTR and in MAAP show that HECTR's predictions are better than MAAP's when compared against test results of the VGES, FITS and NTS experiments. The model in MAAP overpredicts the burn time and underpredicts the steam inerting effect on ignition. For the standard problem, HECTR predicts that pressure generated due to incomplete burning in the lower and upper compartments will have a sharper rise, shorter duration and higher peak value than that predicted by MAAP. MAAP prediction resembles a standing diffusion flame, rather than a flame propagating through a homogeneous mixture.</p>					
14 DOCUMENT ANALYSIS - a KEYWORDS/DESCRIPTORS HECTR computer code MAAP computer code b IDENTIFIERS/OPEN ENDED TERMS				15 AVAILABILITY STATEMENT Unlimited	
				16 SECURITY CLASSIFICATION (This page) Unclassified (This report) Unclassified	
				17 NUMBER OF PAGES	
				18 PRICE	



8232-2/067832



00000001 -



8232-2/067832



00000001 -



8232-2/067832



00000001 -

**UNITED STATES
NUCLEAR REGULATORY COMMISSION
WASHINGTON, D.C. 20555**

OFFICIAL BUSINESS
PENALTY FOR PRIVATE USE, \$300

SPECIAL FOURTH-CLASS RATE
POSTAGE & FEES PAID
USNRC
PERMIT No. G-67